University of Cyprus
Deparment of Architecture

HYBRID CABLE BENDING-ACTIVE STRUCTURES

by

Kristis C. Alexandrou

BA(hons) Architecture and Design, University of Brighton, United Kingdom
Diploma of Architect Engineer, University of Cyprus, Cyprus

DOCTOR OF PHILOSOPHY DISSERTATION

A Dissertation Submitted to the University of Cyprus in Partial Fulfilment of the Requirements for the Degree of Doctor of Philosophy

Nicosia, May 2018

HYBRID CABLE BENDING-ACTIVE STRUCTURES

by

Kristis C. Alexandrou

Research Supervisor:

Dr. Marios C. Phocas, Associate Professor
Department of Architecture, University of Cyprus

Examination committee:

Dr. Aimilios Michael, Assistant Professor (Chairman)
Department of Architecture, University of Cyprus

Dr. Marios C. Phocas, Associate Professor
Department of Architecture, University of Cyprus

Dr. Odysseas Kontovourkis, Assistant Professor
Department of Architecture, University of Cyprus

Dr. Dimos Charmpis, Associate Professor
Department of Civil and Environmental Engineering, University of Cyprus

Dr. Ramon Sastre Sastre, Professor
Deparmento de Tecnologia de l'Arquitectura, Universitat Politècnica de Catalunya

VALIDATION PAGE

Doctoral Candidate: **Kristis C. Alexandrou**

Doctoral Dissertation Title: **Hybrid Cable Bending-active Structures**

*The present Doctoral Dissertation was submitted in partial fulfilment of the requirements for the Degree of Doctor of Philosophy at the **Department of Architecture** and was approved on the 24/04/2018 by the members of the **Examination Committee**.*

Examination Committee:

Research Supervisor: _____

Dr. Marios C. Phocas

Committee Member (Chairman): _____

Dr. Aimilios Michael

Committee Member: _____

Dr. Odysseas Kontovourkis

Committee Member: _____

Dr. Dimos Charmpis

Committee Member: _____

Dr. Ramon Sastre Sastre

DECLARATION OF DOCTORAL CANDIDATE

The present doctoral dissertation was submitted in partial fulfilment of the requirements for the degree of Doctor of Philosophy of the University of Cyprus. It is a product of original work of my own, unless otherwise mentioned through references, notes, or any other statements.

……..……..

……

ΠΕΡΙΛΗΨΗ

«Υβριδικές Δομικές Κατασκευές Καλωδίων και Ενεργά Εύκαμπτων Μελών»

Τις τελευταίες δεκαετίες, ο τομέας της Προσαρμοστικής Αρχιτεκτονικής με έμφαση στη στατική επάρκεια, στις μεταβαλλόμενες μορφολογικές ικανότητες και στην εναλλακτική σχεδιαστική προσέγγιση για ελεύθερη μορφή, διαδέχεται σημαντική αναγνώριση με αυξανόμενο αριθμό ερευνητικών προτάσεων και πειραματικών εφαρμογών. Οι κυρίαρχες επιδιώξεις της ερευνητικής αυτής κατεύθυνσης στοχεύουν στην αναβάθμιση του δομημένου περιβάλλοντος με γνώμονα την αειφορία, την ενεργειακή αποδοτικότητα και τη σχεδιαστική προαγωγή του, διαμέσου επιτυχούς ενσωμάτωσης ενός ευρύτερου φάσματος αποδοτικών κριτηρίων βελτιστοποίησης, όπως αυτά ορίζονται από τις σύγχρονες κατασκευαστικές μεθόδους και τη χρήση νέων υλικών.

Σε αυτό το πλαίσιο, η παρούσα διατριβή επικεντρώνεται στη διερεύνηση εναλλακτικών αυτό-εντεινόμενων συναρμολογούμενων υβριδικών δομικών συστημάτων, βασιζόμενων στη χρήση ελαστικών μελών. Στοχεύει στην παροχή επίγνωσης σε μη-γραμμικές διαδικασίες εξεύρεσης μορφής, στη στατική ανάλυση και στην αποκωδικοποίηση της φέρουσας ικανότητας υπό ανόμοια διαμορφωμένους σχηματισμούς. Η διερεύνηση στηρίζεται σε περιπτώσεις μελέτης προτοτύπων, με αφετηρία την εις βάθος εξέταση έξι υβριδικών δομικών μονάδων. Η πρωταρχική αυτή διερεύνηση παρέχει τον κατάλληλο βαθμό πληροφορίας για περεταίρω εξέταση πιο σύνθετων δομών με μεγαλύτερο άνοιγμα, συμπεριλαμβανομένων της μορφολογικής και δομικής βελτιστοποίησης τους, η οποία ενεργοποιήται με μείωση του μήκους των καλωδίων.

Το κεφάλαιο 1 εισηγείται στοιχεία τόσο σχεδιασμού, όσο και αποτελεσματικής χρήσης του υλικού που συνεισφέρουν στην επίτευξη προσαρμοστικών δομικών αναβαθμίσεων. Στο ακολούθως επόμενο κεφάλαιο 2, παρουσιάζονται ιστορικά και σύγχρονα παραδείγματα από χωρικές κατασκευές, η σύσταση των οποίων αποτελείται από μέλη ενεργής κάμψης. Ο ρόλος του καλωδίου σε υβριδικές κατασκευές και οι δυνατότητες για υβριδοποίηση με

ενεργά-εύκαμπτες κατασκευές, όπως και επισκόπηση γενικευμένων μεθόδων υπολογισμού για εξεύρεση μορφής περιγράφονται στο κεφάλαιο 3. Το μοντέλο ανάλυσης, το οποίο έχει υοθετηθεί στην παρούσα μελέτη, παρουσιάζεται στο κεφάλαιο 4. Οι προτεινόμενες περιπτώσεις συστημάτων αποτελούνται από μονά, απλά-συνδεδεμένα ζεύγη και εσωτερικά-διασυνδεδεμένα ζεύγη από ελαστικά μέλη σε συνδυασμό με αποκλειστικά εφελκυστικής ικανότητας δευτερεύοντα γραμμικά στοιχεία, όπως περιγράφονται στο κεφάλαιο 5. Τα αποτελέσματα ανάλυσης των συστημάτων παρέχουν δεδομένα για την κατανόηση τις δομικής συμπεριφοράς, με ειδική έμφαση στους συσχετισμούς που προκύπτουν από την κατάσταση εσωτερικής έντασης και της φέρουσας ικανότητας τους. Η πληροφορία αυτή αξιοποιείται περεταίρω προς όφελος ακόλουθης διερεύνησης υβριδικών διαμορφωμένων φορέων μεγαλύτερου ανοίγματος. Τα συστήματα εξετάζονται σε ζητήματα βελτιστοποίησης μορφολογικής και στατικής επάρκειας, με βάση τη μείωση του μήκους καλωδίων για την επίτευξη αυξανόμενης προένασης και ελέγχου παραμορφώσεων των συστημάτων, όπως περγιργάφεται στα τελευταία δύο κεφάλαια της παρούσας μελέτης. Τα συγκεντρωτικά συμπεράσματα όσον αφορά τρόπους σχεδιαστικής προσέγγισης, όπως επίσης και κριτήρια βελτιστοποίησης, περιέχονται στα συμπεράσματα της παρούσας διατριβής.

ABSTRACT

"Hybrid Cable Bending-Active Structures"

In the last decades, the concept of Adaptive Architecture in terms of the structure's static performance, morphological altering capabilities and free-form design is increasingly acknowledged with growing number of research projects and experimental applications. Predominantly, this research field's objective is oriented towards transforming our build environment into a more sustainable, energy efficient and design-wise augmented reality, by succeeding into a broader variety of performance and optimisation criteria, set by both, contemporary construction techniques and new material exploitation potentials.

This thesis refers to the investigation of alterative self-stressed hybrid structural system assemblies, based on application of elastic members. It aims at providing insight in nonlinear form-finding processes, structural analysis and load-deformation behaviour of dissimilar configurations. The work is based on a prototypes analyses approach and is initialised with an in-depth examination of a series of six hybrid structural single-segment configurations. These provide necessary information for the subsequent examination of longer span assemblies, including their morphological and structural optimisation, activated by the cables length reduction.

In Chapter 1, aspects of design and material's performative use for achieving unique adaptive structural enhancements are introduced. Historical background and present examples of elastically deformable space structures are discussed in Chapter 2. The role of the cable in hybrid structures and its potentialities in hybrid bending-active systems, as well as general form-finding calculation techniques are overviewed in Chapter 3. The analysis model adopted for this study is presented in Chapter 4. The case studies models proposed, are composed of simple, simply-paired and paired interconnected elastic members, hybridised with tension-only elements, as presented in Chapter 5. The analysis results provide general understandings of the structural behaviour and explicit information with regard to the interdependencies of the inner stress state of the members and their load-bearing capacity. The information collected is utilised for further examination of more

complex hybrid configurations of longer span. These are then subjected to global form and capacity optimisation strategies, based on the cables length reduction for achieving increased prestress and load-deformation control of the systems as stated in the final two Chapters of the present report. An overview of the results obtained with regard to design aspects and optimisation criteria is included in the Coclusions of the present thesis.

ADKNOWLEDGEMENTS

Throughout this long and challengeful journey, I have gained a lot by learning to persevere despite difficulty and precariousness. I am feeling grateful to all those who supported me along this journey. I would have never reached my goals without the assistance and all valuable forms of support of numerous people who I am indebted to.

First and foremost, I would like to express my absolute gratitude to my thesis supervisor, Professor Dr.-ing. Marios C. Phocas, for his continuous support and encouragement for completing this research. He has been a true mentor and endless source of inspiration. I will never forget his support and effort for providing me numerous opportunities to learn and develop as a researcher. To him I wish to say, “you are a wonderful person, mentor and professor”.

I am also very grateful to Dr. Odysseas Kontovourkis and Dr. Dimos Charmpis, for serving as committee members and providing valuable insights and suggestions during the initial phases of this work.

I would like to extend my sincere thanks to my fellow postgraduate colleagues in MSc Energy Technologies and Sustainable Design, at the Faculty of Engineering, University of Cyprus, Stella Athini, Christina Zakou and Ioanna Anastasiadou for their fruitful exchange of knowledge and collaboration in our mutual research interests and objectives. Team working has significant impact for keeping the research spirit alive.

Words cannot express the feeling I have for my parents. Their relentless unconditional support, both sentimental and financial, consists primary reason for the successful completion of this thesis.

Finally, I would like to acknowledge the most important person in my life, my brother, Marios Alexandrou. The person who has always been there for me, responsible to endure and strengthen my motivation during this course.

Dedicated to those who are fascinated with the design of kinetic, reconfigurable structures…

TABLE OF CONTENTS

LIST OF FIGURES

LIST OF TABLES

CHAPTER 1 **INTRODUCTION**

1.1 Adaptivity in Architecture

The word *adaptive* is used as a technical term and it is defined as the object or objective that is ''characterised or given to adaptation'' that can go through ''actions or processes of adapting or being adapted'' (*Adaptive*, 2016). In this respect, in the field of architecture, all existing buildings comply in some degree with adaptive characteristics, since they have been designed for having the capacity to adapt or show adaptation to explicit aspects, such as inhabitant's activity needs, environmental phenomena alterations or changing loading conditions. These attributes of *adaptivity* correspond to particular objectives in a unique way that express distinct level, scale, method and effect of *adaptation* (Schnädelbach, 2010). By extent, an evaluation of buildings' adaptive behaviour can be classified in two main criteria. Criteria that can be described numerically (quantifiable), for instance the response to temperature, light, loading circumstances etc., or criteria that are more subjective to inhabitant's satisfaction (qualitative), such as response to users' personal space organisational preferences or aesthetics. Likewise, buildings that can adapt to more than one architectural aspect can be characterised with multi-adaptational behaviour.

Consequently, in architecture, *adaptation* can be defined as the process that describes either the generation or emerged behavioural performance of buildings, according to respective aspects. Adaptive architecture may be either the result of a design process that incorporates functioning aspects, which makes it *adaptable* (*Adaptable*, 2016) to a particular domain of shifting conditions, or *adaptive*, in terms of being able to adapt to readjusted conditions. Despite their differences, the terms *adaptable* and *adaptive* are often conceived by designers as similar, due to confusion between design objective and actual performance. Both words describe processes or actions that provoke adaptive effects. *Adaptable* and *adaptive* is concerned within buildings that in multiple levels and

frequencies can enable changes to themselves and sustain a space-time adaptation, whether this is attained naturally or manually via human intervention. This approach frequently involves digital technology such as sensing devices, actuators, controllers, or communication technologies (Sterk, 2003). Taking the above information into account, these definitions and the associated framework therein may apply to a variety of particularities to architecture, such as those labelled *interactive, responsive, dynamic, intelligent, smart, flexible, hybrid,* with each unfolding complementary adaptation features with explicit area of focus, depending on the kind and effect of adaptation.

Adaptive attributes of space may be achieved using either passive or active characteristics of the overall building. These characteristics are based on mechanical, chemical, or other procedures, which result into transformational, thermal, or other adaptive responses (Fox, 2016). Passive adaptive characteristics of space may refer to material properties that can maintain the same level of space characteristics (e.g. temperature) during different environmental changes, a structural form syntax that provides highly optimised static performance, or reconfigurable spatial forms that can be transformed by the users and adapt to functional or structural requirements. On the other hand, active adaptive characteristics of space are attained using systems with shifting mechanical characteristics, able to obtain a real-time control of specific reconfigurations and adapt to predefined objectives, sustaining in this respect a constant adaptive behaviour. In this case, an active control system is required depending on the type of activation, as well as the supply of energy from an external source to actuate the transformation. In other words, architectural applications that aim at succeeding on a real-time adaptive function with regard to a particular purpose, are directly related to the type and kind of the approach followed to activate the particular adaptive functions (Schnädelbach, 2010). Passive approaches are usually less responsive to adaptation operations and take more time to effect, compared to active ones.

The ability of a building to transform itself to a specific static state and therefore adapt to time-depended external forces or user demands, necessitates the formulation of a

design strategy that intersects with multiple objectives and research means. The integration of motion with ultimate purpose to reach an adaptive character and behaviour with regard to space and time, is discussed in the field of *Kinetic Architecture*.

The classification of kinetic systems departs mainly from the structural transformation action performed, such as folding, sliding, swivelling, rotating, squeezing, extending etc. In order to achieve an independent behaviour, kinetic structures are directly associated with activation methods and automation systems of active control (embedded computation) responsible to stimulate command signals to the structure to react according to the input of the surrounding environment or user (Elkhayat, 2014).

The multi-parametric character of the approach needed to follow in the design of such systems can be identified as *data driven design*, where multiple constraints, limitations or restraints are mostly assigned as numerical domain restrictions or geometrical interdependencies. In the basis of parametric associative design logic, knowledge from multiple fields contributes in sustaining the success of the outcome in all dimensions (Menges and Ahlquist, 2011).

1.1.1 Kinetics in rigid components

The kinetic structural systems have been firstly explored in mechanical systems in 1700 (Reuleaux and Ferguson, 2012). The employment of rigid elements and materials, as well as the application of hinge or similar connection typologies and support conditions, enable the structure to transform energy – force into motion. The geometry of the members, the connections typology and the boundary conditions are the basic critical parameters for the design of such systems. They define the kinematics and therefore the transformational possibilities and kinetic characteristics of the system (direction and magnitude of transformation) (Schumacher, 2010).

The work of the German engineer Franz Reuleaux shows a comprehensive description of typological models of mechanisms, which can convert the actuating force into different

structural expansion. The main principle behind the conceptualization of such mechanisms is the assignment of different constraints, either derived from the geometrical characteristics (i.e. dimensions in 2D and 3D) or nodal restraints (i.e. connection typology), to define the degree of freedom, motion transformation typology and direction. As a result, mechanisms are in position to rotate, slide, fold extend, swivel etc. (Khoo, Salim and Burry, 2012).

Reuleaux, also stated that a chain of elements and nodal constraints, can form more complex mechanisms and therefore different motional behaviours, otherwise called as the *kinematic chain*. Following this method, multiple new structural reactions and behaviour could be calculated and analysed (Khoo, Salim and Burry, 2012).

The framework of 'hard' mechanics has been however formed long before the 19th century. What Franz's work seemed valuable, is his effort to classify and describe in a more detailed and precise way the possibilities of kinematic machine synthesis. In the field of architecture and structural engineering, several kinematic systems have been conceptualized using the main principles already developed; each with different potential with regard to architectural applicability, system assembly, structural expansion range, or possible reconfigurable transition (Moon, 2003).

Hard mechanical systems in global scale are set in function through the process of translating and converting an input source force of specific direction and magnitude into an output motion of indifferent kinetic character. The generated motion is a result controlled both by the geometrical characteristics of the elements that describe the kinetic chain, as well as the degrees of freedom that the connection between consecutive elements is defined of. Fundamentally, this approach follows the principle of utilising rigid, high strength materials that can transmit the triggering loads effectively without causing any buckling effects. The synergic synthesis of geometrical characteristics and hinge constraints are responsible to determine the scale of the output transformation and the type of motion that mediates during the stage of transformation (Fig. 1.1).

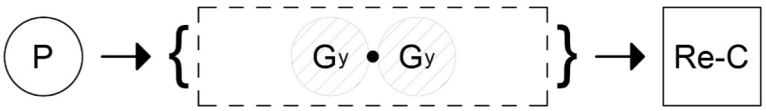

Figure 1.1 Kinetic principles for rigid elements. P: Actuation force; G: Geometry; Re-C: Reconfigured shape

In architecture, the category of typological motions is directly derived from the main principles of the hard mechanical approach. In particular, motion is a result of energy conversion from dynamic to kinetic. The movement of rigid architectural elements can be reduced down to basic types of movement such as: rotation, translation or combination of the two. The classification of movement principles presented in Fig. 1.2 demonstrates the basic syntax of respective typologies in different dimensions, which can be used to compose a more complex sequence or synergy of motion (Schumacher, 2010).

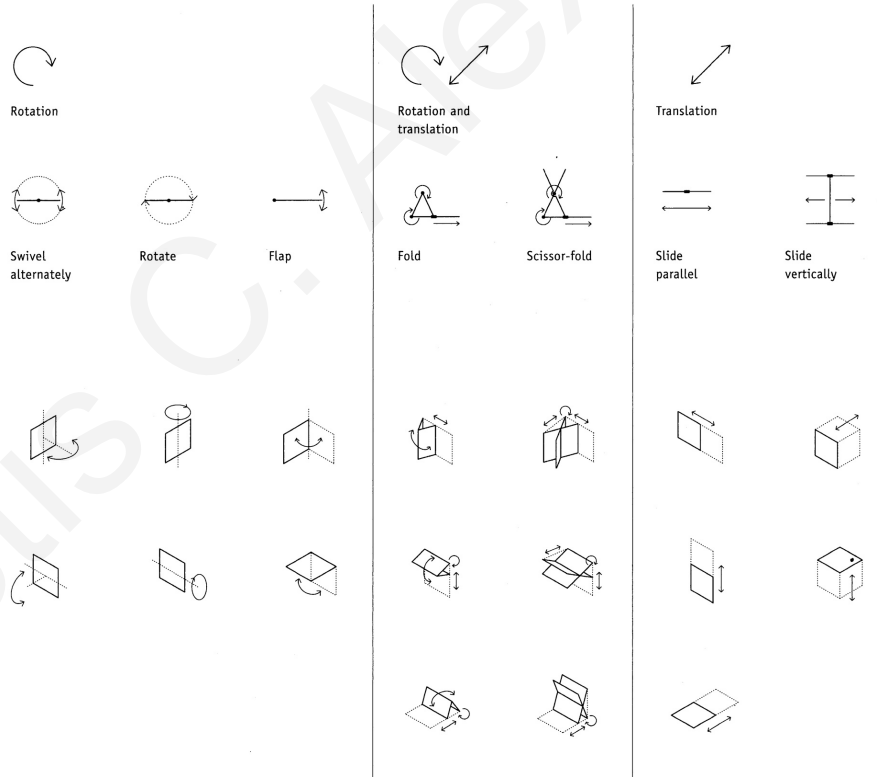

Figure 1.2 Movement principles of rigid elements (Schumacher, 2010)

According to Michael Fox, there are three kinetic typologies that one can distinguish. *Embedded, Deployable and Dynamic Kinetic Structures*. The classification is based on

possible architectural scales of application, as well as the purpose that a structure may achieve, as follows (Fox and Yeh, 2000):

- *Embedded Kinetic Structures:* Systems that exist within an architectural whole, in anchored location. They can be responsible for either human or environmental factors.

- *Deployable Kinetic Structures:* Deployable systems for temporary use. Characteristics such as mobility, lightness and transportability.

- *Dynamic Kinetic Structures:* Dynamic systems that can act independently in an architectural whole.

1.1.2 Kinetic principles in deformable elements (compliant mechanism)

Flexible architectural elements compared to rigid, hinge connected ones, utilize the material's elastic capacity in bending, stretching or buckling to generate motion, realized through the members' deformation (Fig. 1.3). Force is not directly translated into kinetic motion and displacement, instead, it is stored temporarily into the material's molecular structure (residual force) allowing an incremental distortion in the material. In particular, bending moment is not an internal effect, but rather a visual one. Within this frame, planar surfaces can form single or double curvature surfaces according to the type and magnitude of the force applied. Transformation takes place as long as the force remains active. Once the force is released, the elastic elements can regain their initial form without need of additional energy. Elastic deformation reveals a whole new way of creating motion (Fig. 1.4). The principles of soft mechanics have been primarily used so far in product design industries (Lienhard, La Magna and Knippers, 2014). The classification of these structures according to their action is as follows:

1. Surface-active (surfaces and membranes)

2. Bending-active (planar elastically deformable solids)

Figure 1.3 Kinetic Principles of Deformable Elements. P: Actuation force; G: Geometry; Re-C: Reconfigured shape

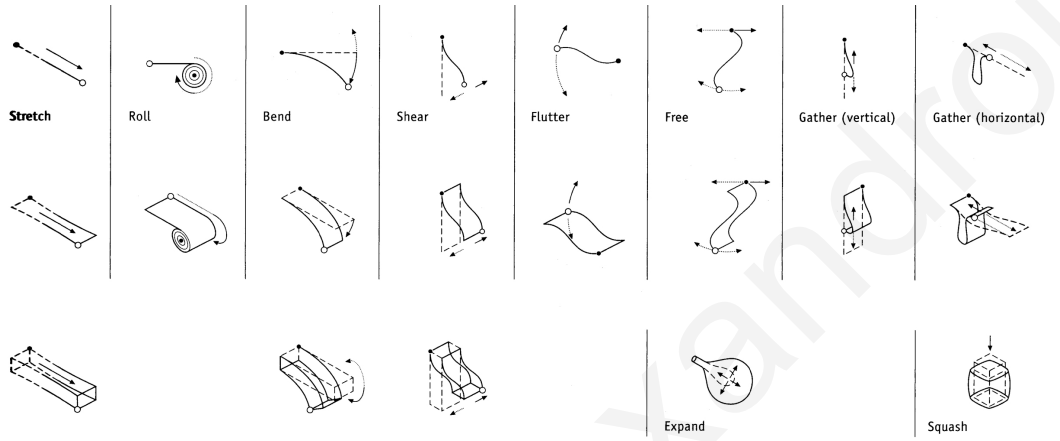

Figure 1.4 Movement Principles of Deformable Elements (Schumacher, 2010)

1.1.3 Reconfigurable structural systems

The structural synthesis of adaptive systems necessitates the overcoming of static, heavyweight and energy inefficient building components and processes (Schnädelbach, 2010). The outcome of most established structural design approaches that exist today and are able to deliver systems with characteristic capabilities to justify with demanding adaptive objectives, can be traced in the dynamic features of deployable tensegrity or pantographic structures (Escrig, 2013). These systems have been principally influenced in their development by architectural form requirements, aesthetical factors, structural optimisation criteria, performance capacity and economy (Phocas, Kontovourkis and Nicolaou, 2014). The typical rigid elements' geometrical arrangement and connectivity often play a significant role in achieving the expected structural behaviour and adequate transformation capacity (Sterk, 2003). Several further aspects of critical consideration relate to self-weight minimisation, modularity, ease of connectivity and constructability (Elkhayat, 2014).

Kinetic systems with dynamic relationships between their constituent parts were developed in recent Centuries (Schnädelbach, 2010). References of flexible structures have only been outlined on deployable systems, which had central design stimulus, ease of transportation and reassembly, capable to accelerate mobility and general adaptation needs. Today, systems that integrate motion are mostly applied as part of the second typology (deployable kinetic structures) and are mostly architectural elements.

Currently, existing structural systems with aforementioned adaptive characteristics have been industrialized following hard mechanical principles. These systems however have been criticised as brutal, complex and energy-depended solutions during assembly and reconfigurational activation respectively. In contrast to the hard mechanical apparatus undertaken so far by the construction industry, soft mechanical principles, conceptually derived from the study of natural systems behaviour patterns, have shown their potential in succeeding a vast diversity of morphological adaptation, allowing at the same time a promising outcome in terms of energy performance, stability, aesthetics and material minimisation.

1.1.4 Interdisciplinary design

Any adaptive features that reflect the final building behaviour or state, may also have a direct reflection of the design's hierarchy of criteria or building's construction processes. The notion of *adaptability* in the design of contemporary architecture is not something new. It is a notion of serious concern and matter that has troubled the architecture discourse along its theoretical and practical development, for a diversity of reasons and purposes. The question however that fully-defines *adaptability* is: being adaptive to what and in what terms?

In the past decades, adaptive attributes of form, space and structure, followed by environmental, cultural, societal, organizational, communicational, or other requirements have been examined separately, implemented in passive forms and evaluated in isolation from secondary objectives or criteria. All these isolated adaptive strategies forced

architecture to ramify its focus into singular case studies, orienting attention into gathering explicit information and developing knowledge and tools for object-specific tasks. This one-fold tactic has led to the pop-up of multiple relevant courses that provide design guidance to discrete design methodologies, often referred as *bottom-up approaches*. Today contemporary design acknowledges the fact that architecture is part of other disciplines and number of distinct modes of research to be further nonlinear and interdisciplinary (Phocas, 2015).

Bioclimatic, environmental, kinetic design and sustainability are some of the indicating courses of individual developments carried out and brought to architecture from relevant fields. Those courses are responsible to provide design guidance and strategic plans, to consolidate a more advanced and efficient design outcome with regard to particular adaptation objectives. Part of the investigated knowledge includes favourable geometrical vocabularies, material properties knowledge, fabrication and construction techniques and compatible structural system knowledge for different purposes and logics mainly adopted from engineering, biology or other adjacent fields (Hensel, 2013).

In static adaptive forms, stimuli such as contextual adaptation, structural performance optimization and aesthetical adaptation, triggered the need for an architecture that can reach complex and organic forms for the design of space, minimizing at the same time the constraining parameters that planar shapes cause to the design. This gave ground to architecture to make its first step into *free-form* shapes. Construction logics, fabrication techniques and assembly logics borrowed from automotive and aerospace industries, contributed positively for this shift to happen. Computerized data and visualization tools, originally developed in film and computer graphics industries have been integrated to architectural design, either for organizing early design decision thoughts, or used for structural optimization processes during the finalization of the design product. Having as common aim the improvement of performance in adaptation purposes, all negotiated disciplines have formed a new relationship and made a great step towards an *interdisciplinary design* approach in the early 90s.

Adaptive architectural design development has also been the triggering agent for many architects and structural engineers to search for adaptive systems in terms of shape, aesthetics, geometry and structural behaviour; systems, which emerge from processes that follow principle lows of nature. For instance, the use of environmental forces acting as driver for discarding any unreasoned material and therefore, approaching more fluid forms like the ones found in natural surroundings. Martijn Veltkamp in his thesis on *free-form structural design*, examines a vast amount of existing construction techniques and structural systems potentials on establishing a truly sustainable (material efficient) and formal-free construction and design approach. The conclusion of his work covers many possible ways on reaching a well-defined, optimized construction strategy, however, he mentions that there is still more to be expected. Building construction experienced certain changes, because the disciplines involved in the technical realization of such building designs prefer to deal more with digitalizing methods of working, instead of establishing a more vital interdisciplinary support (Veltkamp, 2007). Veltkamp's suggests the use of more science and interaction of scientific fields as means for making architecture construction more efficient and effective.

1.1.5 Performance-based design

The parameters responsible for a building's performance can be set to multiple, in order to achieve a higher level of adaptation, however, all these parameters cannot be treated equally. It is helpful to separate and categorize the parameters into sub-sets and define a hierarchy between them, in order to achieve balanced design actions and processes. In addition to that, the most essential part that characterizes the parametric sets, responsible for a performance-based design outcome, is the type of the parameters considered. There are aspects of design that can be considered as quantifiable and can be measured in numbers, shaped under geometrical constraints, or maintained under a particular domain. In the area of structural engineering, these parameters could be referred to with either forces, weights, moment, cost, or deformation. If the design aspects could only be conceived as of qualitative content, they cannot be understood or calculated using this

method. In this respect, recent developments focus on methods to convert quantitative aspects into quantifiable objects. Such numerical progress in essential for the computer to be able to calculate and translate these values into meaningful and helpful information for the design (Woodbury, 2010).

Adaptive architectural interventions entail a composite and multidimensional design approach, since the physical outcome includes multiple parameters of consideration. In this mode, the designer must think simultaneously at a vast amount of critical aspects that constitute the adaptive behaviour of the structure, its performative efficiency and the overall aesthetical aspect. In order to do so, multiple tools and principles must apply to the design strategy, in order to both, guide the designer to the correct decisions and verify the choices that have been applied so far (Ahlquist *et al.*, 2014).

1.1.6 Form-finding

The development of user-friendly modelling interfaces signalled and encouraged the search of adaptive free-form architecture. These concerns however, gave opportunities for architecture and structural engineering to intersect and to provoke a true search into natural systems, not only as static monolithic forms, but more importantly in terms of their structural aspects, force distribution and scale. All these numerous practical problems, forced alternative structural solutions to come to force, making the search for adaptive systems more interesting and innovative. This approach also contributed to the simplification of already known structures, using the logics of nature and therefore removing any unsound properties, processes or ornamenting elements in the design of architectural structures (Hensel, Menges and Weinstock, 2013).

Such logics include minimization of structural self-weight, and follow form patterns that are more familiar with shapes formed out of natural processes. Examples from natural systems, organisms and life in general has always been a primary inspiration area for architects, in search for logic and appropriateness of form in design of buildings (Olsson, 2012). Pioneer architects and structural engineers, Frei Otto, Felix Candela, Edmund

Happold, Heinz Isler and Horst Borger followed and demonstrated multiple approaches that can treat architecture with a more natural performative way, provoking a truly adaptive character of the overall structural form. This development took place during the 50s until 90s, where *free-form* architecture was determined by form-finding methods and techniques (Adriaenssens *et al.*, 2014).

During the shift of the 90s and the significant development of software tools, as well as computing speed and capacity of computers, form-finding approaches are further conducted through *performance-oriented and -based* design approaches (Hensel, 2013). Such approaches adhere the logic developed during the previous Century. Nowadays, such design approaches are supported with simulation tools and computational design thinking. This realisation implies an urge to enhance some aspects of performance in the design using the rapid calculation power of computers (Menges and Ahlquist, 2011). By extent, the term form-found is not an absolute designation to the structure's material characteristics, but rather derives from a broader directory of design parameters of different sort that can generate a unique morphological result according to the hierarchy or magnitude of importance factor of the selected aspects.

1.2 Motivation and Aims

The design of adaptive structures towards embracing attributes of multi-performance characteristics and coinciding trajectories with both architectural and structural objectives is a complex task. In principle, the primary factors that lead research into innovative investigation paths of unique system designs or approaches, include focused considerations of minimal material use, modularity, connectivity and constructability. In literature, lightweight adaptive systems such as those with reconfigurable characteristics or moment-free component configurations, mainly used for temporary shelters or roof structures, comprise a good source of information on dealing with these issues.

Although existing transformable systems have verified their multimodal capabilities to adapt and provide adequate flexibility in terms of modular and overall morphological

adaptation, the initialising platform of the hard mechanical approach, whose principal design guidelines have been actually articulated since the early 19th Century, seems to be a limiting parameter in view of extensive advancements and future innovation (Moon, 2003). In the majority of implemented examples, the resultant system reconfigurations are limited between a 'closed' and an 'open' state, or realised through integration of 'locking' techniques and mechanisms, for achieving an increase of the number of obtainable configurations. In cases where unique adaptive behaviour is aimed at, with attributes of optimised kinetic adaptation and increased cohesiveness in structural control, the systems rely on embedded computation and mechanical actuators (Sterk, 2003; Kontovourkis, Phocas and Tryfonos, 2013). Such mechanisms often lead to an energy inefficient and complex kinetic behaviour (Phocas, Christoforou and Matheou, 2015).

The recently developed framework of bending-active system design has made significant contribution and generated new potentials in the field of adaptive architecture. The alternative material utilisation enables a far more morphologically-free and connectivity-less design outcome that can induce a new prospect era of ideas and innovation. Although this design approach is not new, contemporary means of analysis and simulation can accelerate the calculation phase, increase the accuracy and enable a much easier experimentation process in dealing with it.

Along these lines, the aim of this thesis is to suggest alternative lightweight hybrid structures based on the use of elastically deformable members and linear tension elements. The hybrid synthesis of elastic members with tension-only elements may achieve post-assembled systems with optimised structural performance, whereas the tension-only element takes the role of actuation for the fastening and erection process, as well as the prestress and load-deformation control of the system. The compatibility of the components hybridisation derives from the necessity of the elastic members to rest in static equilibrium, or to succeed in a wider domain of geometrical adjustments. The form-found and load-deformation behaviour of the single-segment configurations aims to follow a numerical Finite Element analysis (FEA) of increased preciseness, taking into account

geometrical nonlinearities and large system displacements that take place during all transformation stages.

1.3 Literature Review

The literature review is divided into two areas of focus, and covers critical aspects that can provide insight towards a bending-active and tension-active system hybridisation (Fig. 1.5). It aims at providing discrete information towards creating systems with adaptive characteristics, as described further in this chapter.

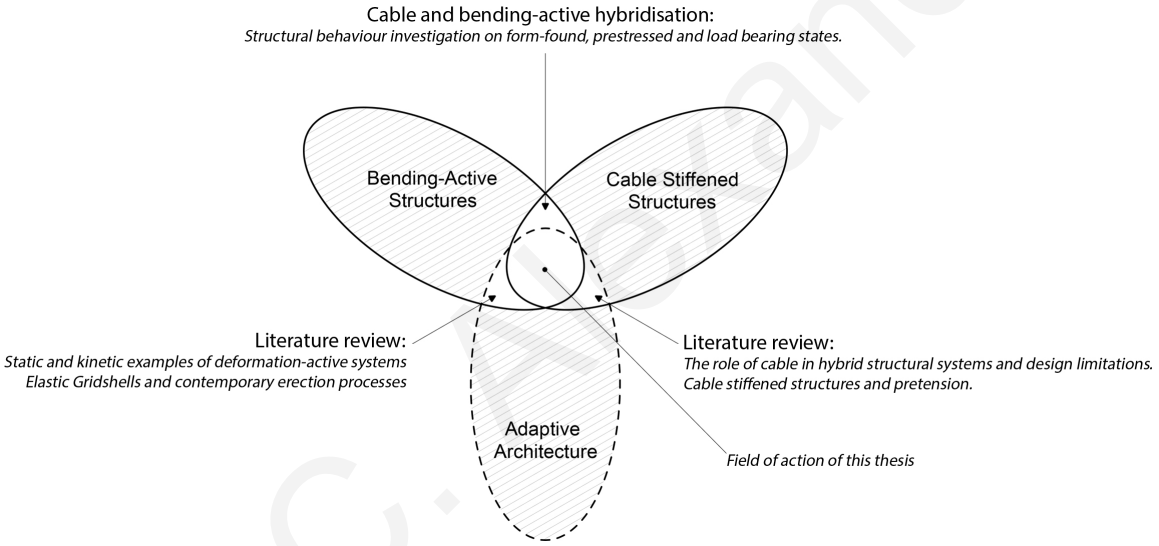

Figure 1.5 Present thesis overview diagram

In a preliminary phase, the research will review existing examples of bending-active systems of both passive and active adaptive behaviour, within a broader area of actual and experimental applications. The examined systems will be classified as to their initially configured state (assembly), also related to the elastic member's initial shape and proportions. Consequently, general remarks with regard to their efficiency and applicability will be made. This also includes reviews on different form-finding techniques and mechanical aspects of consideration. In a second phase, the role of cables in lightweight structures will be introduced, for examining their compatibility and possible operation with bending-active members. The general outcomes from these two phases of research

reviews will foster the case studies analysis objectives, with regard to a series of proposed cable bending-active structural single-segment configurations and multible segments systems.

1.4 Research Summary and Contribution

This research will run through a preliminary literature review on soft lightweight static and transformable structures, their historical and architectural context of development, Chapter 2. The hybridisation of bending-active and tension-only elements will be examined through existing examples of hybrid structures, Chapter 3. In a further stage, a set of both single, simply-paired and paired-interconnected, hybrid cable bending-active configurations (structural single-segment configurations) will be proposed and analysed, Chapter 4 and 5. The form-finding of the single-segment configurations follows a FEA with custom programming technique to enable accuracy in the calculations, due to the nonlinear geometrical effects of the systems, as well as a progressional multi-stage static analysis, also necessary in reaching the final form-found shape (SOFiSTiK Structural Desktop and text editor Teddy). Cable elements take the role of active components responsible to regulate their length and therefore readjust the bending radii of the elastic members. The residual stresses that are stored inside the elastic members are absorbed by the cable elements allowing an adequate stabilization of the systems during any inactive mode. The results obtained are focused on identifying the nonlinearities of the structural deformations, the interdependencies between the involved structural components, as well as the performative static and dynamic domains of action. The results will be used to provide feedback in the further development of the structural systems through linear repetition of the structural single-segment configurations, which are proposed in the last two Chapters 6 and 7 of the present thesis.

The present research aim is to contribute to the formulation of a design methodology that can handle such complex, multi-stage form-finding design processes. The dual combination of the systems proposed brings innovation in self-reconfigurable structures

and generates operative and efficient adaptive behaviour, due to their high elastic and strength properties and their hybrid composition.

The contribution of the proposed research refers to the following aspects:

1. Application of interdisciplinary design methodology for form-finding and analysis of lightweight bending-active structures.

2. Classification of load-deformation behaviour of bending-active members according to different structural typologies implemented.

3. Apprehension of cable compatibility with bending-active members in hybrid elastically deformable systems, both in terms of delivering optimum structural behaviour and actuating the system into different configured states.

4. Development of hybrid cable bending-active systems, whereas the cable element actuates reconfigurations and controls the load-deformation behaviour of the system.

5. Development of FEA simulation techniques of cable bending-active systems, whereas the analysis process considers fastening, erection, prestress and loading of the members as well as the residual stresses of the elastic members developed from the initial non-deformed state of the system.

6. Development of step-by-step form-finding analysis strategies for complex hybrid systems of procedural stepwise assembly processes.

7. Identification of favourable aspects in dealing with the design of coupled interconnected hybrid cable bending-active systems.

CHAPTER 2 **BENDING-ACTIVE STRUCTURES**

In search for alternative approaches towards structural flexibility, improved elasticity, higher controllability and minor energy dependent design solutions, recent research activities have focused on applications of soft, pliable materials, characterised by their passive elastic properties (Deleuran, Tamke and Thomsen, 2011). In principle, the soft mechanical approach is based on the utilisation of the materials' mechanical properties, in particular those of low elastic modulus, E, and high strength, σ_{Rd}, to enable physical actions of increased transformational accuracy acquired by the members' elastic deformability (Kotelnikova-Weiler et al., 2013). The overall system complexity can be minimised by replacing numerous consecutively joined segments with a single elastic, i.e. bending-active member, providing thus a wider spectrum of single- or multi-curvature configurations (Adriaenssens and Barnes, 2001; Lienhard and Knippers, 2013; Phocas, Kontovourkis and Alexandrou, 2013). Bending-active members may autonomously sustain a variety of form-found shapes during their prestressed state and undergo further natural configurational transitions, excluding at the same time the need for supplementary external energy provision. Thus, the structural design task concentrates on the search for ideal slenderness for active deformation of the actual bending-active systems, initially composed of straight, planar elastic members of respective section dimensions, and the actuation member. In comparison to section or vector-active actions, whereas inner stresses developed in the members should not exceed the section's maximum load-bearing capacity, form-active actions are designated to systems, where the acting load or pressure can be expressed visually on the structural members' own shape distortion (Lienhard and Knippers, 2013). These actions also result to a members' stiffness increase.

In architecture, the morphological exploration and investigation of lightweight adaptive structures, while using active deformation as a consolidating design agent, has raised a new challenge for the role of representation and prototyping, with most recent examples

following an analytical and dynamic-based approach (Nicholas and Tamke, 2013).This has been fairly characterised as an approach instead of being classified and treated as a separate structural system or action (Lienhard, 2014). Critical aspect that drove to this designation lies on the progressional form-finding phase that necessitates the assembly process and precedes the final form emergence.

2.1 Historical Development

Precedent examples of lightweight structures that utilize their members' high capacity in bending, can be found in strained gridshells and plydome pavilions (Adriaenssens *et al.*, 2014). These types of structures are formed through controlled, externally induced deformation to individual members or global system assemblage (Lienhard, Alpermann, *et al.*, 2013). In a successive post-formed state, the structures are stabilized and stiffenced thought additional deformation manipulation or secondary members superposition. In the case of strained gridshells, a series of identical straight members is used to construct a planar lattice surface, purposely bent, to generate a three-dimensional curvilinear deformed geometry (Liddell, 2015). At post-formed stage, the strained shell structure is anchored to the ground and stiffened though diagonal bracing or a prestressed interconnecting cable network (Quinn and Gengnagel, 2014) (Fig. 2.1(a) – Table 2.1). In a similar manner, a plydome structure is constructed from identical slender plates, partially fastened together to obtain a global polyhedral shape (Fig. 2.1(b) – Table 2.2). The amount of the overlapping area between two adjacent plates defines the degree of the members self-induced single curvature tilting (Schleicher *et al.*, 2015).

The significance of these implemented structures lies within the design and construction principles adopted, enabling the production of a complete structural system characterized with modularity, low self-weight, ease in constructability and diversity in form configurability (Lienhard, 2014). Design-wise, the form-finding process of a bending-active structure may result into a global three-dimensional shell shape formation, similar to synclastic curvature. Compared to conventional frame structures, shell structures have a more efficient form in terms of the system's structural capacity, and therefore contribute

highly towards limitation of material overuse. Construction-wise, the utilization of members high capacity in bending enables the creation of self-generated organic shapes, providing in this respect a qualified substitute of cold-formed members. This results into reduction of the fabrication energy and cost. Construction expenses are further shrinked when comparing the transportation ease achieved over conventional prefabricated free-form assemblies. By extent, ease in constructability can also be achieved by following modular design principles. In strained gridshells with high level of modularity, the use of universal joint connections simplifies the construction stages and maintains the projects economy within a lower balance (Harris *et al.*, 2003).

All these beneficial construction and design advances granted over conventional structures come at a cost when dealing with the construction duration. In the case of strained gridshells, the active formation process (erection) necessitates the use of external infrastructural support or mechanical actuators for pulling, pushing or lifting the structure into the desired position. The erection process of the Mannheim Multihalle gridshell for example, was performed using a series of forklifts and scaffolding units, for gradual pushing and supporting the structure's upwards bending (Adriaenssens *et al.*, 2014). In the example of the Weald and Downland Museum gridshell, the non-deformed planarly assembled lattice structure was elevated at a higher level, left to gravity, and further weighted at the edges for it to be pulled towards the ground level to form a doubly curved shell. Alternative erection suggests the use of mobile crane and light auxiliary columns, practically applied for the erection of the Essen Pavilion. Some of the most frequently applied erection and forming approaches are also known as ''pull up'', ''push up'' and ''ease down'' (Quinn and Gengnagel, 2014). Despite the diversity of applicable techniques, almost every major gridshell project suffered from increased construction energy and excessive erection duration. In addition, most of the erection approaches induce point load or high, full-span compression forces to the constituent members causing the structure to experience breakages, due to exceeded levels of concentrated stresses. Although modern examples have reduced the amount of breakage failures through use of modern machinery and tools,

this issue remains an important aspect of consideration when dealing with the construction of bending-active structures (Liuti, 2016).

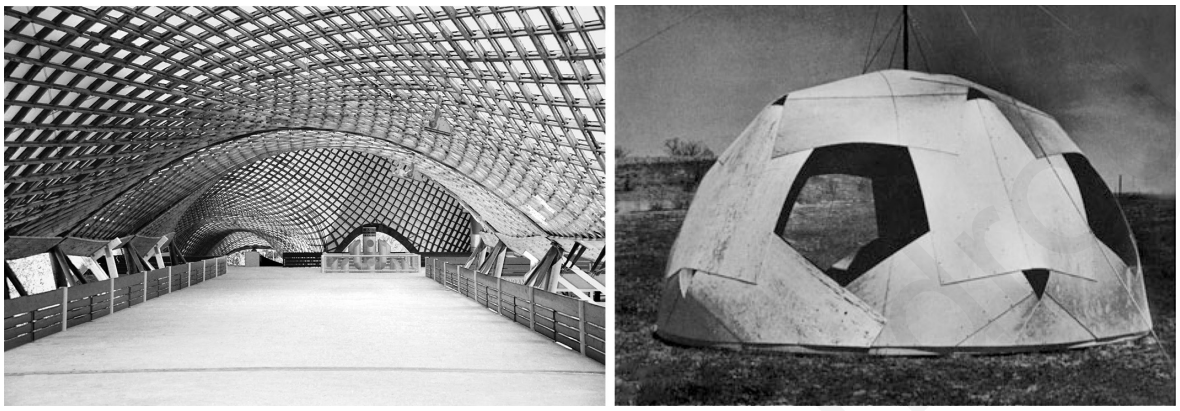

(a) (b)

Figure 2.1 (a) Gridshell: Mannheim Multihalle, Germany, 1975, by Frei Otto; (b) Geodesic plydome: Des Moines, Iowa, 1957, by Buckminster Fuller (Adriaenssens *et al.*, 2014; Schleicher *et al.*, 2015)

Table 2.1 Manheim Pavilion Project

Project	Mannheim Pavilion, Germany
Year	1973
Form - Geometry	Synclastic shell shape
Construction	
Material	Nonlinear Elastic (Western Hemlock Timber 50 x 50 mm)
Manufacturing	Industrial product of identical properties and dimensions - Continuous length timber laths of up to 6 m, finger joined together to form longer members of approximately 30 to 40 m.
Fabrication	Regular grid. Four layers of timber laths pin connected at each 0.5 m, with shear block between the layers at vertical distance of 50 mm.
Duration	1973 - 75
Post erection stiffening	Twin 6 mm cable diagonal bracing at every 6^{th} node
Assembly	
No. of elements	-
Scale	60 x 60 m span
No. of constr. stages	3 - planar assembly, erection and post-stiffening using cable bracing and fixing of the lattice nodes.
Assembling tools	Human resources for assembling the planar lattice structure and cladding the roof.
Form-finding calculations	Hanging chain model technique and simplified computer generated mathematical model.
Boundary conditions	Four different boundary types: arches, concrete, laminated timber beams and cable boundaries, with concrete being the most often used.
Erection	'Push up' using scaffolding jacking towers.
Forming Process	Double axis bending
Application	
Architectural	Exhibition space - "a light, airy construction to harmonize with the landscape of flowers, trees and artificial hills".
Structural	Lightweight strained Gridshell - funicular and distributed loading scenarios.

Table 2.2 Des Moines geosedic plydome Project

Project	Buckminster Fuller's geodesic plydome in Des Moines, Iowa
Year	1957
Form - Geometry	Synclastic shell shape - Spherical
Construction	
Material	Nonlinear Elastic (marine plywood 6.4 mm)
Manufacturing	Industrial product of identical properties and dimensions
Fabrication	Perforations at sheets tangent to ground and near the corners of the sheets so that the sheets will be fastened together both in the areas of the grid lines.
Duration	Unknown
Post erection stiffening	Secondary system of single strut with diagonal cable bracing
Assembly	
No. of elements	± 16 parts
Scale	7.3 m span
No. of constr. stages	-
Assembling tools	Human resources for placing and tilting of the elastic plates – According to Fuller, it would also be feasible to use adhesive means to for holding the sheets together in the proper geodesic alignment.
Form-finding calculations	Overall structure was constructed purely out of experimentation and estimation of its deformed geometrical morphology
Boundary conditions	Point supports – peripheral support
Forming Process	Single axis bending
Application	
Architectural	Temporary / Ephemeral use
Structural	Lightweight Self-strutted Geodesic structure – Uniform stressing of all sheets

The design of actively deformable structural components has traces from more recent decades. Kinetic structures, which rely on bending principles have been firstly developed in parallel fields of architecture, such as mechanical engineering (product design), aircraft industries and robotics. Inspiration for the design of such systems is mainly derived out of natural systems classified as bio-inspired systems. Recent developments in architecture can be observed in the work by the Institute of Computational Design and the institute of Building Structures and Structural Design of the University of Stuttgart with the development of active-bending structures and respective techniques applied (Menges, 2012). CITA (Centre for Information Technology and Architecture) of the Royal Danish Academy of Fine Arts has also undertaken several approaches in using the material's mechanical characteristics as an active agent for the design conuction of responsive skins and facades (Fig. 2.2) (Deleuran, Tamke and Thomsen, 2011).

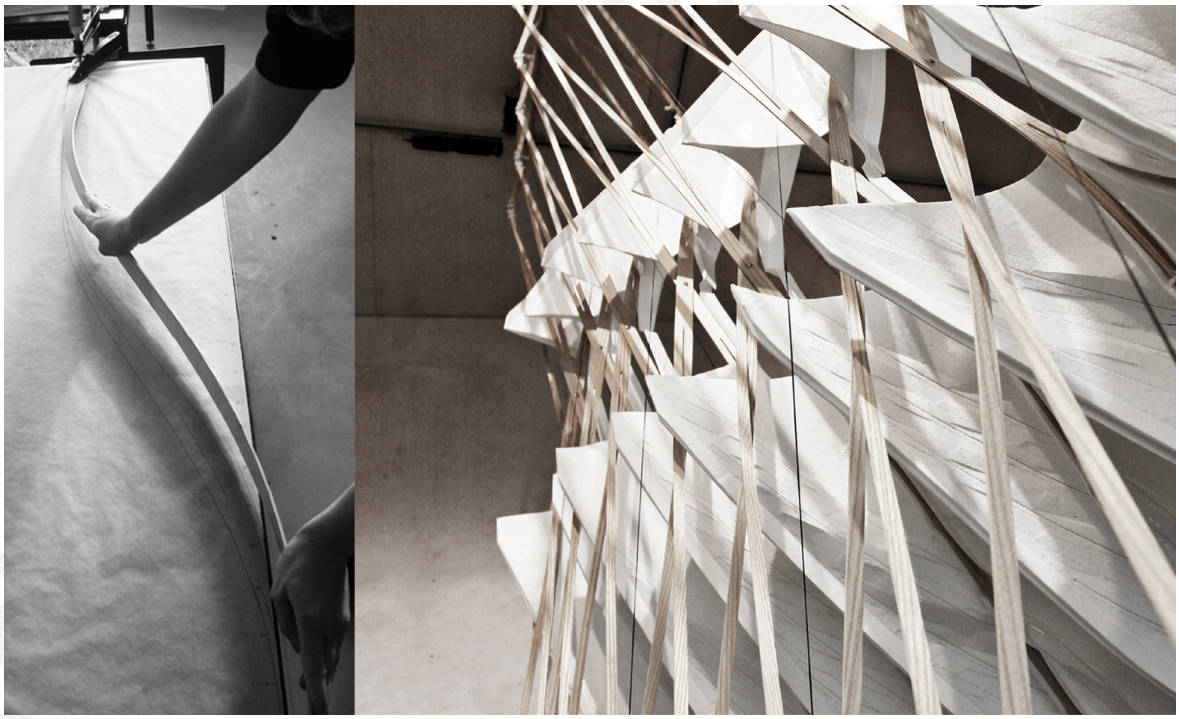

(a) (b)

Figure 2.2 Shading Device: CITA – Thaw Architectural Installation, Copenhagen, Denmark, 2010. (a) Physical material deformation measurement, (b) Actual model (Nicholas and Tamke, 2013)

2.2 Implementation of Bending-Active Systems

The applicability of bending-active members in structural or other purpose form design products triggers a new horizon of research and investigation on making architecture. To begin with, bending-active systems may follow two main categories according to their final behaviour: (a) Static bending-active (passive post-buckling behaviour) and (b) kinetic/transformable bending-active (active post-buckling behaviour). On the one hand, elastic members can simply be used to deliver predefined deformed shapes of prestressed inner state condition. On the other hand, active deformation can alternatively be utilised to deliver real-time deformation-based transformation to enable the kinematics of the system. Both categories can obtain principle designations according to their initially configured state (assembly), or the member's initial shape and proportions. In this respect, taking into account a representative number of existing research and implemented examples, the classification of bending-active systems may refer to the following three main categories: (i) elastic gridshell structures, (ii) elastic plate space structures, and (ii) elastic rod space structures (Fig. 2.3). These may further address supplementary descriptions or determinations according to connectivity methods, configuration aspects or global output shapes.

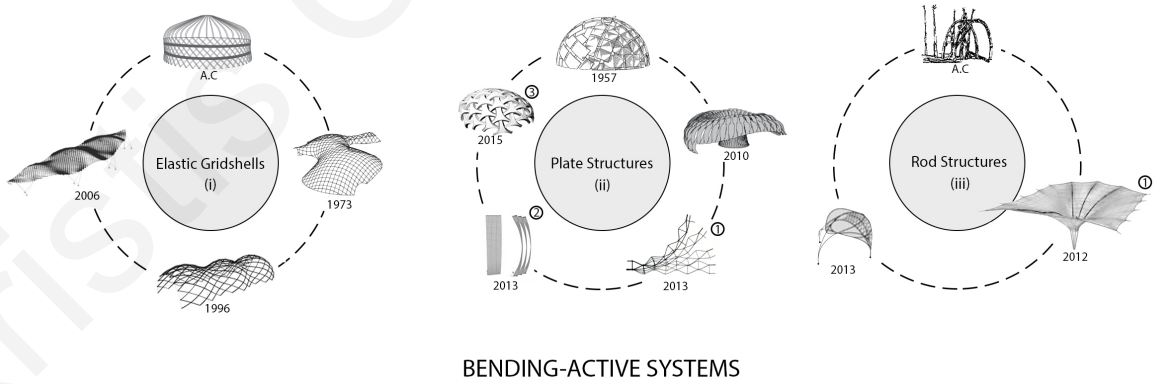

Figure 2.3 Bending-active systems classification; (i) Elastic gridshells; (ii) Plate structures; (iii) Rod structures; (1) Active adaptive installations; (2) Active adaptive skins; (3) Kit of parts

i. Elastic or 'strained' gridshells. Structures made of slender continuous length beams, planarly assembled in regular or irregular grid configuration. The final shell-like shape is achieved through the principle of active bending (Quinn and Gengnagel, 2014).

ii. Elastic plate space structures. Structures made of beam members, whose planar dimensions are substantially higher compared to their thickness. These are often rectangular, square or irregular plates or stripes. Elastic plate structures achieve their final deformed shape by using coupling techniques (interconnection fastenings) of a pair or multiple bending plates, or modification of boundary support conditions. These techniques allow the overall structure to reach a self-stressed equilibrium state without the need of additional elements.

iii. Elastic rod space structures. These structural assemblies are of similar characteristics to the previous category (ii), instead, the slender plate elements are replaced with elastic rods. These structures enable a free morphogenetic approach in their design due to the members' multi-directional bending ability.

2.3 Architecture Examples

2.3.1 Elastic gridshells

Elastic gridshell design is a complex form of structural synthesis and incorporates a large number of parameters that deal with its construction and are of vital importance, in order to reach a successful outcome. Optimisation potentials of these complex but elegant structural schemes focus mainly on topology, geometrical and mechanical characteristics of the members and boundary support conditions. This category does not entail any transformable (active adaptive) examples, since it results into a much complex design effort and cost on the process of sustaining both, structural stability and morphological adaptation purposes.

The gridshell **Weald and Downland** open air Museum in Singleton, United Kingdom, comprises one of the fundamental examples of regular gridshells. It provides a double curved spatial shape controlled by a variety of parameters, including curvilinear support arrangement and degrees of freedom of its inner nodes (timber lath connections). It is worth noting that the shape of the structure was re-evaluated and regenerated to encompass a structurally optimised outcome, in particular as to the shell's resistance to shear (Harris *et al.*, 2003). The shell is initially configured in planar form as a network of two layers of 50 x 35 mm timber laths running in two directions and placed on scaffolding support on an average mid-height level of the estimated form-found shape's height. Despite the structure's initial deformation caused by its self-weight, an additional pulling force was needed to connect the paired laths endpoint to the ground supports (Fig. 2.4 – Table 2.3) During the 'pull-down' erection process the grid-lath joints were subjected to scissoring and sliding and were auto-adjusted to the stress conditions produced from the overall pulling process. Once the form-found shape was obtained, all grid nodes were reinforced with bracings to minimise post-buckling and prevent post-scissoring effects. This also enabled the activation of both layers of the lath pair for external loading scenarios.

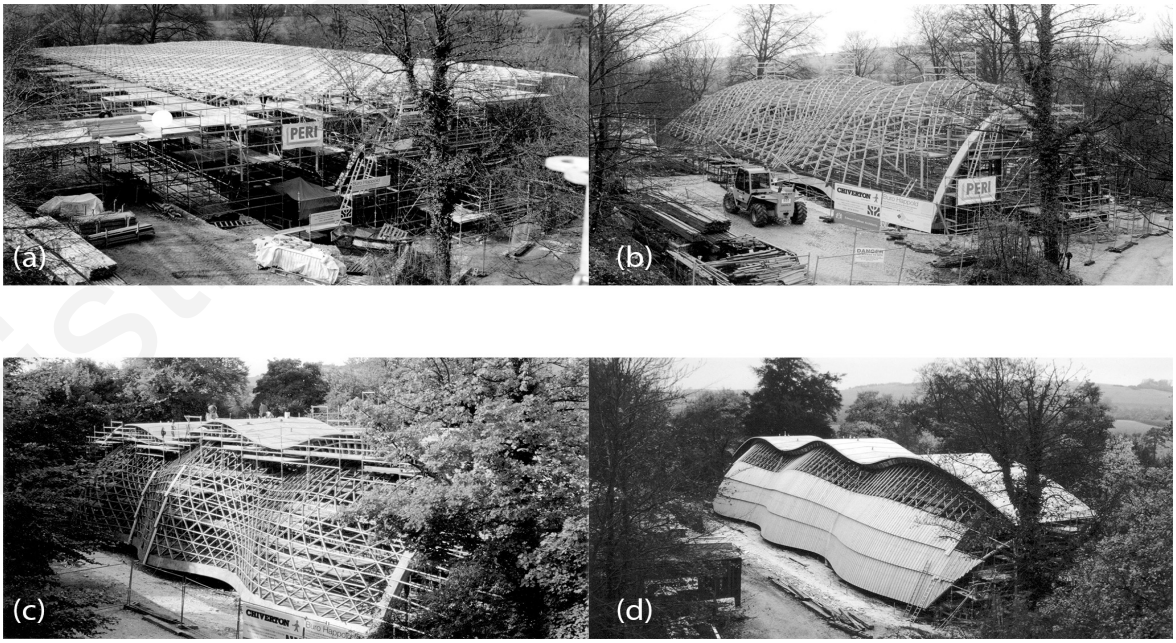

Figure 2.4 Gridshell Weald and Downland Open Air Museum (Singleton, UK); erection stages (a) – (d); Architect: Edward Cullinan Architects; Structural engineer: BuroHappold (Harris *et al.*, 2003)

Table 2.3 Weald and Download gridshell Project

Project	Weald and Downland Open Air Museum, Singleton, UK
Year	2002
Form - Geometry	Anticlastic shell shape
Construction	
Material	Nonlinear Elastic (Oak Timber 50 x 35 mm)
Manufacturing	Industrial product of identical properties and dimensions - Continuous length timber laths of up to 6 m, finger joined together to form longer members of 50 m.
Fabrication	Regular grid. Four layers of timber laths pin connected at each 1 & 0.5 m, with shear block between the layers at vertical distance of 35 mm.
Duration	---
Post erection stiffening	Installation of a ‘’fifth layer’’ lath
Assembly	
No. of elements	-
Scale	50 x 16 m span 9.5 m tall
No. of constr. stages	4 - raised planar assembly on scaffoldings, erection, post-stiffening using ‘’fifth layer’’ of laths and roof cladding.
Assembling tools	Human resources for assembling the planar lattice structure and cladding the roof
Form-finding calculations	Dynamic relaxation
Boundary conditions	All peripheral nodes have been fixed to ground deck
Erection	‘’ease down’’ using scaffolding to raise the structure and prop jacks pull it downwards.
Forming Process	Double axis bending
Application	
Architectural	Museum space. Culture & Leisure
Structural	Lightweight strained Gridshell - funicular and distributed loading scenarios

The next example consists of a more recent implementation and practice on elastic gridshells. The **Saville Garden Gridshell** is the roof structure of the visitor's centre of the Royal Landscape Park in Windson, United Kingdom. The roof's longitudinal span counts to 98 m with varying width dimensions, reaching a maximum of 25 m. The vertical depth of the shell structure fluctuates between 4.5 and 8,.5 m. The grid is made of continuous length, double-layer timber laths (35 Km in total length) of 80 x 120 mm in section, connected via small timber blocks of 20 x 120 x 300 mm. The strained gridshell is locked in its final prestressed state through a perimetrical steel tube (Fig. 2.5 – Table 2.4). Compared to the previously examined project, the current one was not erected following a global planar deformation. Instead, the model was analysed and the prototype tested using contemporary simulation means to accurately calculate the length of each timber stripe and therefore minimise the need of any on-site adjustments. Using this technique, the construction relied on manoeuvring each single lath into position. Following this, the laths were strewed together sequentially. This technique has also minimised the risk of crack or breakage. To enhance the diagonal stiffness of the shell, continuous sheeting was used as top-level layering of the structure, which also serves as a roof cover (Toussaint, 2007).

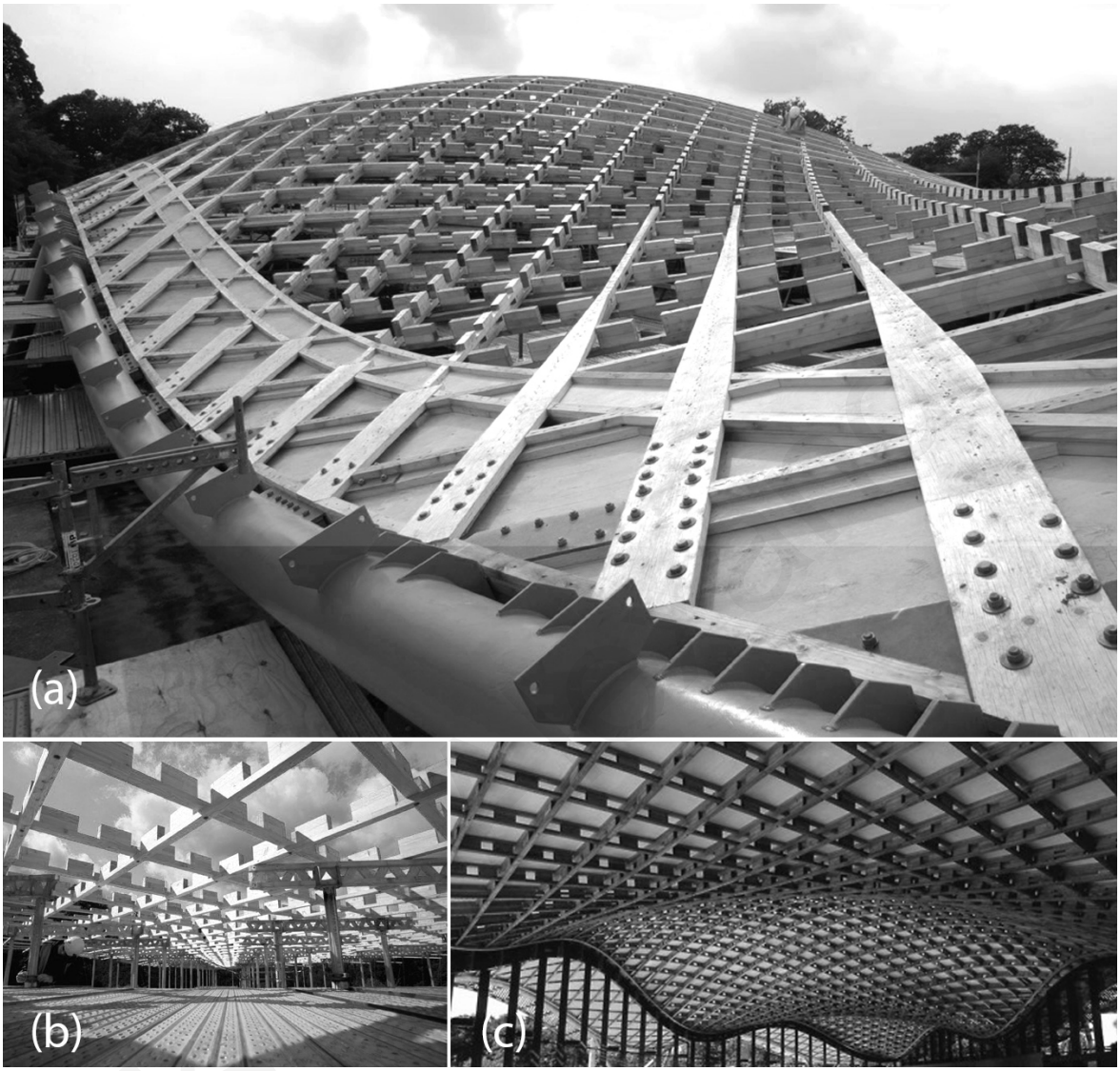

Figure 2.5 Savill Garden Gridshell, Windson, U.K., 2006; Architect: Glenn Howells Architects; Structural engineer: BuroHappold (Harris and Roynon, 2008)

Table 2.4 Savill Garden gridshell Project

Project	Savill Garden Gridshell, Windson, U.K.
Year	2006
Form - Geometry	Anticlastic shell shape – Sinusoidal wave
Construction	
Material	Nonlinear Elastic (Lark Timber 80 x 50 mm)
Manufacturing	Industrial product of identical properties and dimensions - Continuous length timber laths of up to 6 m, finger joined together to form longer members of 35 m.
Fabrication	Regular grid. Four layers of timber laths pin connected at each 1 m, with shear block between the layers at vertical distance of 120 mm.
Duration	---
Post erection stiffening	Ridge braces
Assembly	
No. of elements	Up to 1000 timber laths
Scale	28 x 98 m span 4.5 – 8.5 m height
No. of constr. stages	4 - raised planar assembly on scaffoldings, erection, post-stiffening using ‘’fifth layer’’ of laths and roof cladding.
Assembling tools	Human resources for assembling the planar lattice structure and cladding the roof
Form-finding calculations	Physical and computational form-finding
Boundary conditions	All laths have been anchored to steel roof boundary structure
Erection	‘’ease down’’ lowered down with special scaffolding
Forming Process	Single axis bending
Application	
Architectural	Museum space. Culture & Leisure
Structural	Lightweight strained Gridshell - funicular and distributed loading scenarios

2.3.2 Elastic plate space structures

The structural design examples of elastic plate structures are limited to a small number of research or experimental cases, since this field does not have any prolonged practice. However, the amount of related research and projects currently under development shows constant increase, due to the applicability and the free-form design potentials that emerge from this approach. The design approach has been supported by recent technological advancements in multiple sciences and the intersection of new knowledge within the field of architecture. As already stated, computational design, performance-based design methodologies and easy to use material performance simulation tools are three of the most critical factors that led to a research interest increase in this area of study. By extent, the applicability of these structures except from being utilised to create lightweight, free-form designs, also exhibits high potential in creating active adaptive systems, mainly used as building skins or envelops to control environmental or other architectural purposes.

The work of the **ICD/ITKE pavilion** (Fig. 2.6 – Table 2.5), stands out as an iconic example of pure active-bending elements' utilisation for the construction of a lightweight structural system. The prototype Pavilion reflects the fabrication and construction principles followed in Mannheim Multihalle in the category of static structures. However, the depth of complexity with regard to the design process and construction detailing applied is much higher. The structure is composed of 500 planar plywood stripes, which are paired in groups of two longitudinal stripes that form an inversely bent assembly. This combination allowed the stored energy between consecutive member pairs to neutralise and therefore bring them to force an equilibrium state. At global scale, all bending-active members are digitally fabricated with uniqueness in geometry, as determined by the force distribution for the coupling stripes configurations. The overall structure has a torus-like shape and serves as a temporary pavilion. The purpose of the final outcome is to demonstrate how thin elements of elastically deformable characteristics can form an overall system that can sustain a structural rigidity for its scale and purpose, maintaining at the same time the benefits of a highly lightweight construction (Menges, 2012).

Figure 2.6 ICD/ITKE Research Pavilion, Stuttgart, Germany, 2010 (Lienhard, 2014)

Table 2.5 ICD/ITKE Research Pavilion 2010 Project

Project	ICD/ITKE Research Pavilion, Stuttgart, Germany
Year	2010
Form - Geometry	Monoclastic shell shape – Torus like global shape
Construction	
Material	Nonlinear Elastic (Birch Plywood Timber stripes 6.5 mm thick)
Manufacturing	Industrial product of identical properties and dimensions – Stripes are robotically fabricated as planar elements.
Fabrication	Radial arrangement and interconnection coupling of the stripes to form arch system of 4 m span.
Duration	1 week
Post erection stiffening	None
Assembly	
No. of elements	Up to 500 geometrically unique timber stripes
Scale	10 x 10 m span 2.14 - 3.37 m height
No. of constr. stages	2 – Parts assembly and global structure construction
Assembling tools	Human resources for assembling the planar stripes to equilibrated parts
Form-finding calculations	Computational FEA – elastic cable approach
Boundary conditions	All stripe configurations have been anchored - fixed ground conditions
Erection	Assembly of structural parts using scaffolding formwork
Forming Process	Single axis bending
Application	
Architectural	Temporary space
Structural	Lightweight structure using bending-active principles

The **Twist installation** at timber expo in London also reveals how material efficiency can be of significance for the design process (Greenberg, et al., 2015). In this example, low thickness timber profiles are twisted, allowing an increased complexity in the outcome geometry of the deformed structure. The primary forced-to-bend elements exhibit a double-side connection with the secondary planar non-deformed curved elements, in parallel direction (Fig. 2.7 – Table 2.6). Due to length and planar geometry differentiations between the two groups, the primary elements are potentially required to both bend and twist, to fit the secondary elements planar curvature, and enable a set of flexural stresses to be developed into the primary elements (ITKE Research Pavilion, 2010). The component configuration is duplicated along the structure's length allowing a natural form-finding process to take place, in providing overall stability for the structure (Lienhard, 2014).

Figure 2.7 Twist Installation – Timber Expo, London, U.K., 2015 (*AA Twist installation*, 2015)

Table 2.6 Twist installation Project

Project	Twist installation – Timber Expo, London, U.K.
Year	2015
Form - Geometry	Synclastic Surface
Construction	
Material	Nonlinear Elastic (Birch Plywood Timber stripes 6 mm thick)
Manufacturing	Industrial product of identical properties and dimensions (Plywood sheets) - Stripes are CNC milled to obtain the desired planar profile.
Fabrication	The secondary elements 'wings' have been fastened to already assembled system of ribs'
Duration	1 week
Post erection stiffening	None
Assembly	
No. of elements	Up to 300 'rib' and 'wing' elements
Scale	10 x 10 m span 2 m height
No. of constr. stages	2 – Parts assembly and global structure construction
Assembling tools	Human resources for assembling the planar stripes to equilibrated parts
Form-finding calculations	Computational Form-finding
Boundary conditions	All stripe configurations have been anchored - fixed ground conditions
Erection	Assembly of structural parts using scaffolding formwork
Forming Process	Double axis bending
Application	
Architectural	Temporary space
Structural	Lightweight structure using bending-active principles

Another interesting example, which follows a unique and rather simplified approach on utilising material efficiency is the temporary shading structure **Pavilion EmTech**, in Zurich, developed in research collaboration with the Architectural Association (AA) and Swiss Federal Institute of Technology (ETH). Compared to previously examined modular structures, this example proposes a simplified approach by regulating the bending stiffness and resistance of a single uniform timber plate, through introduction of precise cuts to form the primary stripes (Fig. 2.8 – Table 2.7). The design process has been informed by material testing and computed in such a way, in order to deliver a final product of minimum material use. Secondary bending-active members are added to the structure, which are interconnected with the primary members through cables, responsible to distribute the load evenly over the vaults, while aiming at sustaining low post-buckling deformations over unplanned loading conditions (*EmTech Pavilion*, 2012).

Figure 2.8 Temporary shading Pavilion, Zurich, Switzerland, 2012 (*Temporary shading structure*, 2012)

Table 2.7 Temporary shading pavilion Project

Project	Temporary shading Pavilion, Zurich, Switzerland
Year	2012
Form - Geometry	Monoclastic Surface
Construction	
Material	Nonlinear Elastic (Birch Plywood Timber stripes 18 mm thick)
Manufacturing	Industrial product of identical properties and dimensions (Plywood sheets) - Stripes are CNC milled to obtain the desired planar profile.
Fabrication	-
Duration	1 week
Post erection stiffening	Installation of a secondary system of cable elements, interconnection the upper and lower bending-active members.
Assembly	
No. of elements	5 elastic stripes of 11 m long and variable width
Scale	9 x 2.5 m span 4 m height
No. of constr. stages	2 – Erection and post-formed installment of cables
Assembling tools	Human resources for both active formation process and installment of secondary elements
Form-finding calculations	Computational Form-finding
Boundary conditions	The system has been fixed to 4 ground supports
Erection	Human resources
Forming Process	Single axis bending
Application	
Architectural	Temporary shading pavilion
Structural	Lightweight structure using bending-active principles

Similar approaches that undertake pliable material characteristics have been investigated for the development of kinetic structures. The transformational ability that is inherent in the material mechanical properties provides an ideal starting point to enable a constant deformability of the system. Along these lines, the **Hyper Membrane Project** designed by the Hyper team in 2011, demonstrates how material deformability can achieve real-time adaptive behaviour and an immense variety of complex structural morphologies (Ferre, 2007). The kinetic gridshell is assembled of a continuous pairing of thin composite material stripes. The paired stripes are bent inversely between each grid point, reaching maximum bending radii at mid-distance of each grid's consecutive points (Fig. 2.9 – Table 2.8). Linear actuating elements connect the inversely bent members at their mid-points, allowing the structure to reach an equilibrium state. The actuators can adjust their length and therefore modify the bending radii of each opening of the bent stripes individually.

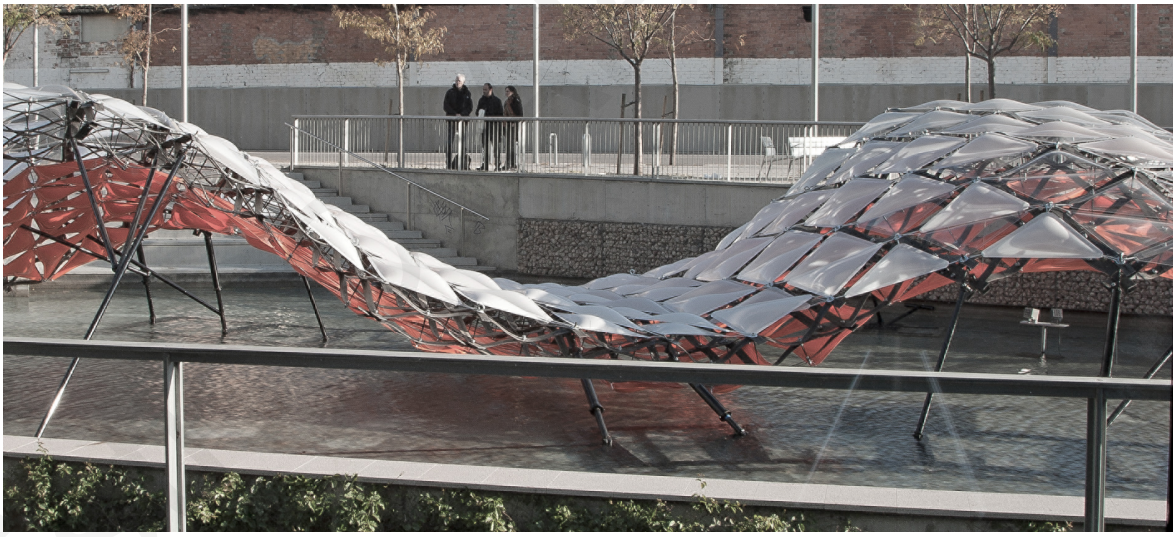

Figure 2.9 Hypermembrane, adaptive installation at the Design Hub Museum, Barcelona, Spain, 2013 (*Hypermembrane Project*, 2013)

Table 2.8 Hypermembrane Project

Project	Hypermembrane, adaptive installation at the Design Hub Museum, Barcelona, Spain
Year	2013
Form - Geometry	Kinetic double curvature geometry
Construction	
Material	Nonlinear Elastic (composite material 18 mm thick)
Manufacturing	-
Fabrication	-
Duration	-
Post erection stiffening	Real-time stiffness correction – depending on form alteration
Assembly	
No. of elements	Pair of elastic stripes of continuous length
Scale	20 x 5 m span 3 m height
No. of constr. stages	2
Assembling tools	Human resources
Form-finding calculations	Computational Form-finding
Boundary conditions	The system has been fixed to point ground supports with rotational degrees of freedom
Erection	Human resources
Forming Process	Single axis bending
Application	
Architectural	Temporary - transformable
Structural	Lightweight kinetic structure – soft mechanics

Although the design of active adaptive systems with elastically deformable elements provides immense possibilities for the development of advanced and morphologically unique system designs, respective applications are only limited to building skins and envelops. The spectrum of variable transformations according to respective structural requirements in real time extend the complexity and the amount of tests to be performed, in order to verify and achieve the effectiveness of the members.

2.3.3 Elastic rod space structures

The last category of bending-active rod members provides similar potentials in achieving prestressed systems, however, due to the enhanced 3D flexibility resulting from the sectional shape of the members used, the design may provide more freedom and the static behaviour of the systems reaches higher complexity. Therefore, these structures are combined with form-active members, such as membranes, textiles or linear tension members, to more easily sustain a 'locked' configuration.

The first example presented of the **Yurt-dome**, Shelter System (Fig. 2.10 – Table 2.9) consists of a deployable hybrid bending-active and textile system. The shelter dome is initially assembled with elastic pipe stripes of continuous length, following geodesic design principles in their construction, i.e. the shortest line on sphere. Compared to previously presented strained gridshells, the elastic pipes are fastened together by using a unique mechanism, which allows sliding and rotation on each connection node. The textile member installed in a consecutive construction phase, apart from covering purposes, also increases the structure's global stiffness (*Shelter Systems*, 2016).

Figure 2.10 Yurd-dome Shelter System, 2013 (*Yurd-dome*, 2013)

Table 2.9 Yurd-dome Shelter System

Project	Yurd-dome, Shelter Systems, Nevada, USA
Year	2013
Form - Geometry	Synclastic dome
Construction	
Material	Nonlinear Elastic (Birch Plywood Timber stripes 18 mm thick)
Manufacturing	Industrial product of identical properties and dimensions (Plywood sheets) - Stripes are CNC milled to obtain the desired planar profile.
Fabrication	-
Duration	1 week
Post erection stiffening	Installation of a secondary system of cable elements, interconnection of the upper and lower bending-active members.
Assembly	
No. of elements	5 elastic stripes of 11 m length and variable width
Scale	20 x 5 m span 3 m height
No. of constr. stages	2 – Erection and post-formed installment of cables
Assembling tools	Human resources for both active formation process and installment of secondary cable elements
Form-finding calculations	Computational Form-finding
Boundary conditions	The system has been fixed to nodal ground supports
Erection	Human resources
Forming Process	Single axis bending
Application	
Architectural	Temporary shelter use
Structural	Lightweight structure using bending-active principles

The **Bending-active Membrane roofing Marrakech** consists of elastic rod members that enable an easy to deploy mechanism through their active elastic capacity. The installation (Fig. 2.11 – Table 2.10) is a student project, which demonstrates the hybridisation potentials of an integrated textile and bending rod structure. The supportive structure is constructed out of 7.5 m continuous fibreglass rods and single surface membrane textile. The synergy of the system components may provide elegant and variable organic shapes.

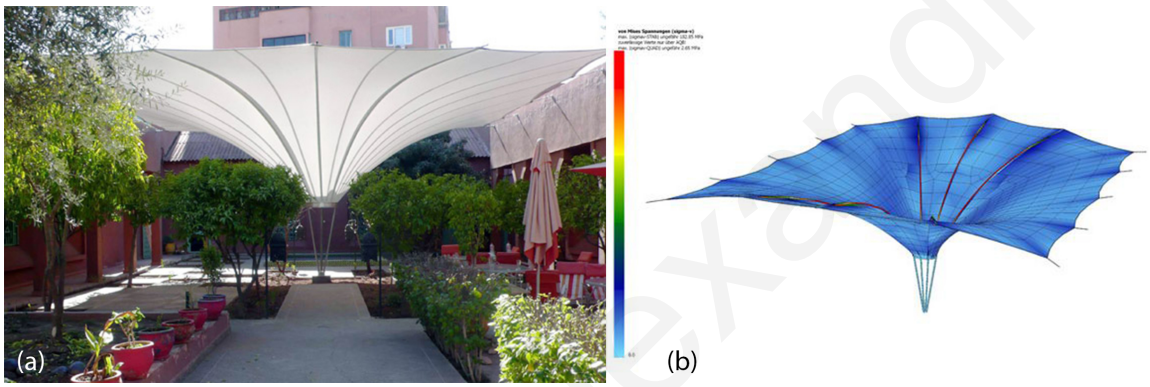

Figure 2.11 Bending-Active Membrane Roofing Marrakech, ICD, University of Stuttgart, Germany, 2012 (*Bending active membrane roofing Marrakech*, 2012)

Table 2.10 Marrakech Umbrella Project

Project	Bending-Active Membrane Roofing Marrakech, ICD, University of Stuttgart, Germany
Year	2012
Form - Geometry	Synclastic surface – funnel shape
Construction	
Material	Nonlinear Elastic (Fiberglass rods mm)
Manufacturing	Industrial product of identical properties and dimensions (Fiberglass rods) -
Fabrication	-
Duration	1 week
Post erection stiffening	Further stiffness improvement was achieved by bundling rods, wherever they ran parallel, through simple lacing connections.
Assembly	
No. of elements	6 elastic rods of 7.5 m length and thickness of 3 to 24 mm / 110 m^2 of membrane surface.
Scale	11 x 12 m span 5.5 m height
No. of constr. stages	2 - Formation process and periphery cables prestressing
Assembling tools	Human resources for both active formation process and installment of secondary cable elements.
Form-finding calculations	2 stage - FEA analysis.
Boundary conditions	The system has been fixed to main nodal ground support and multiple nodal periphery points for avoiding lateral buckling.
Erection	Human resources
Forming Process	Single axis bending
Application	
Architectural	Temporary shading structure
Structural	Lightweight structure using bending-active principles (textile hybrid)

Bending-active rod structures, serving as temporary pavilions have shown a high potential in lightweight and rabidly assembled structures. These are however limited to dome-like shapes or global shapes with enclosed geometrical characteristics. The **Textile Hybrid M1** project developed at the Institute of Computational Design (ICD) at the University of Stuttgart is an example of diversification of possibilities that can emerge from the synergic action of bending- and tensile-active configurations (Fig. 2.12 – Table 2.11). The complex formation of the final outcome is a result of a computational process that takes into consideration the structural behaviour of the constituent elements. It follows a numerical analysis process on the investigation of the equilibrium shape.

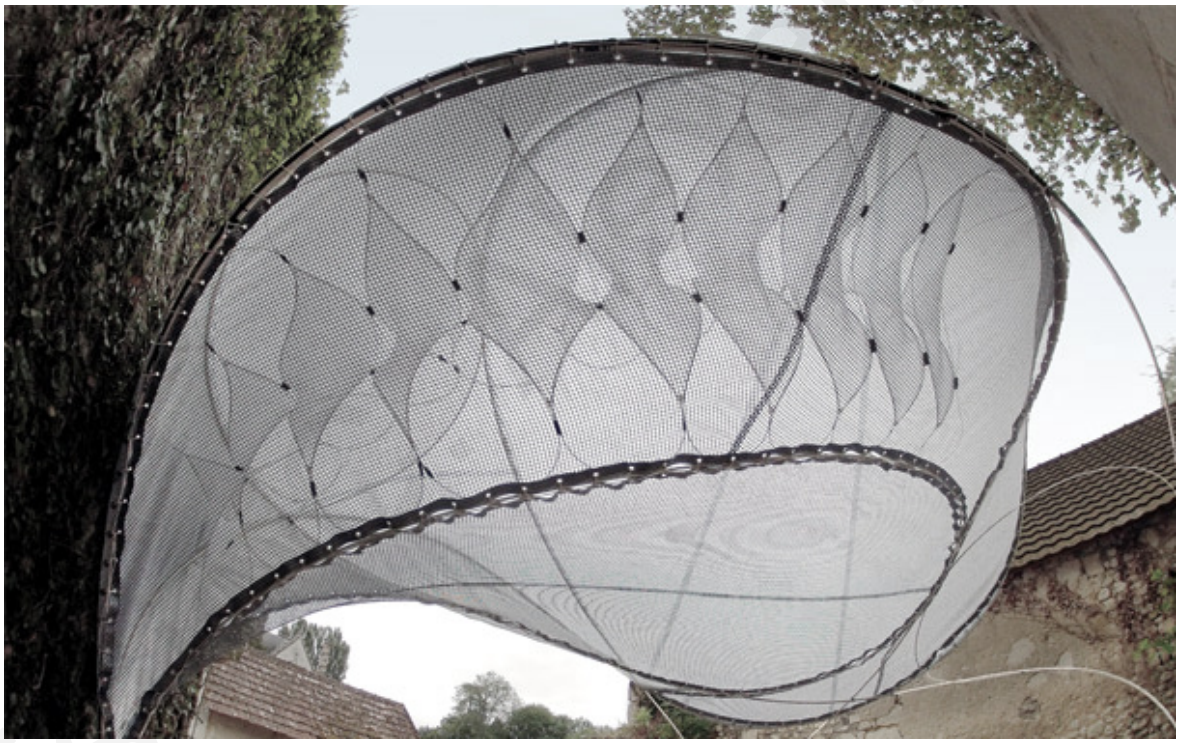

Figure 2.12 Textile Hybrid M1 Project, ICD, University of Stuttgart, Germany, 2013 (*Textile Hybrid M1*, 2013)

Table 2.11 Textile Hyrid M1 Project

Project	Textile Hybrid M1 Project, ICD, University of Stuttgart, Germany
Year	2013
Form - Geometry	Multi-dimension synclastic and anticlastic geometry
Construction	
Material	Nonlinear Elastic (Fiberglass rods mm)
Manufacturing	Industrial product of identical properties and dimensions (Fiberglass rods) -
Fabrication	-
Duration	1 week
Post erection stiffening	
Assembly	
No. of elements	elastic rods of total length of 110 m GFRP rod and thickness of 3 to 24 mm / 45 m^2 of membrane surface.
Scale	6 - 8 m span
No. of constr. stages	2 - Formation process and periphery cables prestressing
Assembling tools	Human resources for both active formation process and installment of secondary cable elements.
Form-finding calculations	Two-stage - FEA.
Boundary conditions	The system has been fixed to main nodal ground support and multiple nodal periphery points for avoiding lateral buckling.
Erection	Human resources
Forming Process	Multi-axis bending
Application	
Architectural	Temporary shading structure
Structural	Lightweight structure using bending-active principles (textile hybrid)

2.4 Conclusions

In the current section, a detailed analysis of bending-active systems applications in architecture has been conducted. The introduction of bending-active principle as a leading design instrument for the conception of structures, gave a great boost towards the development of unique, material and energy efficient free-form lightweight systems. These are realized thought application of interdiciplinary design, computational fabrication, exclusive assembly techniques and state-of-the-art construction and forming methods; aspects that are directly associated with the form-finding process that preoccupies the bending-active members' activation. Along numerous design and construction parameters necessary for the morphological objectives succession, most examples lack design aspects considerations that would associate generative systems' formation parameters with respective post-formed load-deformation behaviour and response.

Furthermore, some of the beneficial construction and design advances granted over conventional structures come at a cost when dealing with the construction duration. In the case of strained gridshells, the active formation process (erection) necessitates the use of external infrastructural support or mechanical actuators for pulling, pushing or lifting the structure into the desired position. The erection process of the Mannheim Multihalle gridshell for example, was performed using a series of forklifts and scaffolding units, for gradual pushing and supporting the structure upwards and or its gradual bending (Adriaenssens *et al.*, 2014). In the example of the Weald and Downland Museum gridshell, the non-deformed planarly assembled lattice structure was elevated at a higher level, left to gravity, and further weighted at the edges to be pulled towards the ground level to form the doubly curved target shell shape. Alternative erection processes suggest the use of mobile cranes and light auxiliary columns, practically applied for the erection of the Essen Pavilion. Some of the most frequently applied erection and forming approaches are also known as ''pull up'', ''push up'' and ''ease down'' (Quinn and Gengnagel, 2014). Despite the diversity of applicable techniques, almost every major gridshell project suffered from increased construction energy and excessive erection duration. In addition, most of the

erection approaches induce point load or high, full-span compression forces to the constituent members causing the structure to experience breakages due to exceeded level of concentrated stress. Although modern examples have reduced the amount of breakage failures through use of modern machinery and tools, this issue remains an important aspect of consideration when dealing with the construction of bending-active structures (Liuti, 2016).

The author acknowledges the emerging problems when dealing with active-bending systems' forming procedures and introduces an alternative approach for structural activation in the case of synclastic shape acquisitions. In Capter 5, 6 and 7 the hybridization of bending-active members is proposed with a secondary system of cable elements to be used as an alternative formative instrument, which may also work as a self-stiffening and stabilization enhancing add-on (Alexandrou and Phocas, 2017). To avoid breakages during the forming of such systems, both the final shape outcome, as well as the entire formation phase should be monitored. The structural activation using installed cable elements may follow a gradual and uniform self-induced deformation distribution, dissolving the members stress concentration effect. In this respect, the construction energy is to be stored in the secondary structure of cables in the form of prestress / strain energy.

CHAPTER 3 **FORM-FINDING**

The design and construction of form-active structures that consist of either tension-only members (cable-net structures) and membranes, or bending-active members, comprise a complex process compared to conventional rigid bar structures. The initial and fundamental aspect of the design is the form-finding; the design stage that determines the final shape of the elastically deformable system prior to its operation. Due to the elastic properties of the materials employed, the shape of any member can vary according to multiple local constraints (i.e. supports and members' connectivity), or global configurations (i.e. assembly), resulting in different deformations.

Form-finding can be defined as the finding process of an (optimal) shape of a form-active structure that is in (or approximates) a state of static equilibrium (Lewis, 2003). At this point, however, questions with regard to the prescription of 'optimal' may confuse the way someone conceives this process. In the field of engineering, optimal shape implies the idea of having a respective high static performance, or having the system form-found out of natural procedures, for example according to the loading conditions. On the other hand, in terms of architecture, optimal is more suitable to the most appropriate form for a specific architectural purpose or application. In this respect, more recent definitions refer to form-finding as *''the process of finding an appropriate architectural and structural shape''* or even *''a structural optimization process, which uses nodal coordinates as variable''* (Veenendaal and Block, 2012). The latter definitions lead to a performance-oriented approach in design than a performance-based one. In the following sections of this thesis, form-finding of the systems is investigated in the frame of a performance-based approach.

3.1 Analysis Methods - Classification

Over the past decades, several form-finding methods have been established and experienced. The foremost methods were mainly developed, in order to calculate form-

finding of shapes such as cable-net structures, while later developments could also be utilized for elastic surfaces and membranes. These methods have been categorized into three main groups according to the chronological period developed, as follows (Veenendaal and Block, 2012):

Stiffness Matrix Methods are among the longest applied, and their logic is based on structural analysis using standard elastic and geometric stiffness matrices (Adriaenssens *et al.*, 2014).

Geometric Stiffness Methods calculate form-finding solely from geometric stiffness, without taking into account any material characteristics. These methods can be used to calculate or simulate elastic behaviour as pure form rather than accurate material-defined elements. By including additional physical properties, simulation of the elements fully defined elastic behaviour may be achieved. Driving force for these methods development is the need to numerically simulate elastic behaviour of pliable objects and represent them though computer graphics (Terzopoulost *et al.*, 1987).

Dynamic Equilibrium Methods can update the geometrically deformed system in time-steps. These methods are equivalent to normal static analysis and in most cases, they are formulated under a time-based solver, as an instrument to unravel the problem of the dynamic equilibrium, until the final form of the system is found. In this case, residual stresses are converted into velocities and the mass of each node determines its acceleration. Compared to the previous methods, dynamic equilibrium methods can handle more complex systems with many degrees of freedom, and perform calculations in less computational time (Veenendaal and Block, 2012).

As already stated, the above-mentioned methods are more suitable for membrane or cable-net structures (tension-only members). When it comes to the design of bending-active structures, where components can embed multiple stress types such as tension, compression and bending, form-finding becomes more complicated. Despite the axial deformation between the nodes of each element, there is a bending moment that takes

live action upon the member itself. For this purpose, the *Particle Spring System* (Fig. 3.1) is a more convenient form-finding method. Particle spring system is an interactive real-time form-finding method, which is based on the application of spring elements to simulate elongation or active bending. Each member is divided into a chain (2D) (Fig. 3.2) of nodes and elements. All interchangeable nodes are connected using spring elements, enabling thus the simulation of bending and swivelling. The stiffness of the spring elements assigned determines the overall stiffness of the members examined (Kilian and Ochsendorf, 2005).

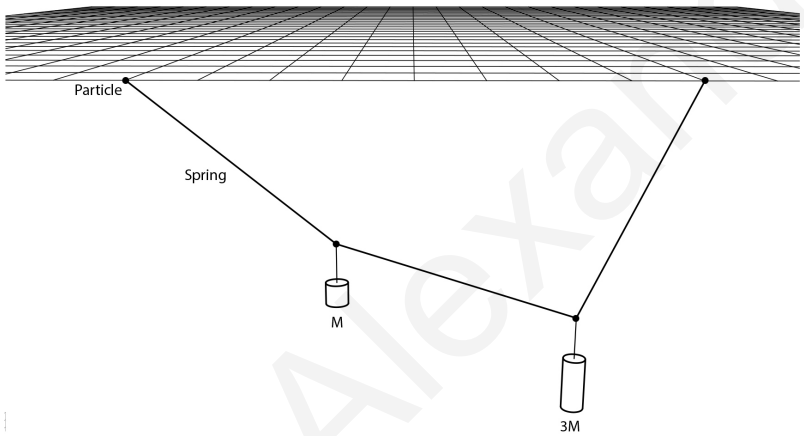

Figure 3.1 Simple Particle-Spring System

Despite the ease of constructing *Particle-Spring based models*, this method is advised to be utilized just in early design stages, due to the fact that the actual mechanical properties of the members are not considered in the analysis and therefore, no realistic stress conditions may be obtained in different stages of the active deformation process. As a result, this method cannot be conducted in the frame of an objectively conclusive numerical form-finding analysis.

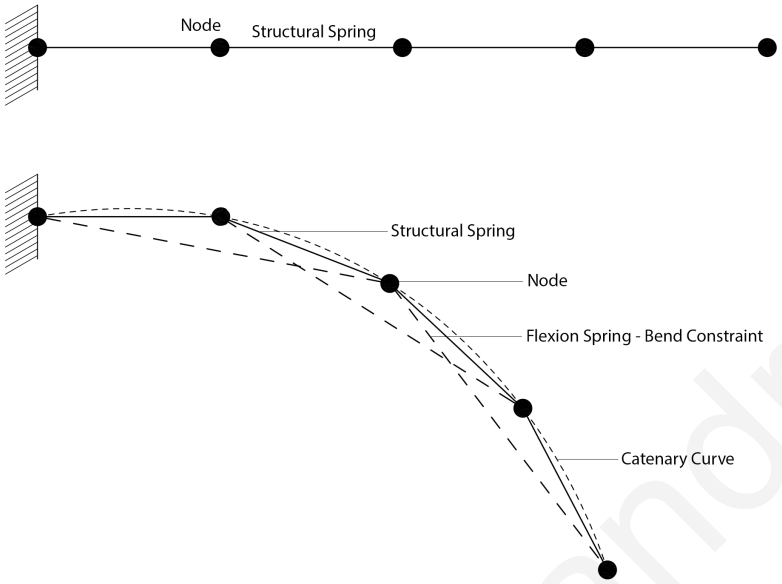

Figure 3.2 Particle-Spring System for simulating active-bending

In literature, multiple numerical calculation methods, analytically described in (Veenendaal and Block, 2012), have been developed to solve flexible systems. Among many, FEA, dynamic relaxation (DR), particle-spring system and force-density methods are the ones widely used today (Dieringer *et al.*, 2013; Lienhard, Ahlquist, *et al.*, 2013; Mele *et al.*, 2013; D'Amico, Kermani and Zhang, 2014). Form-finding techniques in bending-active members based on FEA are presented in (Adriaenssens *et al.*, 2014). FEA proves to be a valid form-finding calculation method (Veenendaal and Block, 2012), and takes into account both material and geometrical nonlinearities that occur during the members' large deformations and displacements.

However, in lightweight elastic structures, large displacements cause numerical instabilities and violate the necessary assumptions of small displacements (Kilian and Ochsendorf, 2005). An alternative approach on decoding and revealing the deformed shape of bending-active system has been recently developed using FEA software and custom programming tools (Lienhard, Ahlquist, *et al.*, 2013). This approach however has been differentiated according to the type and erection process of the structural system

(e.g. hybrid form- and bending-active structures, coupled bending-active members or hybrid form-active structures).

The conventional form-finding methodology of coupled bending-active structures examined in (Fröling and Persson, 2013), points out the need for using both geometrical coordinates, as well as inner stress-state conditions update in the stiffness matrix of the model. In other words, all stresses developed in each deformation step should accordingly be stored inside the updated geometry coordinates of the model before calculating the next step. This is critical, in order to keep a rationalized model that includes all mechanical information in all following static calculations. For the erection and step-wise deformation activation of bending-active members, Lienhard suggests the so-called elastic cable approach (Lienhard, La Magna and Knippers, 2014). Contracting cable elements are used to pull together nodes from both individual members, until they reach the required deformed configuration. The cable elements are assigned to constant pretension and for each static analysis that follows, their elastic stiffness is regulated to a lower level. This process enables cable components to shrink in length and the two end-assigned nodes of the structural members to come together. For the form-finding of coupled bending-active members, this technique allows a complete freedom of the equilibrium paths that are followed during the deformation process.

Traditionally, the calculation of the form-found shape of elastically deformable structures has been performed using physical modelling experimentation or draft numerical calculation. As already stated in the introduction, these techniques have been developed and used for finding the optimum shape of shell structures, and later on of strained gridshells. Although, physical models are considered vital for form-finding purposes, it has been proven that the particular structures are not scale-independent (Adriaenssens *et al.*, 2014). This is due to lack of material's properties such as density, stiffness and poison's ratio.

3.2 Material Compatibility

Taking as an example the simple case of an elastic member, whose ends are interconnected by a cable, the most common mathematical model for the elastic member in structural mechanics may be derived according to the Bernoulli-Euler Model plane sections. This is assumed to remain plane during linear deformation and normal to the member's axis. Therefore, the simplified differential equation of the section's bending is formulated as follows:

$$w''(x) = \frac{M(x)}{EI} \tag{3.1}$$

The Bernoulli-Euler law also formulates a second order nonlinear differential equation for larger nonlinear deformations, as follows (Fertis, 2006):

$$\frac{1}{r(x_0)} = \frac{\Delta dx}{dx} = \varepsilon = \frac{\sigma}{E} = \frac{M(x_0)\cdot t}{E\cdot I} \tag{3.2}$$

Solutions of the above equation lead to the well-known theory of elastic curves (Levien, 2009). The understanding that the Elastica is a curve that generates a minimum of potential bending energy in a constrained system describes best the inseparable interdependency of mechanical behaviour and form-finding in bending-active structures. Further on, FEA based on the equilibrium of forces by applying nonlinear FEA to the problem of form-finding "minimum potential energy constraint bending curves" may be used. The relationship between local bending curvature and bending moment at a differential segment of a largely deflected beam can be formulated as follows (Lienhard and Knippers, 2013):

$$\frac{r(x_0)}{dx} = \frac{t}{\Delta dx} \tag{3.3}$$

whereas r is the bending radius and t the member's section thickness.

By setting t in relation to r and introducing Hook's Law, it is derived

$$\frac{1}{r(x_0)} = \frac{\Delta dx}{dx} = \varepsilon = \frac{\sigma}{E} = \frac{M(x_0)\cdot t}{E\cdot I} \tag{3.4}$$

The above equation shows that the bending moment M is proportional to the change in curvature $1/r$, i.e.

$$\frac{1}{\mathrm{r}(\mathrm{x}_0)} = \frac{\mathrm{M}(\mathrm{x}_0)}{\mathrm{E}\cdot\mathrm{I}} \tag{3.5}$$

For flat sections, the width has no influence on the bending stress, which can therefore be expressed proportional to the thickness t and curvature $1/r$. Therefore, the following bending stress curvature relation may be obtained:

$$\sigma(\mathrm{x}_0) = \frac{\mathrm{E}\cdot\mathrm{t}}{2\cdot\mathrm{r}(\mathrm{x}_0)} \tag{3.6}$$

The formulation of the minimal bending radius for a given permissible stress σ_{Rd} may be written as follows:

$$\mathrm{r}_{\min}(\mathrm{x}_0) = \frac{\mathrm{E}\cdot\mathrm{t}}{2\cdot\sigma_{\mathrm{Rd}}} \tag{3.7}$$

In general, adequate materials for static bending-active structures should offer a ratio of σ_{Rd}/E> 2.5 (with σ_{Rd} [MPa] and E [GPa]) (Fig. 3.3). When it comes to kinetic bending-active structures, additional requirements for fatigue control further limit the permissible permanent elastic stress; therefore, a ratio of σ_{Rd}/E > 10 is recommended (Lienhard, 2014). In this respect, fibre-reinforced polymers (FRP) and certain types of timber and high strength metals are particularly appropriate materials for use in bending-active structures.

In considering an increase of the scale of the system, the radius of curvature r can be expressed as a function of the span l_0 and the rise h_0 of the system, which are equivalent to the pre-scaled ones. The respective equation is based on a scale factor s, as follows (Lienhard and Knippers, 2013):

$$s\cdot\mathrm{r}(\mathrm{x}_0) = s^2\,\frac{{l_0}^2+4\cdot{h_0}^2}{8\cdot h_0} \tag{3.8}$$

Figure 3.4 shows the form-found shape of seven bending-active stripes of 2 to 8 m initial length and 1 to 4 m respective spans. In Eq. (3.8), s can be excluded as a linear factor, i.e.

a linear up-scaling of the system requires linear up-scaling of the cross-sectional thickness of the elastic member in keeping the residual stress constant. This presumes of-course a linear behaviour of the elastic member, whereas only its elastic stiffness is taken into consideration. Since stability plays a decisive role in the structural integrity of the bending-active structure (Takahashi *et al.*, 2016), the consideration of axial forces in the geometrical stiffness of the system is of particular importance for its scaling.

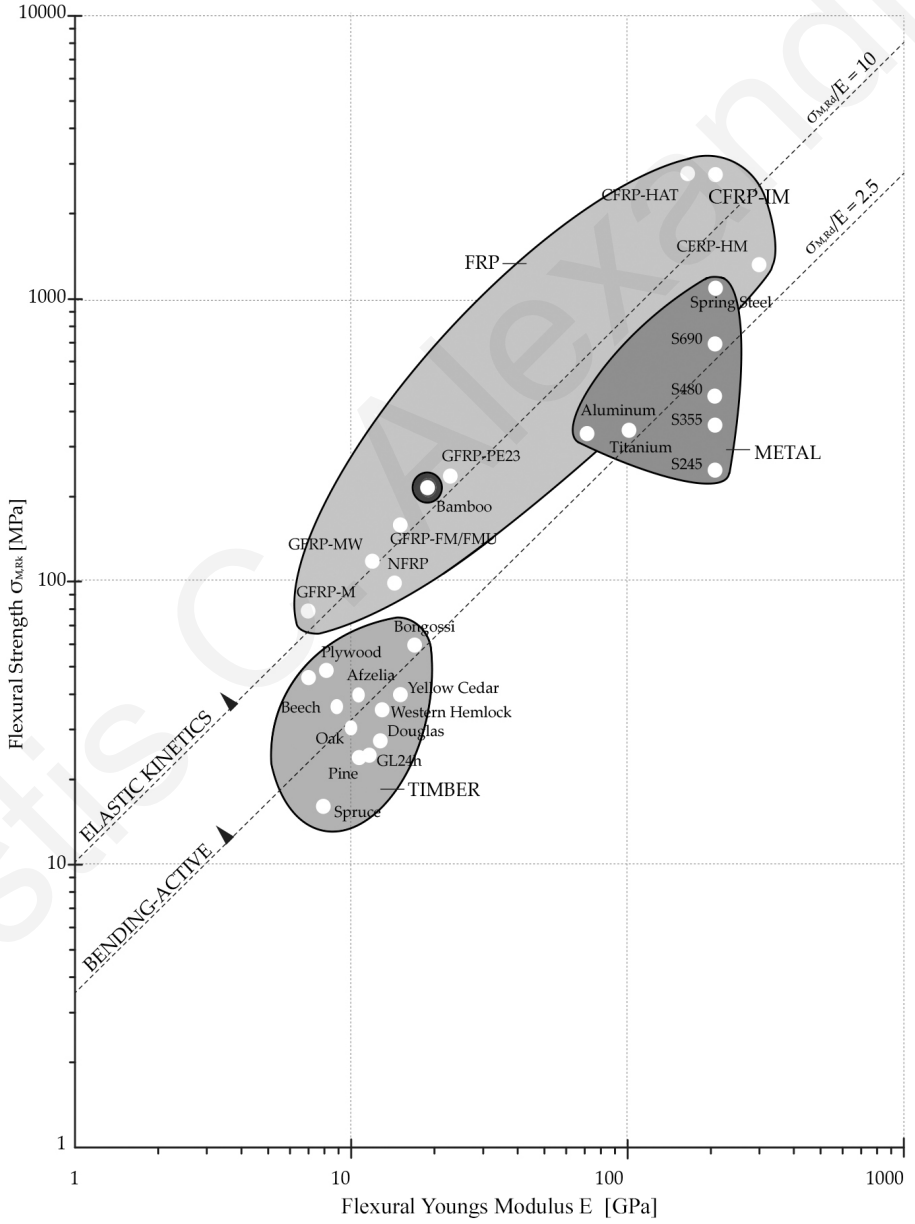

Figure 3.3 Adequate materials for static and kinetic bending-active applications (Lienhard, 2014)

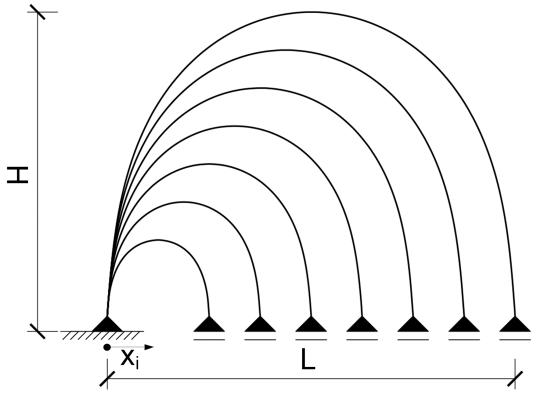

Figure 3.4 Development of elastica curves with increasing system scale

3.3 Hybrid Lightweight Structures

In the context of contemporary structures, lightweight characteristics are often related to modularity, self-weight minimisation and simplicity in constructability. A lightweight structure can be defined as one that uses less material with maximum utilisation. Historically, lightweight structures have shown their peek points in the construction of wide-span structures, temporary, easy to construct spaces, or facades and building envelopes. Lightweight structures have foster a positive attitude towards technology, construction and engineering, and are mainly based on *tensile*, *membrane* or *hybrid tension-compression* structural systems. One of the most important attribute that lightweight structures adopt, is the use of articulately joint connections between the constituent parts, for avoiding bending moments and achieving less material use. This often leads to hybrid systems of interconnected high strength materials. The design of lightweight structures is fundamentally based on material efficiency and this is mainly effecting the configurability and construction details of a system to reach optimum results; in other words, to make best use of the individual materials used. Critical aspects in lightweight structures is the cable prestressing technique (i.e. self-stressed systems). Amongst multiple factors that contributed to the development of lightweight systems, prestress is most significant in achieving low self-weight of the members, as it enables undesirable compression to be converted into tensile stresses and vice versa. However,

lightweight structures still face some major problems, such as their complex interacting design process, high assembly duration and time-consuming construction techniques.

3.4 The Role of Cables in Hybrid Tension-Compression Structures

From a generalised point of view, tension structures can be classified in two main groups depending on the type of tension elements used; (a) Membrane and (b) String structures. String members may either be rods, chains or cables, with cables being the most commonly used. The use of cables in hybrid tension or tension-only structural systems has been adopted and further optimised for both structural and architectural benefits (Saitoh, 1998). Fundamentally, the role of cables in the case of tension-only structures, such as cable-nets, is to enable distinctively lower structural self-weight. In hybrid structures, the cable's role becomes critical in many aspects of the design and structural performance and this may be classified in two classes: (a) The cables are utilised by means of their passive characteristics in tension, and (b) by means of active characteristics of pretension. In this respect, the purpose and effect of cables in hybrid structures is as follows:

Passive use.

1. Formation of a balanced hybrid system, i.e. hybrid string structure (HSS) with regulated stability.
2. Bracing effect, i.e. beam string structure (BSS).
3. In-plane stiffening.
4. Conservation of system's resistance with regard to overall buckling load.

Active use.

1. Stress control of bending or compressive members.
2. Displacement control of global hybrid configuration.

3. Increase in structural stiffness achieved by geometrical stiffness.

In cases of cable's active use, the structural design and construction depend on the amount of the cable members pretension (Saitoh and Okada, 1999). Consequently, an alternative classification may apply, due to different respective conditions or utilisation purposes (Fig. 3.5). These are listed as follows:

[A]: The cable's initial tensile force should be higher than the anticipated compression force (caused by external loads) to prevent cable relaxation.

[B]: The cable's initial tensile force depends on the compression stress to be developed by the rigid members during vertical loading.

[C]: The cable's pretension is actively utilised for the stress and deformation control of the rigid members.

[D]: The cable's pretension is not introduced, but rather self-generated by the existing dead weight of the structure. This enables the achievement and maintenance of a target structure shape.

This leads to a set of general aspects of efficiency, introduced by the cable's pretensioning, closely related to the role of string as noted above:

1. Resistance for compression force that acts on cables.
2. Securing the straightness of cables.
3. Enhanced stiffness (geometrical).
4. Reduction of initial stretch of cables (deformation control).
5. Control of deformation and shape characteristics of a hybrid system.
6. Global stiffening and increase of buckling resistance.

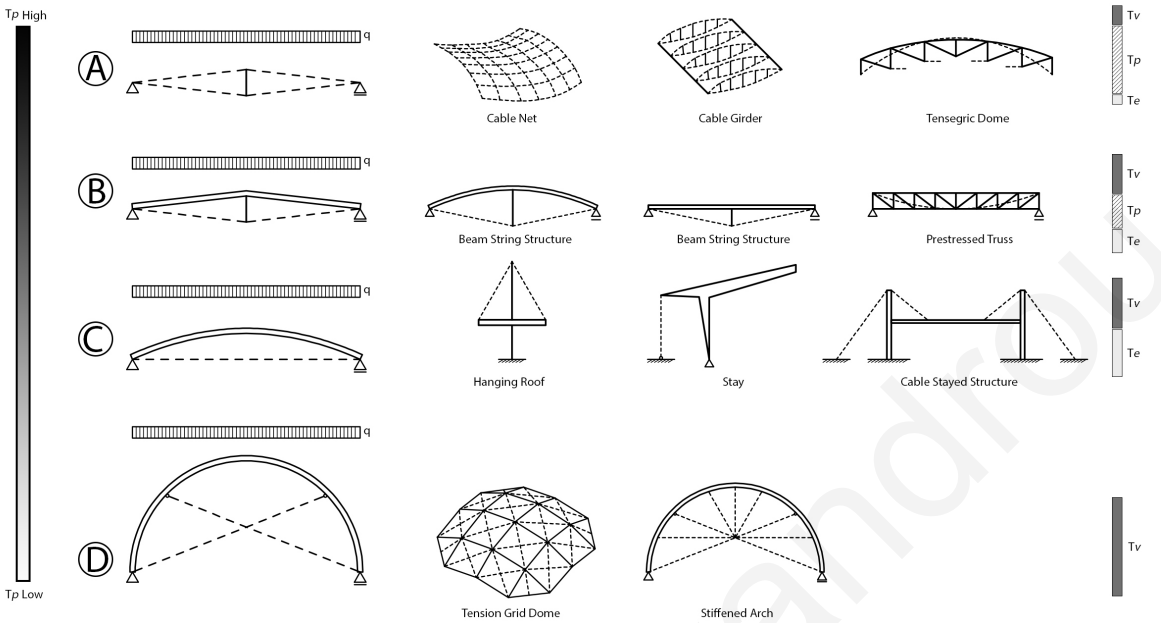

Figure 3.5 Classification of hybrid string structures based on the amount of prestress. Te: existing tensile force; Tp: Pretension; Tv: Tension due to external loading conditions (Saitoh and Okada, 1999)

Among hybrid tensile and tensegrity structural systems, which are frequently applied for achieving long spans, the role of the cables is very critical and aims at sustaining adequate geometrical stiffness of the structure (Saitoh and Okada, 1999). This is however controlled and further optimized through introduction of pretension. For the dome example presented in (Quagliaroli *et al.*, 2015), a comparison between a secondary bracing system and a cable pretensioning solution clearly demonstrates the superiority of self-stress stiffening achieved by using calibrated cable pretensioning, compared to the mechanical rigidity provided by the bracing technique, for both load-deformation control and self-weight minimisation.

In hybrid cable bending-active systems, the role of cables falls into more complex set of criteria with regard to the design and structural efficiency of the system. Due to the active deformation of the primary elastic members, the cables become significant components with regard to the overall shape acquisition of the system. This is primarily based on the need of the elastic members to rest in static equilibrium in their deformed state. Thus, the cable plays a critical role in stabilising the system in deformed shape. By extent,

supplementary aspects such as the initial configuration and connectivity constraints of the elastic members with the cables, are also of importance to the configurability of the system. Subsequently, the role of cables may be characterised as integral. Compared to hybrid rigid elements, in which the cables can be utilised for either passive or active applications, the relation that governs hybrid flexible systems is rather singular, that of active action, applied through length reduction (Fig. 3.6). This action simultaneously induces prestress on both elements (the cables and the elastic members) and results into global stiffening effects. In this respect, the following aspects may characterise the general contribution of the cables in bending-active system hybridisation:

1. As actuator for erection and form-finding of the hybrid system, through initial length reduction

2. As control element for stiffening and prestress of the hybrid system.

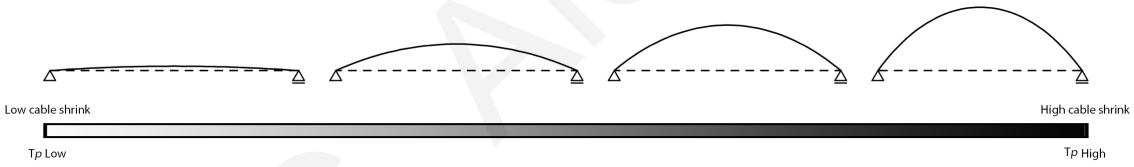

Figure 3.6 Classification of hybrid string structures based on the amount of initial cable length reduction

Consequently, cables are considered as vital components that may actuate and control the system's load-deformation behaviour. Since the deformation and stress-control of bending-active systems are directly related to the length of the coupled cables, there may not be any further post form-found optimisation through pretension.

3.5 The Bow Principle

The principle of a combined compliant-string mechanism can be clearly observed in the case of a bow. The bow technology has been around since ancient years, used in human hunting tribes. The oldest, single-piece bow dates back in 800 B.C. The purpose of the bow was to propel straight arrows using stored elastic energy. The stress conditions of a 'non-recurve' simple longbow are (a) unbraced/unstrung, (b) braced/strung and (c) fully-

drawn/extended (Fig. 3.7). 'Non-recurve' bows are manufactured with initially straight limbs. At strung condition the limbs (compliant mechanism) are elastically bent backwards and the string is tensioned. The bow is then found in equilibrium and the stored energy is also known as strain energy. In extended conditions, the strain energy increases, while the hybrid compliant mechanism reaches equilibrium with the archer's point-pulling force. The maximum fully-drawn distance of a bow depends on the material's yield strength. Bows limbs are traditionally made from wood but nowadays they are made of glass or carbon fibres imbedded in resin. Bows are normally symmetrical and belong to the 'working-recurve' typology, meaning that limps undergo elastic deformation along their entire length. Comparing a 'recurved' with a 'non-recurved' bow of similar dimensions and material, the former can store a higher amount of elastic/strain energy at less backward pulling distance from the archer (Kooi, 1981).

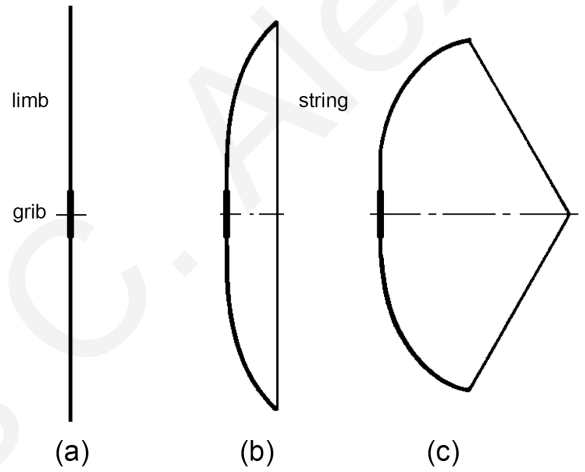

Figure 3.7 Longbow stress conditions; (a) unbraced/unstrung, (b) braced/strung and (c) fully-drawn/extended

CHAPTER 4 **ANALYSIS PROCEDURE**

4.1 Case Study Analysis

The present research focuses on the analysis of six single-segment hybrid bending-active structural configurations of specific dimensions and scale. The design development of the hybrid configurations under examination is based on the exploration of the synergic action of their multiple components with a view to achieve structural efficiency and variation in forms. A simple single-segment configuration, i.e. unit 1, of a fundamental arrangement of a two-component unification, is analysed, while analysis is also provided for five additional single-segment configurations, i.e. units 2 to 6, based on a paired bending-active configuration synthesis (Fig. 4.1). The aim is to parametrically explore the structural behaviour that emerges from a single curvature syntax of structural formation using simple and interconnected pairing techniques on elastic members of identical, or differentiated length.

This investigation aims at addressing and evaluating the structures' geometrical characteristics and load-deformation behaviour in all analysis stages. The proposed analysis model suggests the employment of initially (absolutely) planar geometries (regular beam elements), assigned with elastic material properties, PTFE, while taking into consideration the geometrical nonlinear effects for the calculation of all stages of construction and loading (cables pretensioning and vertical loading). These conditions are considered to be of major importance, in order to allow the analysis calculations to comply effectively with the particular structural principles and construction processes. Throughout the form-finding process, the initially *(i)* non-deformed cable bending-active single-segment configurations are handled in two indispensable assembly stages; namely, *(ii)* the fastening and *(iii)* the prestress stage. Along these lines, the study seeks to create sequential nonlinear analysis stages that follow in an analogous way the actual physical model assembly and subsequently the form-finding process of the system. Aim of the study

is also to conclude on critical aspects that characterize the selected configurations in terms of their structural efficiency and construction design.

4.2 Analysis Steps

During assembly, i.e. fastening and prestress stage (Figure 4.2), the form-found geometry of the systems is completed and the induced bending stresses are stored in the elastic members. The planar elements are bent to form curvilinear shapes, while these should simultaneously preserve adequate prestress for structural stability under respective application requirements. The analysis is achieved through a series of consecutive steps with partial cable shrinkage values, in order to trace the structural behaviour of all components during deformation. For example, the gradual main cable's shrinkage steps 1,…,5, in the prestress stage are set to a constant value of 100 mm, in order to reach a total shrinkage value of 500 mm ($L_0/2$). In the last stage of the analysis, the units are investigated in their load-bearing and deformation behaviour under a vertical uniformly distributed linear load of 2.5 kN/m. This load refers to a surface load of 1 kN/m^2, assuming a linear positioning of the planar structure at 2.5 m relative distance. The self-weight of the members is included in the external loading under consideration in this stage.

4.3 Single-Segment Structural Configurations (Units)

Unit 1 comprises the simplest form of a cable bending-active system configuration, composed of a single elastic member of 1 m length that is connected with a cable at both ends. There should be a small initial curvature in the elastic member to assure its direction of bending. At the form-found state, the system behaviour is based on the bow and string principle, in which a pretensioned cable holds the shape of an elastica arc (bow). The elastic restoring effect of the bending-active arch is used to initiate a pretension force in the cable, which, in turn, assumes the shape of the arch. Unit 2 is based on a pairing configuration of bending-active members, with identical initial lengths, but an opposite deformation direction in span direction. Through activation of the main cable, one member tends to bend upwards while, the other downwards. Unit 1 and 2 are form-found, solely following

the prestress stage, without any fastening. Unit 3 also follows a paired bending-active configuration with two bending-active members of differentiated length of 1.25 ratio. In the fastening stage, the upper member is forced to bend until it reaches the non-deformed length of the lower member and the two end supports are unified. In the subsequent prestress stage, the main cable that connects the ends of both bending-active members, shrinks until it reaches half of its initial length ($L_0/2$). The double arc comprises an externally statically determinate system. The structure forms a closed equilibrium system, while the lower member adds further pretension to the main cable. Unit 4 is identical to unit 3, but with inverted lower member's deformation direction. Consequently, units 2, 3 and 4 are designed based on a pair bending-active members' configuration of equal, or differentiated, lengths. Apart from enabling morphological variation, both elastic members regulate the respective cable axial force. By extent, the deformed curvature of the upper elastic member may counteract the pretensioned cable during vertical loading. Any cable slackening due to sliding of the support, may be prevented by the lower elastic member, which has lower curvature and higher geometric stiffness.

Unit 5 comprises an extension of the unit 3 configuration. A shear-resistant interconnection at the bending-active members' mid-point is applied, in order to provide the alternative form-found shape. The number of the members' interconnections in unit 6 increases to two, and they are placed symmetrically at one third of the members' length. Thus, both, unit 5 and 6 form sequential series of arches and tension elements in the two stripes due to the alternating span between the connection points. In the form-finding process of the coupled arch units, the upper elastic members are forced to bend locally through the imposed edge conditions, while the lower members are prestressed through the elastic restoring action of the bent members. Consequently, in unit 5 and 6, the fastening of the members of variant length, causes force interaction and hence, respective shape distortion until a self-equilibrium state is reached. The larger the arch length difference between the interconnections of both members is, the higher the resulting curvatures are expected to become. In these units, the influence of the main cable is

expected to be relatively small in achieving a target unit's configuration beyond the fastening stage.

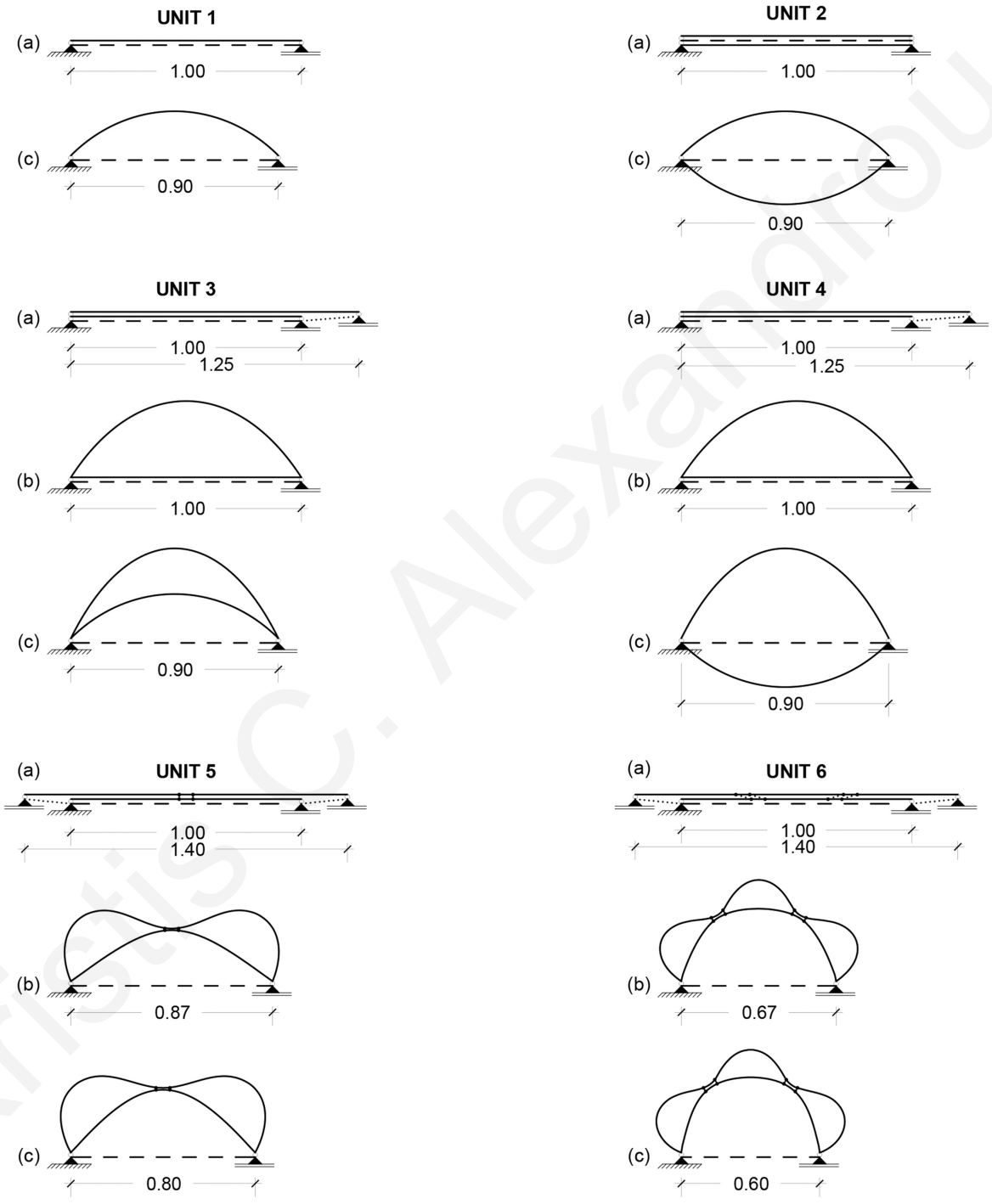

Figure 4.1 Single-segment structural configurations in (a) Non-deformed, (b) Fastening and (c) Prestress stage in initial cable's shrinkage step

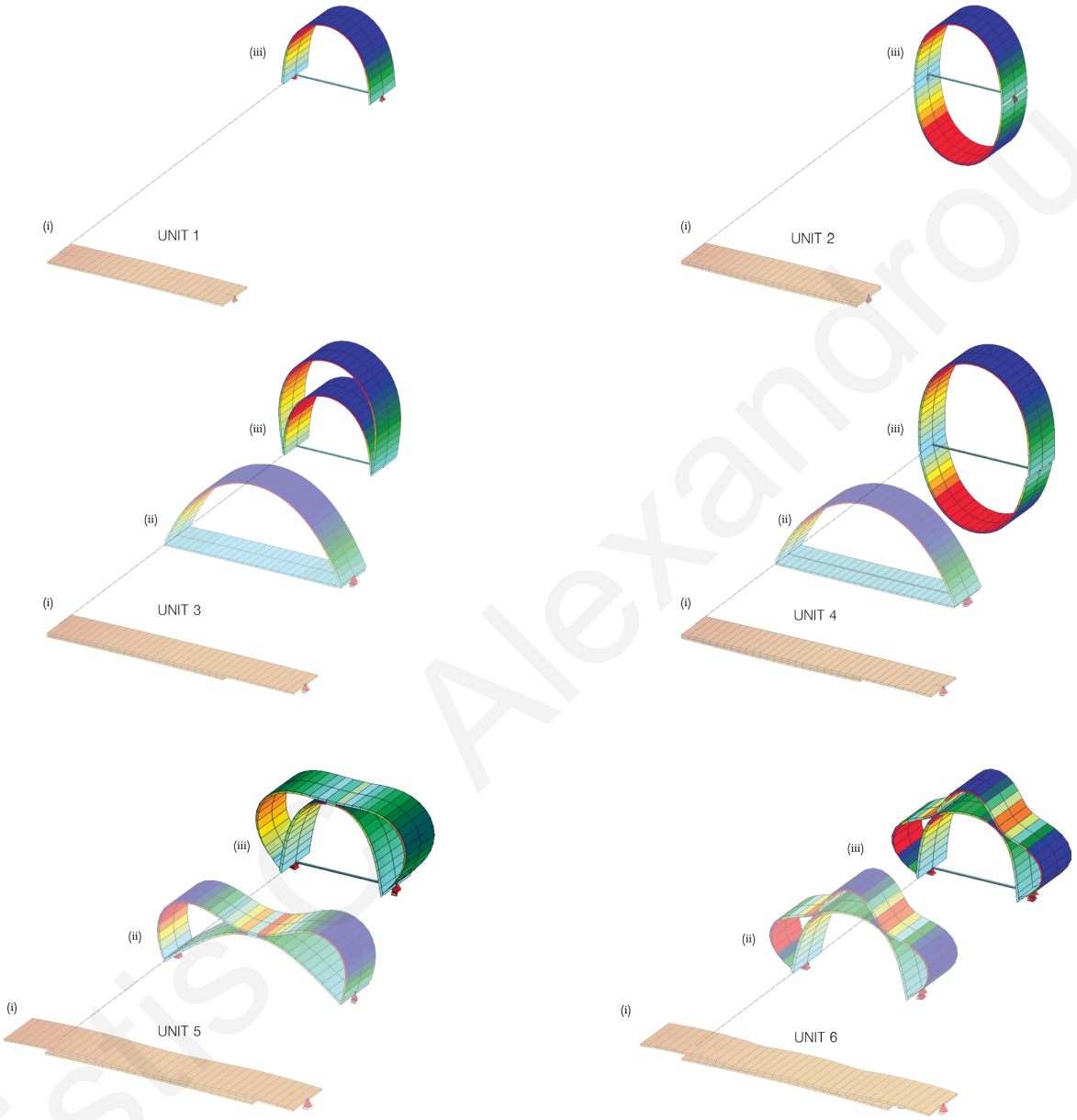

Figure 4.2 Single-segment structural configuration's consecutive analysis stages; *(i)* Non-deformed, *(ii)* Fastening and *(iii)* Prestress stage

4.4 Structural Analysis Model

The structural behaviour of the units was investigated with the FEA software SOFiSTiK (SOFiSTiK AG, 2014a, 2014b). The analysis data was defined and controlled by the alternative input tool of the program, Teddy (text editor), in order to support custom

programming of the commands and control of the load case sequences applied in each analysis stage individually. Fig. 4.3 presents the workflow adopted for the static analysis of the units. For the case of this study, the program modules that have been selected are as follows:

+AQUA	(in SSD): Definition of Materials and Cross Sections.
McNeel Rhinoceros	(Rhino): Geometric Modelling Environment.
+SOFIMSHC	(in SSD): Import and Convert Geometry from Rhino.
+SOFILOAD	(in Teddy): Definition of Loads and Load functions.
+ASE	(in Teddy): General Static Analysis.

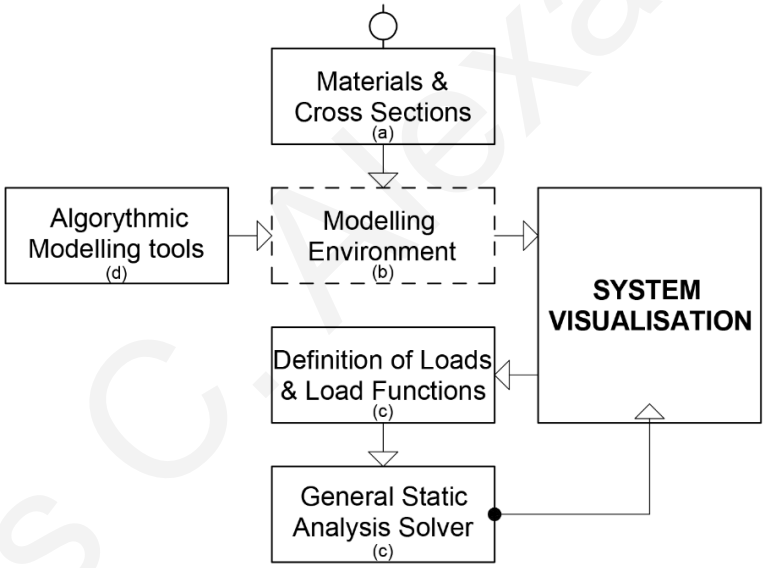

Figure 4.3 Design workflow conducted in (a) Sofistik's window mode default environment, (b) third party, external modelling application, (c) Sofistik's alternative input tool, i.e. TEDDY (text editor), and (d) third party plug-in for algorithmic geometrical modelling

The bending-active members have a small initial curvature to assure their direction of bending, once the contracting elements are activated in the form-finding process. The elastic members have section dimensions of 240 mm width (W) and thickness (T) values of 5, 10, 15, 20 and 25 mm. They are divided in the longitudinal direction into a number of segments of 50 mm length each, so as to increase the analysis accuracy, and are then

assigned to PTFE; that is, a polytetrafluorethylene material with unfilled grades, which exhibits a low elastic modulus, E, of 2.5 GPa and a relatively high yield strength, σ_{Rd}, of 48 MPa. These values have been used in the analyses, whereas a linear stress-strain behaviour of the material has been assumed. The cable elements have 10 mm diameter and are assigned to prestressed steel Y1770 (EN1992) of 195 GPa elastic modulus and 1520 MPa yield strength.

The specific static analyses conducted in accordance to the third order theory (TH3), take into account geometrical nonlinear effects, as well as effects resulting from the geometrical system modification, e.g. snap through effects, length modification and large deformations (SOFiSTiK AG, 2014a). The material selected for the elastic members has a linear elastic stress-strain behaviour to allow the analysis to focus on the geometrical aspects of the active formation process. Buckling of the members under loading has not been considered in the analyses. Throughout the form-finding process, the analysis model seeks to create multiple sequential, nonlinear analysis steps that follow the actual physical model assembly in an analogous way. The absolute tolerance limit of residual stresses in each analysis step is set to 0.001 kN and the iteration cycles are set to 200, in order to ensure successful analysis convergence and adequate calculation precision for each successive step (SOFiSTiK AG, 2014b). As stated in (Lafuente-Hernandez, Baverel and Gengnagel, 2013), the incremental induction of bending deformation (progressional cable shrinkage values) confidently disables any convergence problems that commonly appear in nonlinear analyses with large deformations. The inner stresses and strains, developed in each nonlinear analysis step, are stored in the model, and the respective loads applied in any following step act as complementary to the existing ones. In this frame, residual stresses of the elastic members are referred to as the prestress, which is induced in the form-finding process through shrinkage of the connecting main cable. This impacts noticeably on the stiffness of the systems that works in favour of structural performance (Chini and Wolde-Tinsae, 1988).

Therefore, in bending-active structures, the stiffness matrix is split into the elastic stiffness matrix K_e, the initial displacement stiffness matrix K_i and the geometric stiffness matrix K_g, which is computed based on the stress state of the previous equilibrium iteration.

$$(\boldsymbol{K_e} + \boldsymbol{K_i} + \boldsymbol{K_g}) \cdot \boldsymbol{u} = \boldsymbol{F} \tag{4.1}$$

It can be generalized that in nonlinear system analysis, the geometric member stiffness is influenced by the strains and stresses within the members of the structure. In this frame, stress-stiffening is referred to as the stiffening effect of tension forces or stresses on the geometric stiffness matrix. As this stiffening effect develops primarily in systems with low elastic stiffness, it is usually only considered for slender structures with small bending stiffness compared to axial stiffness, such as thin beams. The geometric nonlinearities that are inherent to bending-active members may lead to stress stiffening effects that work in favour of the structural performance. This influence on the system stiffness will be of importance in the analysis of the structural behaviour of the single-segment configurations. Hence, prestress of the elastic members is used in the case studies analysed, induced through shrinkage of the connecting cable, to increase the stiffness of the elastic members based on the geometric nonlinear consideration of stress stiffening. In this frame, residual stresses of the elastic members are referred to as the prestress that is induced to the elastic members throughout the form-finding process and before their external loading, and remains in the members after their original cause is removed.

The nonlinear FEA form-finding methodology developed in the current Ph.D. thesis has been adopted in a series of graduate bending-active prototype research projects at the University of Cyprus. These are documented in (Kontovourkis *et al.*, 2016; Alexandrou, 2017; Phocas, 2017; Anastasiadou, Alexandrou and Phocas, 2018; Phocas *et al.*, 2018; Phocas, Alexandrou and Zakou, 2018).

CHAPTER 5 NUMERICAL ANALYSIS OF SINGLE-SEGMENT STRUCTURAL CONFIGURATIONS

The structural behaviour of the single-segment structural configurations is investigated for the stages of fastening, prestress and vertical loading. The analyses results are presented separately for each unit, while reference is primarily made to a typical elastic member's section dimensions of 240 x 15 mm. The results obtained for four additional differentiated elastic members' thickness values, of 5, 10, 20 and 25 mm are included in the figures and are briefly documented. Figures 5.1 and 5.4 – 5.7 present the members inner forces (y-axis) developed in all stages of development, i.e. fastening, prestress and vertical loading (x-axis). It is noted that the prestress stage includes all required cable shrinkage steps. Furthermore, the capacity and limitations of the elastic members due to the material's yield limit strength are discussed, while interdependencies in the nonlinear behaviour of the structural components, i.e. elastic members and main cable, are identified.

5.1 Structural Behaviour

5.1.1 Unit 1

Unit 1: Analysis under the action of main cable length reduction (Prestress)

Unit 1 constitutes the simplest system configuration and demonstrates a similar axial forces development between the bending-active member (N) and the main cable (C) (Fig. 5.1). With regard to the typical section of the elastic member, the axial force reaches 1.7 kN in the first 100 mm of cable shrinkage, in analysis step 1, namely, 77 % of its maximum value of 2.2 kN developed in the final step. In the in-between steps, a nearly linear development is recorded, with lower incremental values of approximately 7 %. A similar effect is also observed in the bending moment (M) development of the typical elastic

member; the bending moment of 0.33 kNm from step 1, reaches 40 % of its maximum value of 0.83 kNm developed at the end of the prestress process. However, at this stage, a relatively lower increase rate of 45, 27, 18, 15 % takes place in each consecutive analysis step respectively. The maximum bending moment in step 1, and its increase ratio in the subsequent steps, are directly proportional to the respective deformations of the elastic member at midspan (Fig. 5.2). The shear forces (V) are proportional to the bending moments, due to the fact that unit 1 develops only upward curvature deflections (positive values). In step 1, the shear force amounts to 1.02 kN, i.e. 46 % of the maximum value of 2.22 kN obtained in step 5.

The dynamic behaviour of the structural unit is shown in the first three eigenmodes in Figure 5.3. The dynamic analysis takes into consideration the geometrical modifications and deformations of the system, i.e. P-Δ effects, during the assembly process. While the main natural frequency of the unit amounts to 7.26 Hz, the elastic member has frequencies of 13.18, 50.18 and 102.72 Hz in the first three eigenmodes respectively, without causing any movement to the sliding support.

Unit 1: Analysis under vertical loading

In the consecutive vertical loading stage (Q), the elastic member's and cable's axial force rises further by 14 and 10 %, with maximum values of 2.5 and 2.45 kN respectively. As opposed to the prestress stage, where the axial stresses in both the elastic member and cable element followed an analogous increase, in this case, the external loading primarily influences the elastic member in compressive stress. The maximum bending moment shows a minor decrease of 2.5 % and the shear force increases to 7 %. The maximum vertical deformations of the elastic member at midspan are presented for all section thickness values, and for both stages of analysis, in Table 5.1. The results indicate practically no dependency of the deformations on the elastic members' thickness.

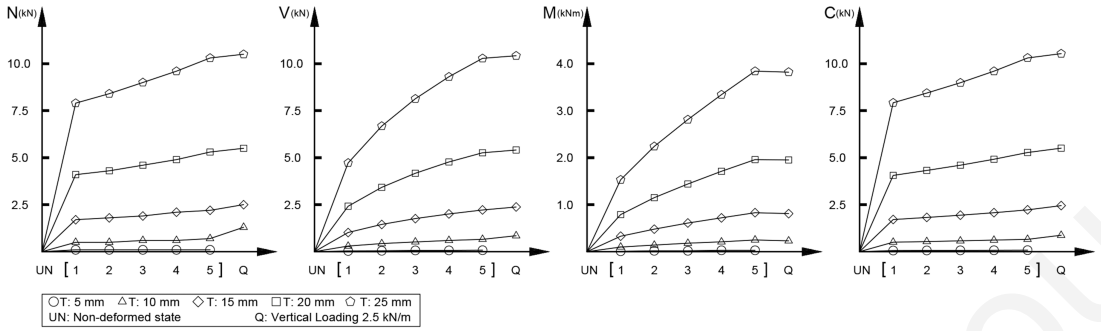

Figure 5.1 Numerical analysis results for unit 1

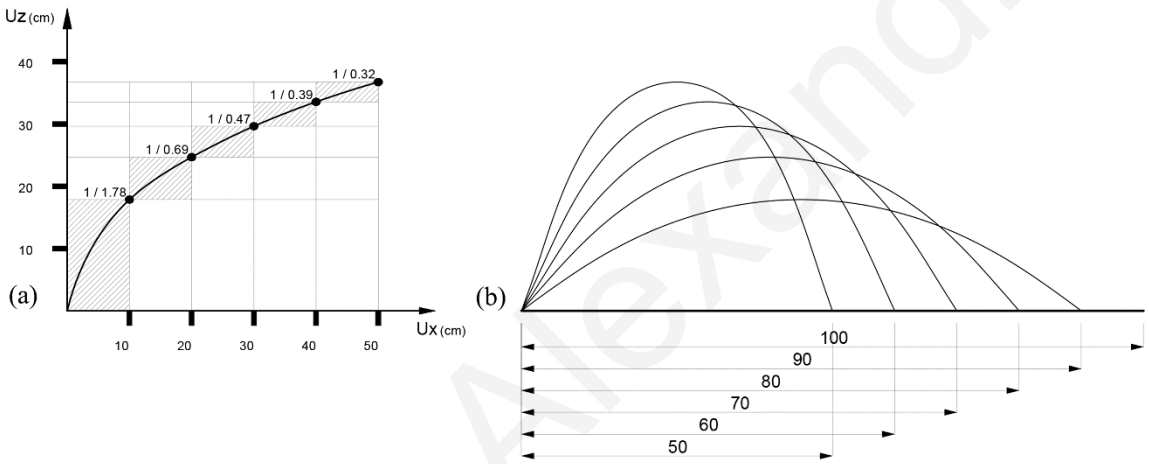

Figure 5.2 Unit 1 deformation analysis. (a) X to Z-direction displacement ratio and (b) deformation curve in each cable shrinkage analysis step of 100 mm

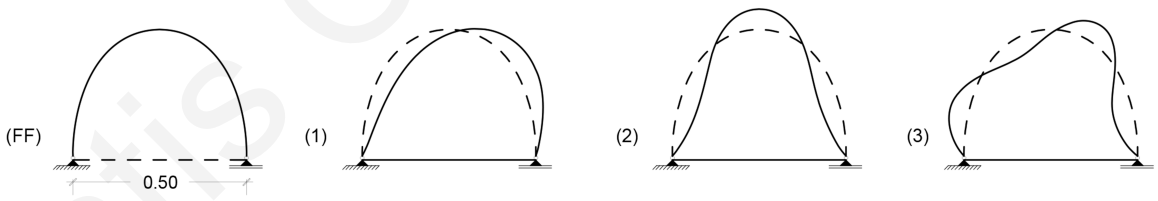

Figure 5.3 Unit 1 and first (1), second (2) and third (3) eigenform of its elastic member

Table 5.1 Unit 1 vertical deformation at midspan in all analysis stages for different thickness values of the elastic member[mm]

Unit	Stage of Analysis	T: 5	T: 10	T: 15	T: 20	T: 25
Unit 1	Prestress	367	367	367	367	367
	Q	-	362	365	367	367

The load-bearing response of unit 1 was analysed individually in all steps of the prestress stage, in order to assess how the initial bending radius magnitude affects the post-stressing of the unit. Hence, the response of the unit was compared at the end of each cable shrinkage step with its response under vertical loading in the respective step (Fig. 5.4). It should be noted that the numerical response values for each step of the elastic member's prestress without vertical loading are identical with the respective values in Figure 5.1. The analysis results indicate substantially increased axial forces in the initial prestress analysis steps, in both, the elastic member and the main cable. In addition, the lower the initial axial force is, the higher the intensification becomes after loading. The vertical load causes an increase of the axial force of the elastic member of 94, 50, 32, 14 and 4 % in all successive prestress steps respectively. In the initial prestress analysis steps, the unit also experiences slightly increased bending moments and decreased shear forces. The vertical deformations of the unit, in its five prestress analysis steps, show minor sensitivity to the vertical loading. While the deformation fluctuation in step 2 is zero, a respective maximum value of 2 mm is registered in the final prestress analysis step (Table 5.2). The non-proportional load-deformation behaviour of the unit throughout the prestress stage is due to the respective change of curvature of the elastic member and thus, the projected uniform vertical load on the elastic member, as well as the inclination of the elastic member on the supports.

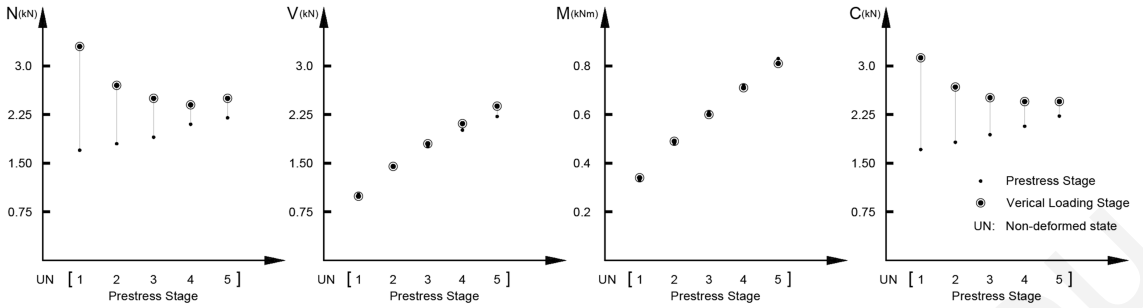

Figure 5.4 Numerical analysis results for unit 1 with elastic member's section thickness of 15 mm, under prestress and vertical loading in different configurations of 100 mm displacement steps in X-direction

Table 5.2 Unit 1 vertical deformation at midspan in all steps of prestress stage [mm]

	Stage of Analysis	Step 1	Step 2	Step 3	Step 4	Step 5
Unit 1	Prestress	190	261	309	343	367
	Q	189.5	261	308.5	342	365

Unit 1: Elastic member's thickness differentiation

The modification of the elastic members' section thickness from 5 to 25 mm causes a uniform differentiation of the developed inner forces and moments of the structural unit (Figure 5.1). Compared to a cross section thickness value of 15 mm, respective fluctuations of the maximum axial forces in the elastic member amount to 5, 32, 140 and 368 % for thickness values of 5, 10, 20 and 25 mm respectively; with 0.1 kN minimum axial force for 5 mm and 10.3 kN maximum axial force for 25 mm thickness. Respective maximum bending moments developed in the elastic member amount to 4, 30, 136 and 362 %; with 0.03 kNm minimum bending moment for 5 mm and 3.84 kNm maximum bending moment for 25 mm thickness. Similarly, respective shear force fluctuations amount to 4, 30, 136 and 363 %; with 0.07 kN minimum shear force for 5 mm and 10.28 kN maximum shear force for 25 mm thickness. The cable's tension force follows the same exponential pattern as the elastic member's axial force. The case of elastic member's thickness of 5 mm fails to enable it to withstand vertical loading due to extreme deformation.

5.1.2 Unit 2

Unit 2 exhibits identical responses by the elastic members in all stages of the analysis as in the case of unit 1. The additional elastic element in the unit induces double the amount of axial force in the main cable element.

5.1.3 Unit 3 and 4

Unit 3 and 4: Analysis in fastening and prestress stage

In unit 3 and 4, the upper (secondary) elastic member exhibits similar behaviour as that of unit 1 (Fig. 5.5). This is due to the absence of any shear connection between the elastic members. In the fastening stage, the initial axial force developed in the upper elastic member amounts to 1 kN; namely, 77 % of the axial force of 1.3 kN developed in the prestress stage. Throughout the form-finding process, the axial force is subjected to a constant increase rate of approximately 6 %. Similar effects are observed in the development of the shear force. In the fastening stage, the shear force reaches 0.88 kN, 69 % of the maximum value of 1.27 kN in the prestress stage. The respective increase rate amounts to approximately 8 %. The lower (primary) elastic member develops higher axial and shear forces compared to the upper elastic member in all prestress analysis steps, reaching an increase of 69 and 34 % in the final analysis step of the prestress stage respectively. The development of bending moments follows a comparatively different trajectory. The upper member maintains a higher value up to step 2, an equal value in step 3 and lower ones in step 4 and 5. This indicates that the developed bending moment in the elastic members is proportional to its bending radius. The upper member reaches 0.42 kNm in the fastening stage, that is, 60 % of the maximum bending moment of 0.70 kNm developed at the end of the prestress stage. The respective increase rates, in the prestress analysis steps, amount to 14, 12.5, 9, 10 and 8 %. At the end of the prestress stage, the lower elastic element has 19 % higher bending moment compared to the upper one. Furthermore, if one compares the two members' responses for similar deformation magnitudes, when both members have a horizontal displacement equal to 1/5th of their

initial non-deformed span, i.e. the upper elastic member at the form-found state and the lower member in prestress step 2, one finds that the lower member develops higher axial and shear forces, due to its relative higher geometric stiffness. By contrast, the curvature of the members and their bending moments are approximately constant. The cable's axial force equals to the sum of the two bending-active members' axial forces in all prestress analysis steps.

Unit 3 and 4: Analysis under vertical loading

The vertical load acts on the outer side of the upper elastic member. By consequence, there is no actual synergy between the simply-paired members, which entails that the upper elastic member is more vulnerable to vertical deformations. The analysis results show clearly that the lower elastic member stays unaffected by the imposed loads, while the upper elastic member's axial force increases by 8 %, reaching the value of 1.4 kN, while, the cable's axial force also increases by 3 %, reaching 3.55 kN. Comparatively, the shear force also increases by 31 %, attaining a value of 1.66 kN, and the bending moment decreases slightly to 0.05 kNm.

Unit 3 and 4: Elastic members' thickness differentiation

Thickness modification of the elastic members causes a similar behaviour of the units to unit 1 with regard to the maximum inner forces and bending moments. Compared to a 15 mm thickness value of the elastic members, the inner forces in the lower elastic member fluctuate between 4, 20, 138 and 362 % for thickness values of 5, 10, 20 and 25 mm respectively. The respective fluctuations for the upper elastic member amount to approximately 4, 50, 135 and 360 %. Similarly, the cable's axial force fluctuates between 4, 28, 136 and 360 %. A section thickness selection of 5 and 10 mm for the elastic members does not prevent collision between them under vertical loading and therefore, fails to provide valid results (Table 5.3).

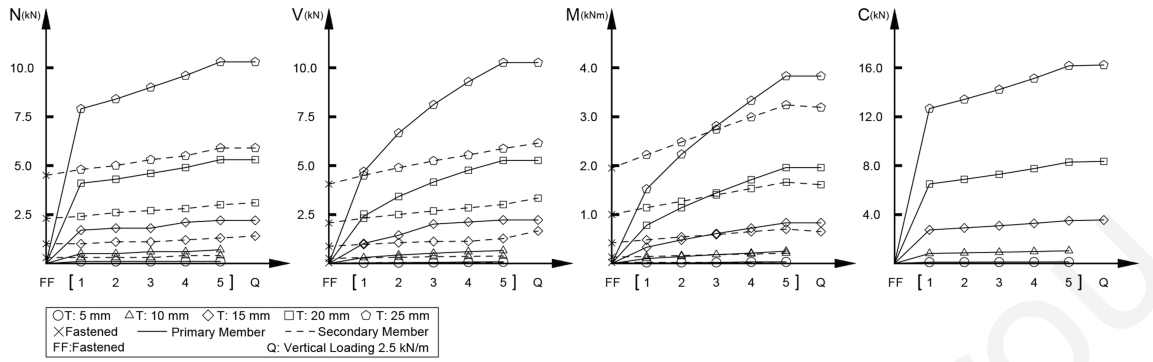

Figure 5.5 Numerical analysis results for unit 3 and 4

Table 5.3 Unit 3 and 4 upper elastic member vertical deformations at midspan in all analysis stages for different thickness values [mm]

	Stage of Analysis	T: 5	T: 10	T: 15	T: 20	T: 25
Unit 3 and 4	Fastening	425	425	425	425	425
	Prestress	547	547	547	547	547
	Q	-	-	537	543	545

5.1.4 Unit 5

Unit 5: Analysis in fastening and prestress stage

In unit 5, due to exceeded horizontal displacements caused on the elastic pair in the fastening stage, the total number of steps in the succeeding prestress stage is reduced to four (Fig. 5.6). In this configuration case, a proportional distribution of axial force between the elastic members and the main cable is no longer evident. The cable's initial axial force developed in step 1 of the prestress process is much lower than the elastic members' axial force sum. Nonetheless, the increase rate in the following steps is exponentially higher; in step 1, a respective value of 0.98 kN is recorded that amounts to 35 % of the maximum value of 2.77 kN developed in the final step. In step 2 and 3 the cable's axial force reaches 63 and 82 % of the maximum value. This indicates that the fastening technique causes a differentiated development of the axial forces in the two members of the unit. In general,

the inner forces and bending moments developed in the elastic members in the fastening stage, differ substantially from the ones experienced in the single, or simply-paired stripes. In both elastic members, the axial force reaches the highest level in the fastening stage and drops significantly in the following prestress stage. Initial axial forces recorded in both elastic members in the fastening stage reach 6.5 kN, which is 195 and 400 % higher in the lower and upper member than the respective unit 3 and 4 prestressed stage, where members are simply-paired. In the prestress stage, the axial force of the lower (primary) elastic member drops to 83, 72, 68 and 66 % of its initial value while, the upper (secondary) member drops to 92, 86, 80 and 75 %, in all four analysis steps respectively. Due to the increased curvature of the upper elastic member, shear forces and bending moments are higher than in the lower member. The shear force in the fastening stage amounts to 5.81 kN and decreases to 94, 88, 83 and 79 %, whereas the initial bending moment amounts to 1.08 kNm and decreases to 98, 95, 94 and 94 %. The shear force of the lower elastic member reaches 3.74 kN and rises further to a percentage of 8, 14, 17 and 19 %. The bending moment amounts to 0.7 kNm and increases further to 20, 41, 60 and 77 %. It is also worth noting that, in the prestress stage, the bending moments and deformations of the lower member exceed those of the upper member.

Consequently, although the lower member's shear force and bending moment increase, the axial force and all inner forces of the upper member tend to decrease at much lower value. Compared to both elastic members' maximum response values, the axial force drops from 6.5 to 5.1 kN, the shear force from 5.81 to 4.59 kN while, the bending moment rises from 1.08 to 1.18 kNm. The elastic members' fastening causes the elastic pair to develop considerably higher inner forces compared to the initial step of the prestress stage. This consequently contributes to an early increase of the stiffness of the system within the fastening process, while, at the same time, it leads the system to a more critical condition in terms of the material's yield limit.

Unit 5: Analysis under vertical loading

In the vertical loading stage, all inner forces of the lower elastic member decrease, whereas they rise in the upper elastic member. The cable's force experiences a negligible tension increase of just 0.01 kN. The lower elastic member's axial force falls to 3.5 kN, i.e. 81 %, compared to the respective value in the prestress stage; the shear force falls to 3.79 kN, i.e. 85 %, and the bending moment to 1.18 kNm, i.e. 95 %. The upper elastic member's axial force rises to 5.1 kN, i.e. 104 %, the shear force to 5.14 kN, i.e. 112 %, while, the bending moment remains stable. This is due to the deformed non-arch-like shape of the upper elastic member, which induces a cantilever-like load transfer on each side of the unit, and slightly releases the lower elastic member.

Unit 5: Elastic members' thickness differentiation

Thickness modification of the elastic members causes a similar behaviour of the units as the previously analysed ones with regard to the maximum inner forces and bending moments. Compared to a 15 mm thickness value of the elastic members, the inner forces in the lower elastic member fluctuate between 4, 30, 130 and 340 % for thickness values of 5, 10, 20 and 25 mm respectively. The respective percentages for the upper elastic member fluctuate between 4, 30, 132 and 350 %. Similarly, the cable's axial force fluctuates between 4, 30, 132 and 348 %. The selection of a section thickness of 5 mm for the elastic members fails to sustain limited deformation and leads to collision of the two elastic members under vertical loading (Table 5.4).

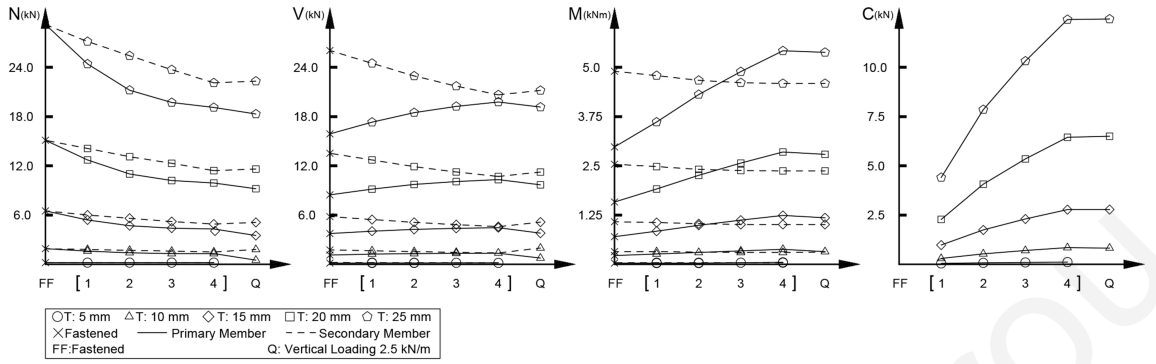

Figure 5.6 Numerical analysis results for unit 5

Table 5.4 Unit 5 vertical deformation at midspan in all analysis stages for different thickness values [mm]

	Stage of Analysis	T: 5	T: 10	T: 15	T: 20	T: 25
	Fastening	216	216	216	216	216
Unit 5	Prestress	370	370	370	370	370
	Q	-	363	368	369	370

5.1.5 Unit 6

Unit 6: Analysis in fastening and prestress stage

Unit 6 comprises a multi-interconnected, hybrid cable bending-active system. The unit necessitated only two steps of cable shrinkage in the prestress stage to reach the span of $L_0/2$, except for the elastic members' section thickness of 10 and 15 mm that merely required a single step to reach the target position. Compared to the other hybrid assemblages, unit 6 experiences a significant shift towards a much higher domain of inner stressing (Fig. 5.7). The initial maximum axial force extends to 19.5 and 18.2 kN for the lower and upper (primary and secondary) elastic member respectively. In the prestress stage, the lower elastic member's axial force drops to 17.9 kN, i.e. 91 %, and the upper elastic member's axial force rises to 18.4 kN, i.e. 101 % respectively. A maximum shear force of 7.83 and 15.61 kN is recorded in the fastening stage, while, in the prestress stage, it exhibits a negligible increase of just 0.02 kN in the lower elastic member. The respective value in the upper elastic member amounts to 15.61 kN, i.e. 5 %. The maximum bending

moment developed in the elastic members in the fastening stage amounts to 1.66 kNm, which is 54 % higher than the respective value of the paired-interconnected elastic members in unit 5. The lower elastic member develops a bending moment of 1.0 kNm while, the upper elastic member reaches 1.66 kNm. In the prestress stage, the upper elastic member records a negligible decrease, while the lower elastic member slightly increases to 0.7 %. The cable's axial force in the prestress stage is 0.51 kN.

Unit 6: Analysis under vertical loading

In the vertical loading stage, both, axial and shear force experience a minor increase, while the bending moment remains constant. The cable's axial force records an insignificant increase to just 0.01 kN.

Unit 6: Elastic members' thickness differentiation

Compared to a 15 mm section thickness value of the elastic members, the inner forces in the lower elastic member fluctuate between 4, 30, 130 and 320 % for thickness values of 5, 10, 20 and 25 mm respectively. The respective percentage fluctuations for the upper elastic member amount approximately to 4, 30, 120 and 300 %. The cable's axial force fluctuates between 86, 30, 272 and 830 %. The selection of a section thickness of 5 mm for the elastic members fails to sustain controllable deformation and leads to collision of the members under vertical loading (Table 5.5).

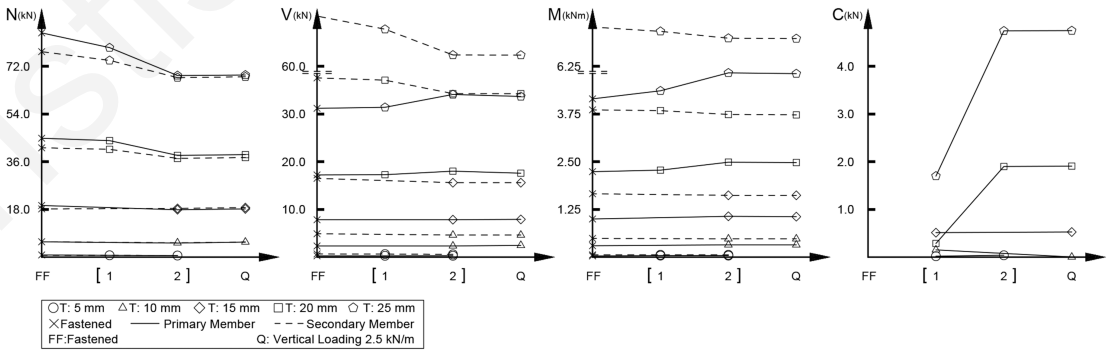

Figure 5.7 Numerical analysis results for unit 6

Table 5.5 Unit 6 upper elastic member vertical deformation at midspan in all analysis stages for different thickness values [mm]

	Stage of Analysis	T: 5	T: 10	T: 15	T: 20	T: 25
	Fastening	403	425	424	411	400
Unit 6	Prestress	438	438	431	434	431
	Q	-	432	435	434	430

5.2 Stress Design

The stresses of the elastic members, developed in the form-finding stage, as well as any additional amount stored under the external loading of the system, should be kept within the elastic region, i.e. below the material's yield strength limit σ_{Rd}. Ideally, materials with high ratio of elastic modulus to yield strength (E/σ_{Rd}) enable a high variety of deformed shapes and consequently, of configurational transitions. The displacement target of $L_0/2$, in the prestress stage of the units under investigation, was deliberately selected to give insight to the deformation behaviour of the units, despite exceeding the selected material's elastic zone of deformation. The structural analyses of the units in the form-finding stage, as well as the subsequent vertical loading stage, have proven that single and simply-paired hybrid configurations like units 1 to 4, extend the range of stress fluctuations, especially in the prestress stage, as opposed to the single, or multiple, paired-interconnected configurations, like units 5 and 6 respectively (Fig. 5.8). The latter have shown that, apart from developing exceeded stresses, they also exhibit very low fluctuations, minimising, in this respect, their configuration potential. The relatively high stresses, developed in the elastic members' sections of over 15 mm thickness, exceed the yield strength of PTFE (48 MPa). This suggests that the design of elastically deformable structural units should be retained at a low thickness value range and low target deformation curvatures.

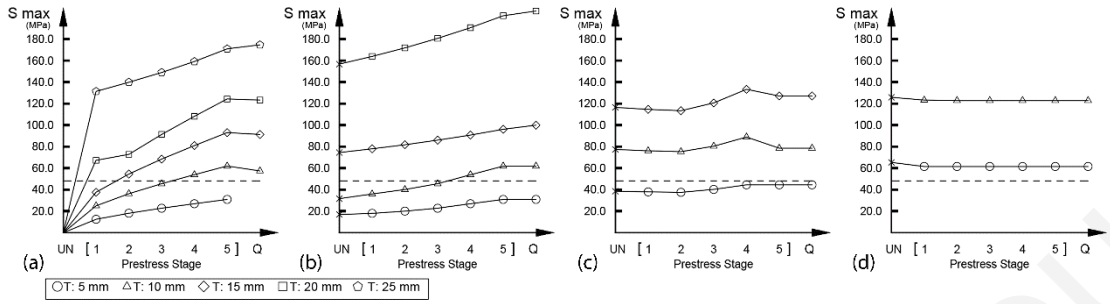

Figure 5.8 Absolute maximum stress of all units in prestress and vertical loading stage; (a) unit 1 and 2, (b) unit 3 and 4, (c) unit 5, (d) unit 6

5.3 Components' Interdependencies

This section discusses the interrelated structural behaviour between the two main components of the hybrid units, i.e. the elastic members and the main cable, and the situations, whereby such interdependencies are considered beneficial in terms of improved performance and applicability of the systems. The results are different for the single and simply-paired units, 1 to 4, and the paired-interconnected units, 5 and 6, following the respective differentiation in their fastening technique (Fig. 5.9).

The cable axial force in the single and simply-paired configurations at the prestress stage corresponds to the elastic members' axial force increase. The coupling of same-length elastic members, as in the case of unit 2, doubles the cable's axial force. The coupling of elastic members with a longer secondary member, as in unit 3 and 4, brings the cable's axial force into an in-between value compared to the single and coupled case of same-length members. In this respect, the length of the secondary elastic member can be used as a design tool in defining, or manipulating, the range of the cable's axial force and the overall stiffness of the unit. In all simply-paired cases, there is a nearly linear increase of the inner forces compared to the gradual cable's axial force increase. In composite, interconnected pairing cases, the nonlinear behavioural relationship already developed between the elastic members in the fastening stage, yields a much higher increase of the tension of the main cable in the prestress stage. The already high amount of inner forces, developed in the elastic members, is further manipulated in the prestress stage, although

at a much lower degree compared to the simply-paired cases. Fluctuations are limited and constrained within a smaller domain. In the vertical loading stage, the interconnected-pairing cases have proven to be very efficient in terms of their load-bearing capacity. Both the cable's axial force and the elastic members' forces remain stable or experience negligible increase.

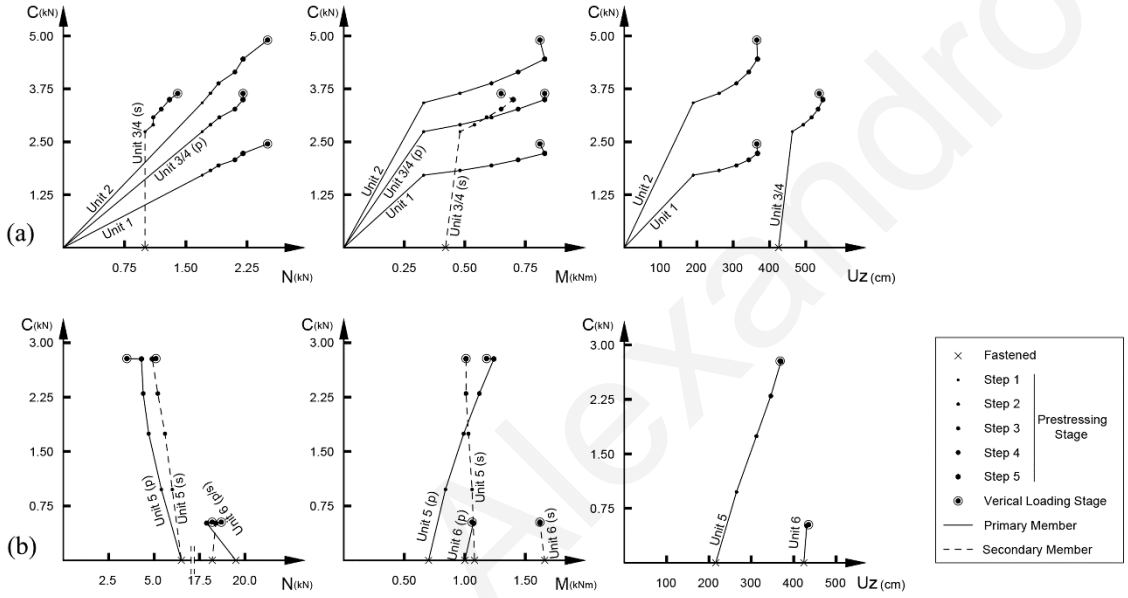

Figure 5.9 Structural interdependencies between cable's axial force and elastic members' inner forces and vertical deformation for (a) single and simply-paired units 1, 2, 3 and 4 and (b) paired-interconnected units 5 and 6. All examined cases are of 240/15 mm elastic members' section thickness

The maximum response values of the units are summarized in Table 5.6, differentiated in simply-paired and paired-interconnected with elastic members' section of 15 mm, for the final stages of prestress and vertical loading, Q. The analyses results verify higher stiffness of the elastic members in paired-interconnected units.

Table 5.6 Maximum units' responses in prestress and vertical loading stage

	Deformation	Elastic Member			Cable	Elastic Member
	U(z) [mm]	N(x) [kN]	V(z) [kN]	M(y) [kNm]	N [kN]	$f_1\|f_2\|f_3$ [Hz]
Simply-Paired Units 1 - 4						
Prestress	547	2.2	2.22	0.83	4.45	13.18|50.18|102.72
Q	537	2.5	2.38	0.83	4.90	
Paired-Interconnected Units 5 & 6						
Prestress	370	18.4	15.6	2.77	2.77	14.22|60.36|89.04
Q	368	18.7	15.6	1.62	2.78	

5.4 Physical Models

All single-segment structures with downward concave configurations (single-segment configuration 1, 3, 5 ,6) have been fabricated and physically modelled in actual scale (Fig. 5.10). The physical prototyping aims at validating the deformation behaviour of the numerical FEA with regard to the systems' form-finding. The elastic stripes are fabricated using white PETG Sheets (VIVAC), a material which exhibits a tensile strength of 53 MPa and flexural modulus of 2.14 GPa. The elastic stripes are hinge connected to rectangular MDF plates at both ends. The supports are able to undergo translation in longitudinal axis and be locked at any location using a series of socket screws. For enabling these physical conditions, the MDF plates are installed on a double rail perforation of a 2 m long elevated MDF deck. The interconnection fastening of case 3, 5 and 6 single-segment configurations has been manually performed using steel bolts and flat washers at 1/4 and 3/4 of the elastic stripe's width. In Figure 5.10, the gradual stepwise physical form-finding process of the selected configurations is demonstrated. The examined cases perform an almost identical deformation behaviour to the digitally analysed models.

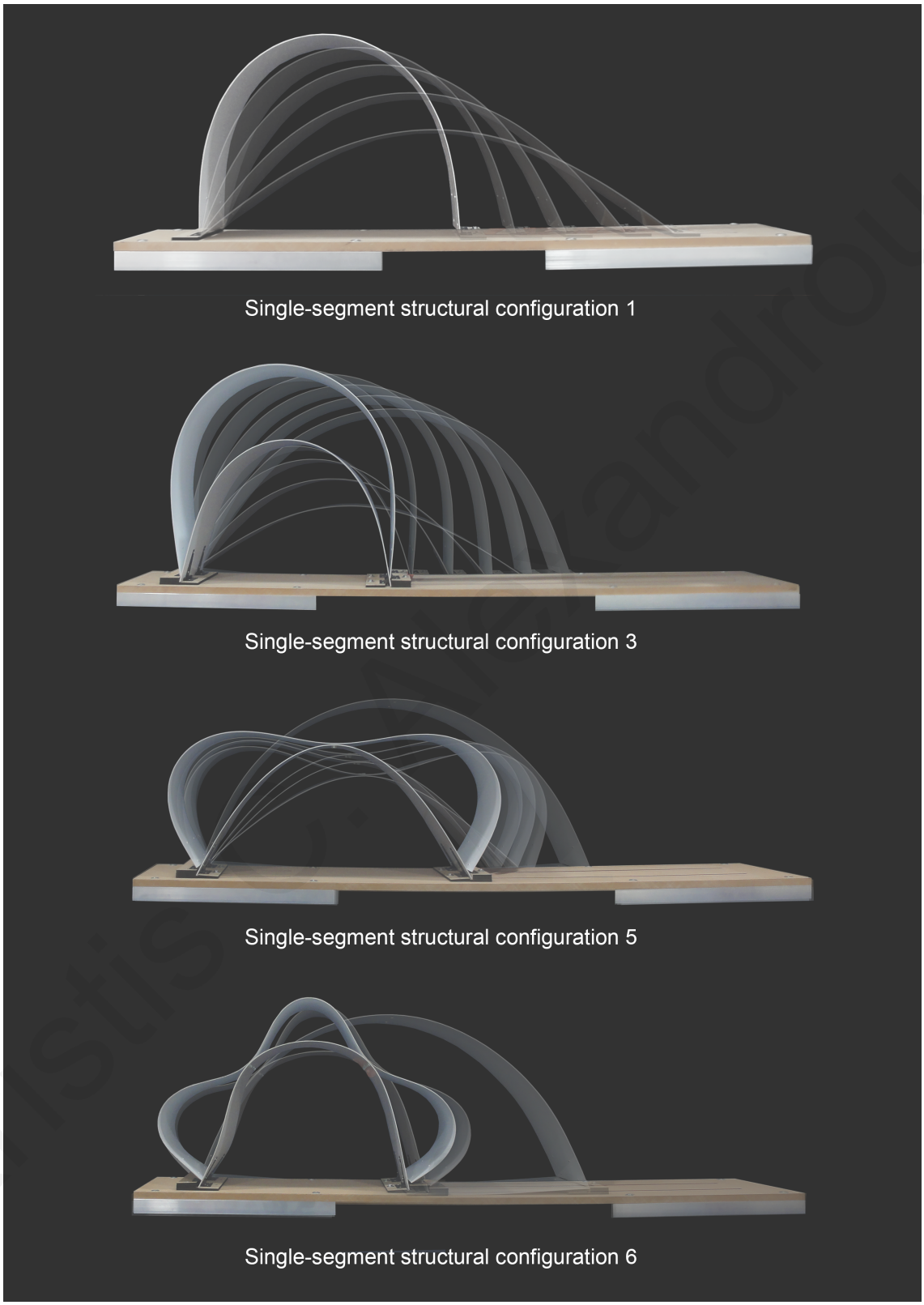

Figure 5.10 Single-segment structural configuration physical modesl; Scale 1:1

5.5 Conclusion

A series of reconfigurable cable bending-active structural single-segment units has been introduced in the present Chapter. The units are composed of single, simply-paired and paired-interconnected elastic members, coupled with a main cable element. The proposed units follow a soft mechanical approach in achieving adaptiveness and configurability, while maintaining vertical deformation resistance under external loading. Both form-finding and vertical load-bearing behaviour investigations follow a progressive step by step FEA, taking into account the geometrical nonlinearities of the systems, in accordance to the principle material characteristics and structural actions associated with the soft mechanical approach. Simulation of the elastic members' fastening and prestress stage was made possible through shrinkage of auxiliary contracting cable elements. The analyses results for different section thickness values of the elastic elements give evidence to the inner forces and bending moments developed in the units' fastening and prestress stage individually. The interconnecting cable's own shrinkage induces deformation control and prestress of the elastic members. The bending moments developed are directly proportional to the deformation curvatures of the elastic members. In single and simply-paired configurations, an adequate stiffness of the systems, with maximum cable force development, is primarily influenced by the elastic members' thickness and the coupling member's overall length; the elastic member's thickness should be kept at a low value range for the material to remain below its yield strength limit. Under vertical loading, the maximum cable forces increase further while, the maximum bending moments of the elastic members decrease slightly. Although a relatively high stiffness is achieved in paired-interconnected units, the prevailing nonlinearities of the system responses, caused by the internal fastening of the elastic members, result into increased stresses in the elastic members and often fail to keep the system responses in the elastic region. Although asymmetrical vertical load cases and horizontal loads have not been considered in the present analyses, it is well acknowledged that they can significantly affect the performance of the units.

CHAPTER 6 NUMERICAL ANALYSIS OF MULTI-SEGMENT STRUCTURAL CONFIGURATIONS – S1

6.1 Multi-Segment Structural Configurations

In this Chapter, the full potentials of cable bending-active multi-segment structures are examined in configurations of larger structural span, to accommodate basic architectural space requirements. The multi-segment configurations design is based on a linear arrangement of multiple single-segment configurations, composed of a continuous length elastic stripe (see single-segment structural configuration 1 in Chapter 4, Fig. 4.1). The initial characteristics of the systems are based on the results obtained from the single-segment configurations' analysis and limitations examined in the previous chapter. This include the preselection of particular features i.e. stripe's to cables interconnecting distance and stripe section dimensions [W: 250 mm and T: 10 mm].

6.2 Hybrid Systems Analysis

The systems are examined in their form-finding and load-deformation behaviour subjected to uniform vertical loading, at the respective erection *(ii and ii&Q)* and post-tensioning stage *(iii and iii&Q)*, Fig. 6.1. The analysis results are presented in Table 6.1. The systems' erection *(ii)* is activated through uniform cables' length reduction and sliding of one of the supports in longitudinal direction (x-axis). All cables are gradually uniformly reduced in length until the sliding support reaches an inward target displacement of half the initial non-deformed *(i)* span length of $L_0/2$. The cables induce local bending deformations to the respective elastic member, forcing the system to obtain a global semi-circular shape. Following modification of the sliding support into fixed, the systems are further deformed through additional cables' length reduction in the post-tensioning stage *(iii)*. The amount of uniform cables' length reduction corresponds to a maximum stress utilization of the

elastic member of approximately 95 %. The value for the vertical loading applied at the end of each development stage *(ii&Q and iii&Q)* is defined based on the stress capacity of the system at its erection stage *(ii)*. The external load has been applied on the systems in increments of 0.01 kN/m, whereas the cables' axial force has been monitored in avoiding complete relaxation of the members.

6.2.1 Erection stage

The amount of uniform cables' length reduction, Δl_c, that is necessary to achieve the target ground support displacement to $L_0/2$, reduces with increasing cable segments in each system. For the two-cable system configuration, a respective value of 211.6 mm is required, whereas with increasing cable segments, the cables' length reduction decreases to 116.6, 67.6, 46.5, 33.9, 26.6 and 21.6 mm respectively. This development corresponds to the stress utilization of the elastic member, σ_x, registering values of 76, 53, 40, 32, 27, 23 and 21 % of its yield strength. The cables' maximum axial force development, C_n, amounts to 0.56, 0.53, 0.48, 0.48, 0.45, 0.44 and 0.43 kN with increasing number of cable segments respectively. In systems with more than two cable segments, the maximum axial force develops in the elements close to the supports. Due to the resulting symmetrical configurations of the systems, the cables' axial forces are equal in the elements to the respective mirror positions, i.e. C_1 with C_8. The elastic members locally developed compression forces are practically proportional to the respective cables' axial tension forces. The bending moments are also proportionally equal to the stress development. The deformed systems span to height ratios, L/H, amount to 1.59, 1.44, 1.48, 1.45, 1.46, 1.45 and 1.45 for the two to eight segments systems respectively.

Load-deformation behaviour

The system response under vertical loading *(ii&Q)* is primarily determined by the cables' axial force development and more prominently by the ones close to the supports, i.e. $C_{1,8}$. These are responsible for absorbing a high amount of the imposed loads, resulting in a respective decrease of their tension force. In systems with high numbers of cable segments,

the elements' tension force at mid-span increases slightly. As mentioned above, the magnitude of the uniformly distributed vertical load assigned at the end of the system erection is calculated following a gradual loading of 0.01 kN/m until the axial force of the cables close to the supports is eliminated. Further increase of the vertical load causes sudden deformations and instabilities, due to lateral bucking of the elastic member at its two ends. In this respect, the maximum vertical loading for each system with increasing number of cable segments amounts to 1.30, 0.60, 0.25, 0.12, 0.08, 0.05 and 0.04 kN/m respectively. The cables maximum axial force records values of 0.0, 0.61, 0.55, 0.71, 0.63, 0.69 and 0.92 kN. The stress utilization of the elastic member undergoes a slight increase of 2, 2, 6, 3, 2, 2 and 4 % in each case respectively. The system deformation at mid-span for the two and three cable segments systems is zero, whereas in systems with more than three cable segments, the maximum deformations amount to 180, 120, 160, 130 and 330 mm.

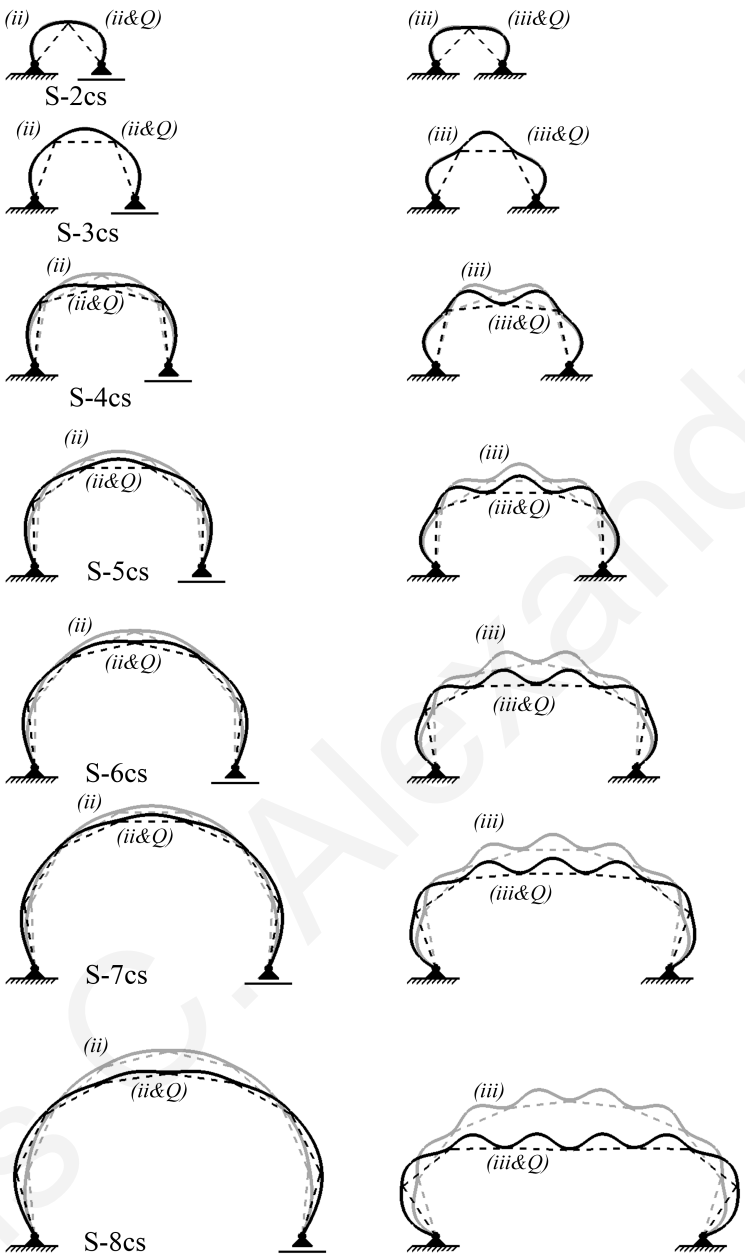

Figure 6.1 Deformation behaviour of hybrid systems with increasing number of cables from two to eight

Table 6.1 Numerical results of the systems behaviour at erection *(ii)*, post-tensioned *(iii)* configuration and consecutive vertical loading stages *(ii&Q and iii&Q)*

System	Δl_c [mm]	σ_x (MPa)	H [m]	L/H	$C_{1,8}$	$C_{2,7}$	$C_{3,6}$	$C_{4,5}$
S-2cs								
(ii)	211.6	36.43	0.63	1.59	0.56			
(ii) & Q: 1.3	-	37.60	0.63	1.59	0.00			
(iii)	64	45.98	0.54	1.83	0.79			
(iii) & Q: 1.3	-	47.88	0.55	1.83	0.01			
S-3cs								
(ii)	116.6	25.48	1.04	1.44	0.53	0.52		
(ii) & Q: 0.6	-	26.19	1.03	1.46	0.00	0.61		
(iii)	105	46.80	0.99	1.52	0.91	1.30		
(iii) & Q: 0.6	-	47.95	0.99	1.52	0.29	1.19		
S-4cs								
(ii)	67.6	19.09	1.35	1.48	0.48	0.46		
(ii) & Q: 0.25	-	21.98	1.17	1.71	0.00	0.55		
(iii)	105	45.49	1.09	1.83	0.88	1.42		
(iii) & Q: 0.25	-	47.96	0.91	2.20	0.42	1.43		
S-5cs								
(ii)	46.5	15.49	1.72	1.45	0.48	0.45	0.45	
(ii) & Q: 0.12	-	16.65	1.60	1.56	0.00	0.29	0.71	
(iii)	100	46.10	1.53	1.63	0.85	1.45	1.62	
(iii) & Q: 0.12	-	47.89	1.35	1.85	0.48	1.40	1.70	
S-6cs								
(ii)	33.9	12.88	2.05	1.46	0.45	0.41	0.41	
(ii) & Q: 0.08	-	13.96	1.89	1.59	0.00	0.07	0.63	

(iii)	95	45.53	1.59	1.89	0.81	1.42	1.69	
(iii) & Q: 0.08	-	48.00	1.26	2.38	0.43	1.28	1.79	
S-7cs								
(ii)	26.6	11.17	2.42	1.45	0.44	0.39	0.39	0.39
(ii) & Q: 0.05	-	11.74	2.29	1.53	0.00	0.00	0.45	0.69
(iii)	93	46.08	2.00	1.75	0.77	1.37	1.70	1.79
(iii) & Q: 0.05	-	47.96	1.64	2.13	0.43	1.16	1.80	1.89
S-8cs								
(ii)	21.6	9.88	2.76	1.45	0.43	0.37	0.38	0.38
(ii) & Q: 0.04	-	11.90	2.43	1.65	0.00	0.00	0.49	0.92
(iii)	90	46.06	2.02	1.98	0.74	1.32	1.69	1.83
(iii) & Q: 0.04	-	48.01	1.48	2.70	0.37	1.01	1.78	1.95

6.2.2 Post-tensioning stage

In the post-tensioning stage *(iii)*, the sliding support of the systems is fixed and a uniform cables' length reduction is further applied. This leads to higher span to height ratios of the systems and axial forces in the cables. The cable length reductions applied amount to 64, 105, 105, 100, 95, 93 and 90 mm for the systems with two to eight segments respectively. The maximum cables' axial forces amount to 0.79, 1.30, 1.42, 1.62, 1.69, 1.79 and 1.83 kN respectively. The cables' maximum axial forces are by 41, 145, 195, 238, 276 and 326 % higher compared to the resulting ones in the erection stage (ii) of the systems. The post-tensioned span to height ratio of the systems equals to 1.81, 1.52, 1.83, 1.63, 1.89, 1.75 and 1.98 respectively.

Load-deformation behaviour

The load applied in the post-tensioning *(iii)* stage of the systems is equal to the one applied at the former stage *(ii)* for comparison purposes. The axial forces in the cables close to the supports, i.e. $C_4 - C_8$, decrease slightly by 48, 56, 53, 56 and 50 %, while the axial

forces close to the mid-span increase slightly from 1 to 7 %. In systems with cables in intermediate chain locations, the axial force differentiation fluctuates within approximately ±20 % of their initial tension value. The elastic member reaches 100 % of its stress utilization. The vertical deformation at mid-span is zero for the two and three cable-segments systems, while the remaining systems register respective values of 180, 180, 330, 360, 542 mm. Compared to the load-deformation behaviour of the systems at the erection stage *(ii&Q)*, these experience higher vertical deformations at mid-span, while the cables have similar axial force reserves. However, the systems with two and three cable segments can withstand a higher amount of vertical loading without undergoing any deformations. The comparative analysis indicates that apart from the maximum cable axial forces, the systems' configuration is decisive in achieving an improved post-tensioned load-deformation behaviour.

6.3 Cables Contribution

6.3.1 Erection stage

A comparison of the system configuration with eight cable segments to a respective system configuration without cables, helps to distinguish the role of the cables in the system's erection *(ii)* and load-deformation behaviour *(ii&Q)*, Fig. 6.2. The numerical results are presented in Table 6.2. The cable system's form-found shape is obtained through 21.6 mm uniform cables' length reduction. A maximum axial force of 0.43 kN is registered in the cables close to the supports. The elastic member has a maximum compression force N_x of 0.43 kN, which is identical to the maximum tension force in the cables. The elastic member also exhibits a maximum value of 0.11 kN in shear force V_z and 0.04 kNm in bending moment M_y. The maximum stress amounts to 9.88 MPa, corresponding to 21 % utilization of the member's yield strength. The overall static height of the erected structure reaches 2.76 m at mid-span. The span-height ratio equals to 1.45. The system without cables is erected through simulated transition of the sliding support and a point load at the elastic member's mid-span. The 'elastica' curve geometry of the system exhibits lower inner forces

and stresses, compared to the system with cables, while it reaches a lower span to height ratio of 1.33. Consequently, the locally induced deformations of the elastic member through the cables' length reduction stress the system at a higher level. The maximum axial force developed in the case with cables is 139 % higher compared to the bare system. By extent, bending moments and axial forces are uniformly developed along the structure, whereas in the bare system, high values of inner forces are only developed at the member's mid-span (higher curvature) and ends respectively, Fig. 6.3.

Load-deformation behaviour

Under uniform vertical load of 0.03 kN/m, the system with cables clearly demonstrates its ability to increase its load-bearing capacity, Fig. 6.2. The cables act as physical restraints to the elastic member, preventing it from lateral buckling. The hybrid configuration of the system with cables responds to vertical loading with axial stressing of its constituent members, whereas, the bare system undergoes further lateral buckling, resulting in instabilities and large deformations. In the case of the system with cables, the respective cables axial forces decrease in the first two segments by approximately 75 and 100 % and increase in the next two segments by 142 %. The elastic member's bending moment increases slightly from 0.04 to 0.05 kNm. In the bare system, the elastic member's tension force increases at a relative percentage of 33 % and undergoes a higher bending moment development from 0.03 to 0.07 kNm. The respective numerical results are included in Table 6.2 while the diagrams of the inner forces before *(ii)* and after loading *(ii&Q)* are presented in Fig. 6.3.

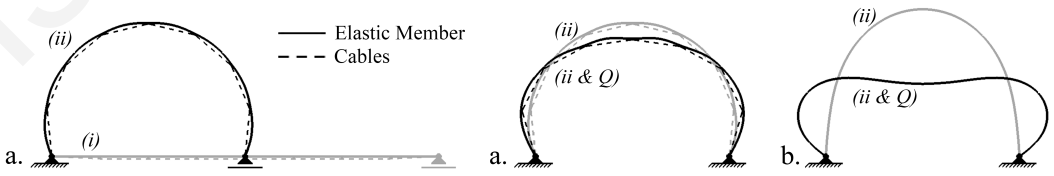

Figure 6.2 System S-8cs with (a) and without (b) cables at erection stage *(ii)* and subsequent vertical loading *(ii&Q)*; Q: 0.03 kN/m

Table 6.2 Elastic member's inner forces and system vertical deformation at erection *(ii)* and consecutive vertical loading analysis stage *(ii&Q)*. Comparison of the proposed system S-8cs with and without* cables. Q: 0.03 kN/m

System	Δl_c [mm]	N_x [kN]	V_z [kN]	M_y [kNm]	σ_x [MPa]	H [m]	L/H	$C_{1,8}$	$C_{2,7}$	$C_{3,6}$	$C_{4,5}$
(ii)*	-	0.18	0.01	0.03	7.93	3.01	1.33	-	-	-	-
(ii) & Q*	-	0.28	0.1	0.07	18.57	1.48	2.70	-	-	-	-
(ii)	21,6	0.43	0.11	0.04	9.88	2.76	1.45	0.43	0.37	0.38	0.38
(ii) & Q	-	0.61	0.34	0.05	9.80	2.63	1.52	0.08	0.00	0.31	0.60

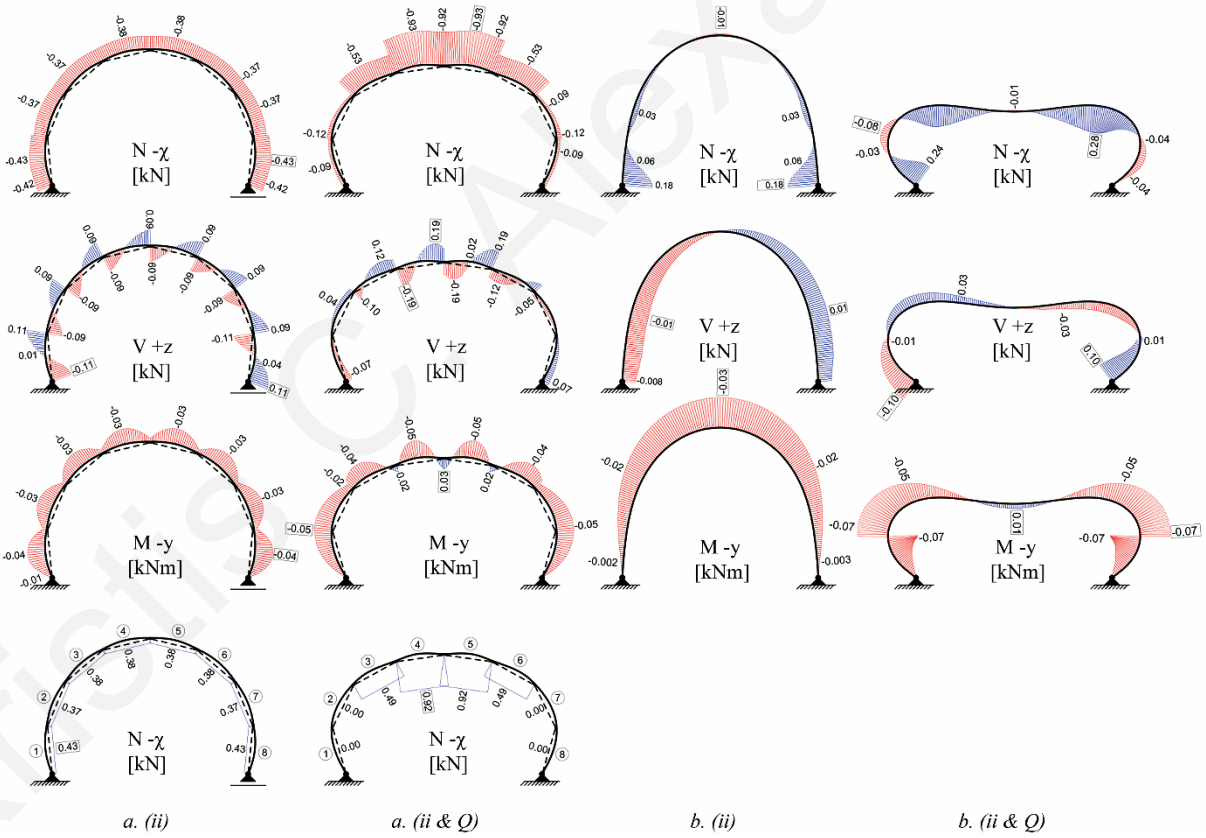

Figure 6.3 System S-8cs inner forces and cables' axial force development at erection *(ii)*, post-tensioning *(iii)* and consecutive vertical loading stages *(ii&Q and iii&Q)*

6.4 Cable Activation

The configurability of the system with eight cable segments is based on custom cable activation scenarios. The system with eight cable segments has been purposely selected for the cables' activation analysis, due to its flexibility, i.e. highest number of cables and lowest stress on the elastic members compared to the other system derivatives at the erection stage *(ii)*. The analysis cases are formulated based on individual or set of cable group activation in the post-tensioning condition *(iii)* of the system. Based on the erected symmetrical system configuration, the cables are divided into four groups, i.e. group A that includes cable 1 and 8, i.e. C_1,C_8, group B with C_2,C_7, group C with C_3,C_6 and group D with C_4,C_5. The examined scenarios are outlined as follows: In scenario one, S-1, individual cable groups are activated, i.e. A, B, C and D. Scenario two, S-2, is based on the simultaneous activation of two cable groups, i.e. AB, AC, AD, BC, BD and CD. Finally, in the third scenario, S-3, a three cable groups' activation is performed, i.e. ABC, ABD, ACD and BCD. The cables' length reduction is limited by two major aspects with regard to the physical and mechanical constraints of the system. Firstly, the cables' action should not lead to inverse bending deformations of any adjacent elastic member's segment. This phenomenon is very likely to occur in S-1, due to the locally increasing bending curvature within the acting segments. In addition, the cables' action should not induce any stress in the elastic member, higher than 95 % of its yield strength, in preserving a respective 5 % stress for the subsequent load-deformation response. All examined scenarios initiate with similar conditions as applied at the erection stage *(ii)*. The elastic member's stress utilization is at 21 %. The cables have tension forces of 0.38 kN and 0.43 kN and have already been subjected to a uniform length reduction of 21.6 mm. The erected system has reached a total height of 2.76 m and a span to height ratio of 1.45.

6.4.1 Scenario 1 – Single cable group activation

Post-tensioning stage

In scenario 1, only individual cable groups are activated. The acceptable amount of cables length reduction for the examined scenario cases verifies that cable groups closer to mid-span are limited to lower length reduction, due to inverse bending deformation of adjacent elastic member's segments. The cables are shortened by 290, 190, 170 and 80 mm from outward to inward cable group activation respectively, i.e. S-1-A, -B, -C and -D. The individual cables' activation provides unique configurations to the system with increased span to height ratios of up to 2, 2.17 and 1.69, except in the S-1-D case, where the system's height to span ratio decreases to 1.36, Fig. 6.4. The cables axial forces in all four cases examined in this scenario are presented in Fig. 6.5. In all activation scenarios, the maximum axial force of the cables increases. The maximum axial force is traced in group D with values of 0.96, 1.67, and 1.96 kN, except in S-1-D traced in group C with a value of 1.42 kN. The lowest cable axial forces are developed in cable group A and equal to 0.59, 0.77, 0.76 and 0.68 kN respectively. In principle, the shortening cable group is responsible for the post-tensioning of the system, also inducing a higher amount of cable axial force in the adjacent cable groups. The elastic member's stress increases. Maximum stress values are obtained in the respective acting cable group segmentations. This effect is directly related to the locally induced bending deformation of the elastic member. Compared to the systems' erection stage *(ii)*, the elastic member's stress is increased by 365, 311, 330 and 213 %, with values of 45.97, 40.69, 42.56 and 30.89 MPa in each case respectively. The elastic member's compression force development is proportional to the cables' axial force in each respective segmentation.

Load-deformation behaviour

In accordance to the preliminary system analysis, and for comparison reasons, the magnitude of uniform vertical load applied on the system in each case separately has been selected to comply with the one used at the erection stage *(ii)* and without exceeding the

maximum value of 0.04 kN/m, Fig. 6.4. In S-1-B and -C, the generated post-tensioned configuration *(iii)* obtains higher stresses under vertical load compared to the erection stage *(ii)*, due to the horizontal position of the cables close to mid-span. In scenario S-1-A, the system may withstand the same vertical load but undergoes a higher deformation of 760 mm at mid-span, Table 3. S-1-D outperforms all examined scenarios with a relatively minor deformation of the system of 170 mm at mid-span, which is almost half of the respective system's deformation of 328 mm at its erection stage. In all cases, the cables close to the supports, i.e. group A and B, absorb a high amount of the imposed loads in compression, thus, reducing their own pretension, whereas the cables close to the mid-span are further tensioned. For a precise depiction of the system's load-absorbing mechanism, all cables axial force fluctuations are presented in Fig. 6.5. In general, S-1-D enables a higher absorption of the imposed load in the form of compression force in the cables close to the supports; consequently, their pretension decreases from 0.68 to 0.25 kN. Furthermore, in group D, the tension force in the cable group close to mid-span is slightly increased from 1.11 to 1.13 kN. The elastic member's maximum stress is slightly decreased in S-1-A and S-1-B, remains stable in S-1-C and is increased in S-1-D.

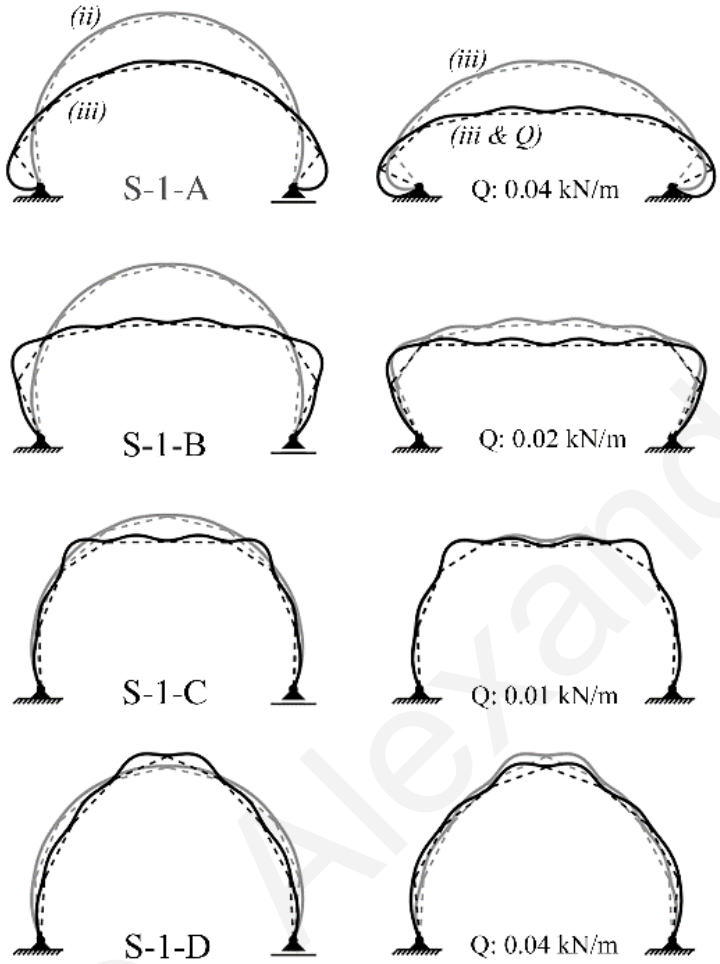

Figure 6.4 Deformation diagrams in scenario 1 for S-8cs with single cable group activation

Table 6.3 Numerical results for S-8cs with single cable group activation (cGRP)

S-1	Δl_c [mm]	N_x [kN]	V_z [kN]	M_y [kNm]	σ_x [MPa]	H [m]	L/H
(ii)	21.6	0.43	0.11	0.04	9.88	2.76	1.45
cGRP: A							
(iii)	290	0.94	0.54	0.18	45.97	2.00	2.00
(iii) & Q	-	1.47	0.94	0.17	43.48	1.21	3.32
cGRP: B							
(iii)	190	1.61	0.89	0.16	40.69	1.85	2.17
(iii) & Q	-	1.74	1.08	0.15	38.90	1.49	2.68
cGRP: C							
(iii)	170	1.91	1.05	0.17	42.56	2.37	1.69
(iii) & Q	-	1.95	1.09	0.17	42.45	2.29	1.75
cGRP: D							
(iii)	80	1.51	0.54	0.12	30.89	2.94	1.36
(iii) & Q	-	1.43	0.78	0.13	31.80	2.77	1.44

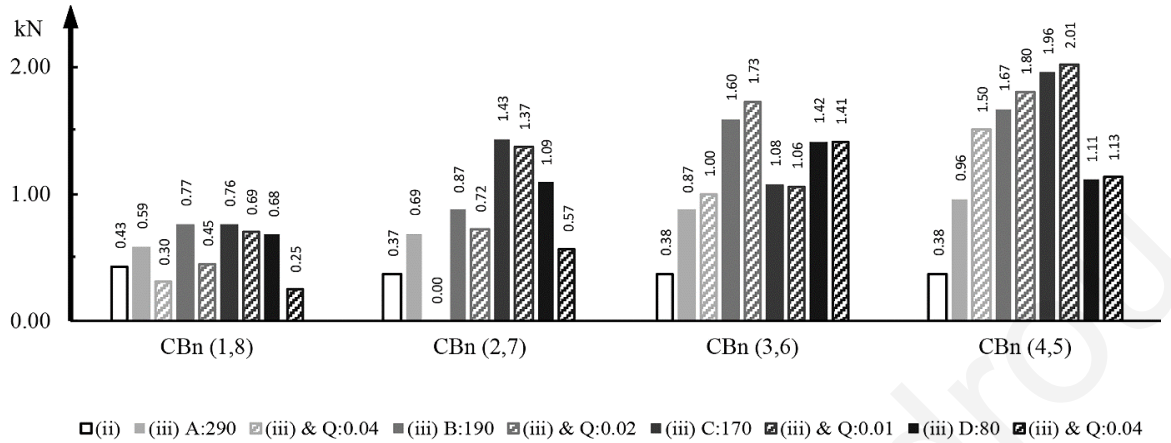

Figure 6.5 Cables' maximum axial force in S-8cs with single cable group activation

6.4.2 Scenario 2 – Two cable groups activation

Post-tensioning stage

In scenario 2, all six possible combinations with simultaneous two cable groups' activation have been examined, Fig. 6.6. In the cases where the active cable groups are not adjacent to one another, or are both located close to mid-span, i.e. S-2-AC, -AD, -BD and -CD, the cables' length reduction is limited to lower values, as shown in Table 6.4. The respective constraining factor is the inverse deformation developed at adjacent member segments. The maximum self-induced reduction value for the cables is registered in S-2-AB with 160/160 mm for both acting cable groups. The maximum elastic member's stress development is not proportional to the cables reduction value. Rather, the location of the acting cable group is more critical for the stress development of the elastic member. For example, in S-2-AC the reduction values of cable groups A and B equals to 230 and 80 mm inducing to the elastic member a maximum stress of 42.70 MPa, whereas in S-2-CD, the reduction value of cable groups C and D equals to 90 and 50 mm, inducing a respective maximum stress of 37.29 MPa. The cables' maximum axial force develops in the adjacent cable groups of the acting ones. In all cases, except in those of the acting cable group D, the maximum axial force is developed in cable group D. A maximum axial force of 1.71 kN is registered in S-2-AC, which is 350 % higher compared to the maximum value developed at the erection stage *(ii)*. The respective lowest value of 0.58 kN is registered in S-2-AB,

which is 35 % higher compared to the minimum value developed at the erection stage *(ii)*, Fig. 6.7. The post-tensioned configuration *(iii)* activated by S-2-AB, -AC and -BC undergoes an increase of the span to height ratio compared to the previous stage, obtaining values of up to 2.00, 2.01 and 1.73. In S-2-AD, the system's span to height ratio also increases at a lowest degree of up to 1.50, whereas in S-2-BD and -CD, the respective ratios undergo a slight decrease of up to 1.44 and 1.42 respectively.

Load-deformation behaviour

The analysis results clearly demonstrate that the systems with higher length to height ratio, primarily caused by length reduction of cable group A, have a significantly reduced load-bearing capacity compared to the erection stage *(ii)*, Fig. 6.6. S-2-AB, -AC, -AD are denoted with limit vertical loads of 0.1, 0.1 and 0.3 kN/m respectively in avoiding collapse. As already observed in the single cable group activation, reconfigurations with horizontal alignment of the cable groups close to mid-span and small angles in relation to the horizontal axis of the cables, close to the supports, do not contribute towards structurally efficient configurations. As a matter of fact, only S-2-BC, -BD and -CD can be compared to the system's erection stage *(ii)*, since all systems can withstand a uniform vertical load of 0.04 kN/m. S-2-CD outperforms all examined cases with minor deformations at mid-span, of only 153 mm, Table 6.4. In S-2-BC and -BD the systems have higher deformations, of 293 and 240 mm respectively. In S-2-AD, -BD and -CD, the cables' behaviour in absorbing the imposed vertical load is identical to the previous activation scenario. The absorbing level in compression force reaches 78 % in S-2-BD and 51 % in S-2-CD, followed by a reduction of their tension force from 0.67 to 0.15 kN and from 0.78 to 0.40 kN respectively, Fig. 6.7. The elastic member's stress is reduced in the structurally inefficient systems of S-2-AB, -AC and -AD and increased in S-2-BD and -CD. All inner forces' diagrams for S-2-CD are presented in Fig. 6.8.

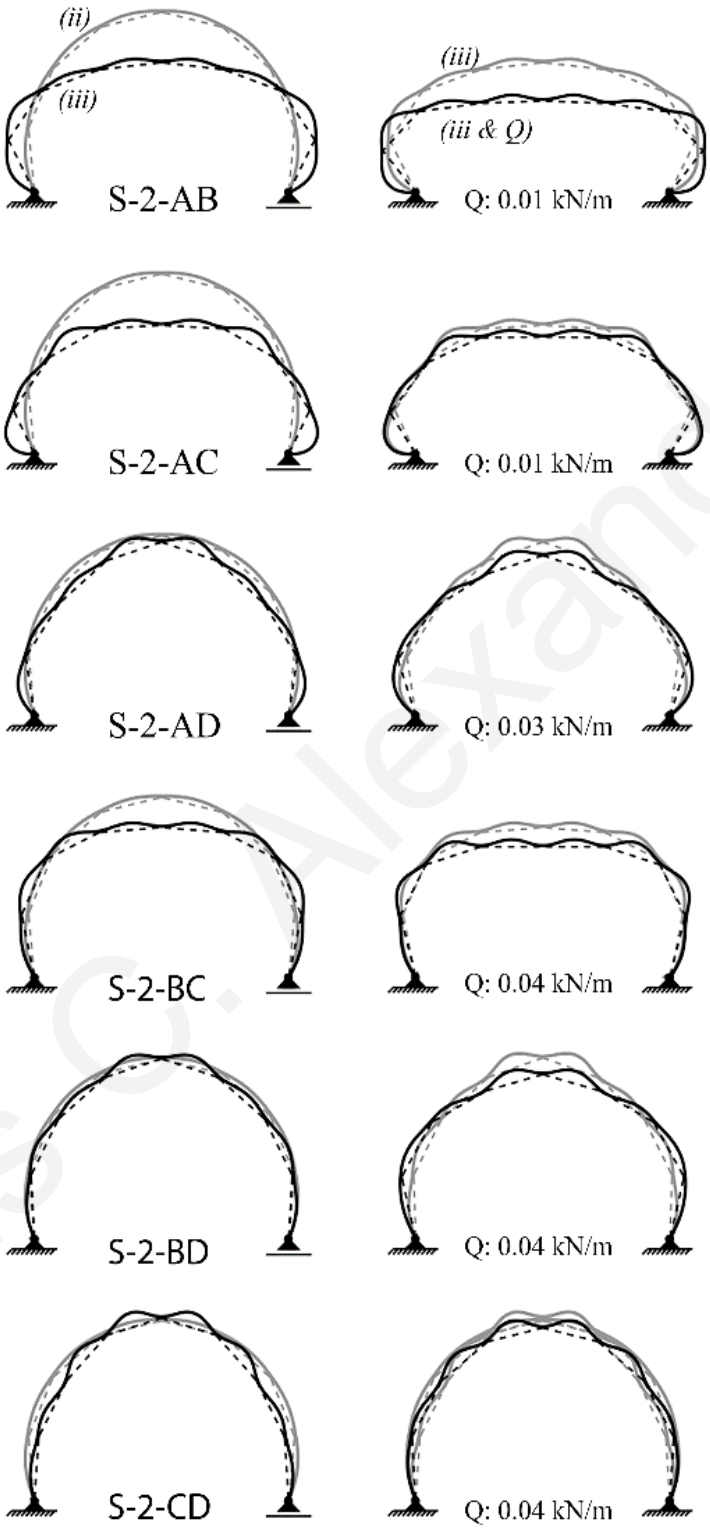

Figure 6.6 Deformation diagrams in scenario 2 for S-8cs with two cable groups activation

Table 6.4 Numerical results for S-8cs with two cable groups activation (cGRP)

System	Δl_c [mm]	N_x [kN]	V_z [kN]	M_y [kNm]	σ_x [MPa]	H [m]	L/H
(ii)	21.6	0.43	0.11	0.04	9.88	2.76	1.45
cGRP: AB							
(iii)	160/160/0/0	1.34	0.54	0.10	26.43	2.01	2.00
(iii) & Q	-	1.71	0.93	0.15	38.32	1.42	2.82
cGRP: AC							
(iii)	230/0/80/0	1.67	0.88	0.17	42.70	1.99	2.01
(iii) & Q	-	1.77	0.77	0.16	41.06	1.81	2.21
cGRP: AD							
(iii)	70/0/0/70	1.44	0.56	0.12	30.62	2.67	1.50
(iii) & Q	-	1.57	0.90	0.12	30.56	2.47	1.62
cGRP: BC							
(iii)	0/110/80/0	1.56	0.53	0.10	25.79	2.31	1.73
(iii) & Q	-	2.00	0.83	0.14	34.35	2.02	1.98
cGRP: BD							
(iii)	0/20/0/60	1.39	0.51	0.11	28.47	2.78	1.44
(iii) & Q	-	1.43	0.92	0.11	29.18	2.54	1.58
cGRP: CD							
(iii)	0/0/90/50	1.46	0.72	0.15	37.29	2.81	1.42
(iii) & Q	-	1.40	0.77	0.15	38.76	2.66	1.50

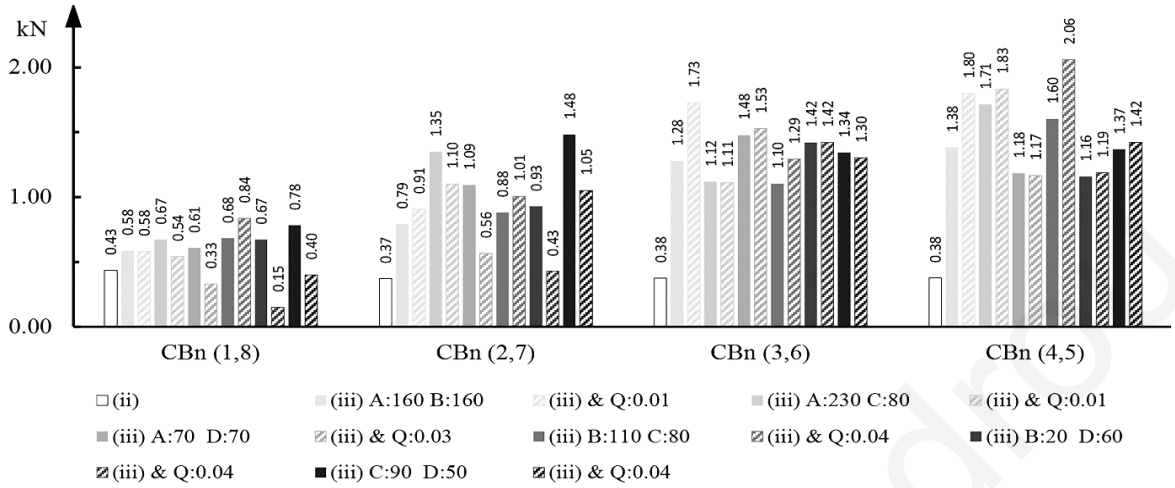

Figure 6.7 Cables' maximum axial force in S-8cs with two cable groups activation

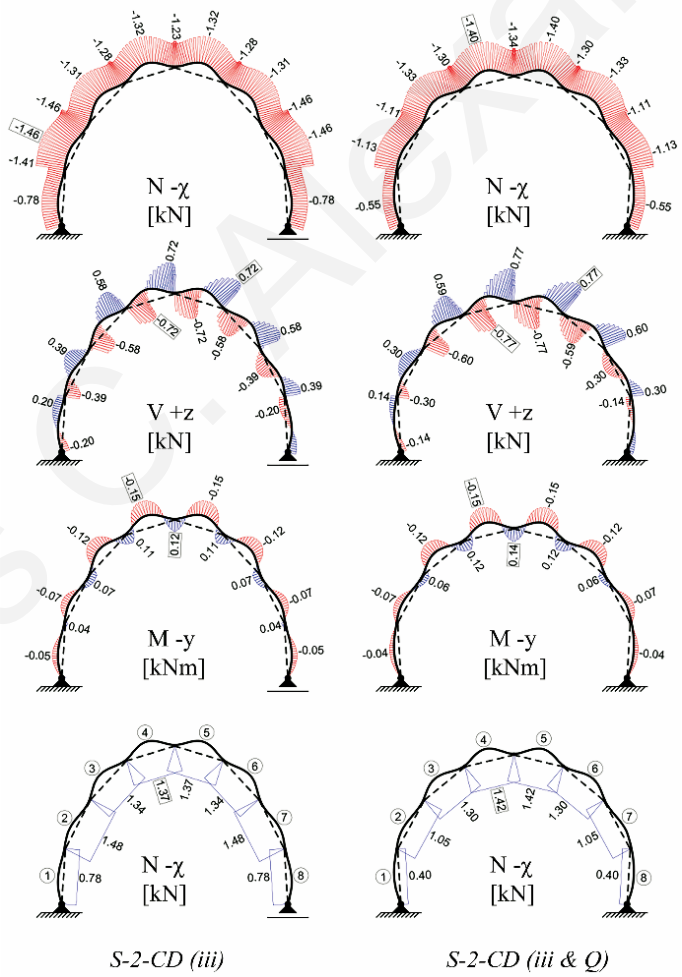

Figure 6.8 System scenario S-2-CD inner forces and cables' axial force development at post-tensioning *(iii)* and consecutive vertical loading stages *(iii and iii&Q)*

6.4.3 Scenario 3 – Three cable groups activation

Post-tensioning stage

In scenario 4, all four possible combinations of three cable groups' activation in parallel are investigated, Fig. 6.9. As to the above-examined scenarios, activation of cable groups close to the supports, i.e. A and B, generate small angles to the horizontal axis and do not provide structurally efficient systems. Consequently, S-3-ABC and -ABD can only withstand vertical loads of 0.2 and 0.3 kN/m and are left out of the comparison. The total cable reduction values of the remaining system activation cases equal to 160 and 240 mm, Table 6.5. Due to the multiple cable groups activation performed, cable group D may be reduced at a higher level compared to the previous scenario, i.e S-3-ACD and -BCD enabling in this respect an inward deflection of the systems' curvilinear shape. S-3-ACD maintains the erected system's span to height ratio, while S-3-BCD increases the respective ratio from 1.45 to 1.59. The cable's maximum axial force in S-3-ACD and -BCD amounts to 1.46 and 1.62 kN, i.e. 284 and 326 % higher compared to the respective values of the system at the erection stage *(ii)*, Fig. 6.10. In S-3-ACD, the cables' reduction is limited, due to inverse deformation caused at the elastic members' segment B, and in S-3-BCD, the cable reduction is limited, due to the maximum utilization of the elastic member's yield strength. The stress utilization of the elastic member reaches values of 80 and 98 % in each activation case respectively.

Load-deformation behaviour

In S-3-ACD and -BCD the loaded system undergoes vertical deformations at mid-span of 218 and 199 mm, which is respectively 34 and 40 % lower than the erection stage *(ii)*, Fig. 6.9. The maximum axial forces in cable groups C and D reach 1.46 and 1.66 kN, which are identical and by 2 % higher than the respective values in the system's erection stage *(ii)*, Table 6.5. The cables close to the supports undergo a tension force relaxation of 54 and 48 % respectively, reaching values of 0.32 and 0.48 kN, Fig. 6.10. The elastic member's stress utilization increases by 3 and 1 % respectively.

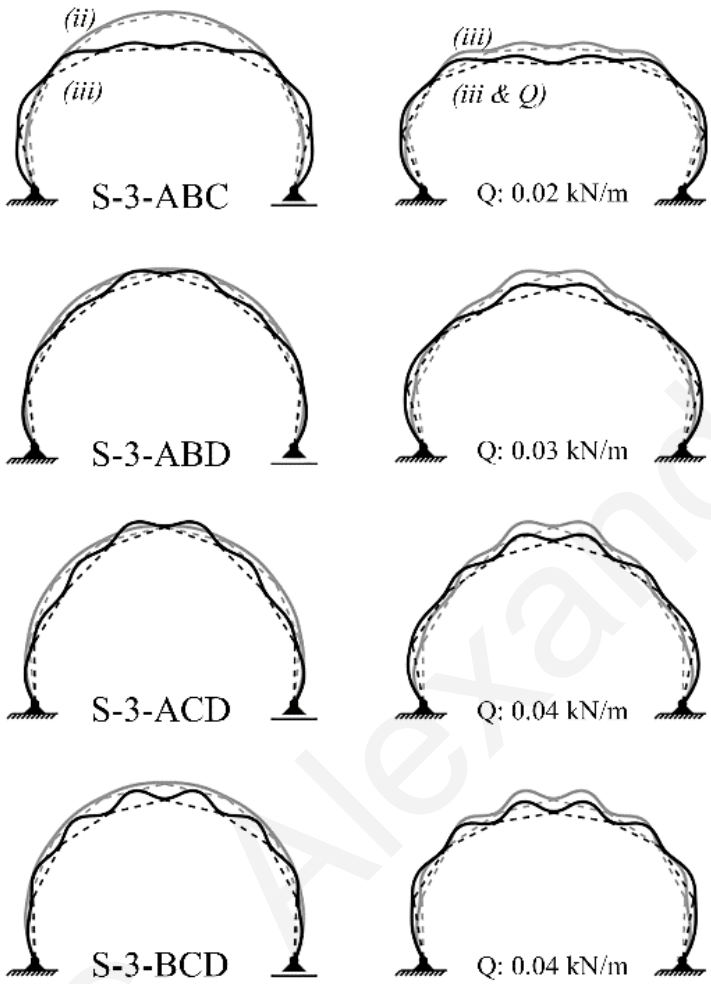

Figure 6.9 Deformation diagrams in scenario 3 for S-8cs with three cable groups activation

Table 6.5 Numerical results for S-8cs with three cable groups activation (cGRP)

System	Δl_c [mm]	N_x [kN]	V_z [kN]	M_y [kNm]	σ_x [MPa]	H [m]	L/H
(ii)	21.6	0.43	0.11	0.04	9.88	2.76	1.45
cGRP: ABC							
(iii)	30/40/60/0	1.64	0.6	0.11	27.99	2.24	1.79
(iii) & Q	-	1.82	0.76	0.11	28.03	1.98	2.02
cGRP: ABD							
(iii)	20/20/0/60	1.45	0.53	0.11	28.87	2.70	1.48
(iii) & Q	-	1.51	0.88	0.12	29.35	2.49	1.61
cGRP: ACD							
(iii)	30/0/30/100	1.43	0.73	0.15	38.29	2.77	1.45
(iii) & Q	-	1.47	0.77	0.16	39.51	2.55	1.57
cGRP: BCD							
(iii)	0/40/80/120	1.55	0.98	0.19	47.41	2.52	1.59
(iii) & Q	-	1.61	1.01	0.19	48.05	2.32	1.72

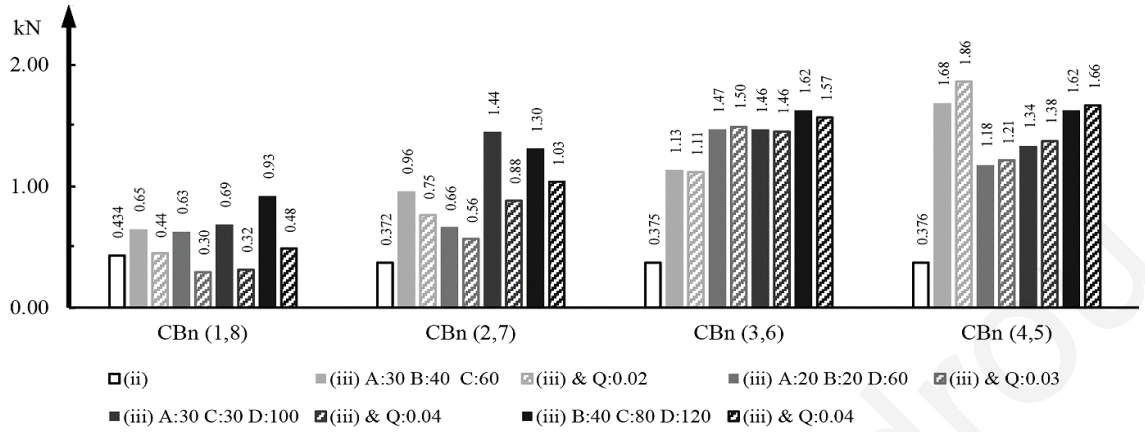

Figure 6.10 Cables' maximum axial force in S-8cs with three cable groups activation

6.4.4 Cables activation for increased system height

The results obtained in the preliminary and multiple cable activation scenarios for S-8cs clearly indicate that the system's load-deformation behaviour at the post-tensioning stage *(iii)* is directly related to morphological aspects and the amount of cable pretension, in particular in cable group A. Considering the geometrical characteristics of the post-tensioned system's configurations in S-1-D, S-2-CD and S-3-BCD, as the ones with the most favorable load-deformation response under vertical loading, relative large angles of the cables as to the horizontal axis at the supports and at mid-span are of high significance in enabling an efficient distribution of the imposed loads to the cables. The aforementioned system cases experience respective vertical deformations at mid-span of 170, 155 and 199 mm, which are by 48, 53 and 39 % lower compared to the system's erection stage *(ii)*. The cables force utilization in cable group A reaches 64, 49 and 48 % whereas, in cable group D at mid-span, it undergoes a minor increase of 1, 4 and 2 %.

Post-tensioning stage

A custom cable group activation serves as an example for achieving improved geometrical characteristics of the system, following a non-uniform length reduction of cable groups, Fig. 6.11. The examined system case is form-found *(ii)* using differentiated cables reduction values of 10, 10, 20 and 30 mm for each cable group A, B, C and D

respectively, as included in Table 6.6. The system reaches half of its initial non-deformed (i) length, $L_0/2$, with a span to height ratio of 1.36. The static height of the system equals to 2.94 m. The elastic member's stress utilization reaches with 12 MPa, 25 %. The cables' highest maximum axial force of 0.49 kN is developed in cable group D, and the respective lowest value of 0.39 kN, in cable group B, Fig. 6.12. In the post-tensioning stage, only cable group D is further reduced in length by 40 mm. The elastic member's stress utilization reaches 56 %. Further cables length reductions result into inward deformation of respective adjacent segments of the elastic member. The cables' highest maximum axial force amounts to 1.24 kN in cable group C, and the respective lowest one of 0.68 kN in cable group A. The total static height of the system reaches 3.01 m, providing a length to height ratio of 1.33.

Load-deformation behaviour

The load-deformation behaviour of the system subjected to a uniformly distributed vertical load of 0.04 kN/m improves significantly compared to the previously examined activation scenarios, Fig. 6.11. The vertical deformation at mid-span amounts to merely 49 mm, Table 6.6. The force utilization in cable group A reaches 52 %, while the tension force increases in cable group D by only 2 %, Fig. 6.12. The elastic member's stress increases by 2 %, reaching 27.40 MPa. Furthermore, the elastic member's maximum compression force reaches a value of 1.21 kN. The cables' maximum axial forces and the elastic member's inner forces are presented in Fig. 6.13.

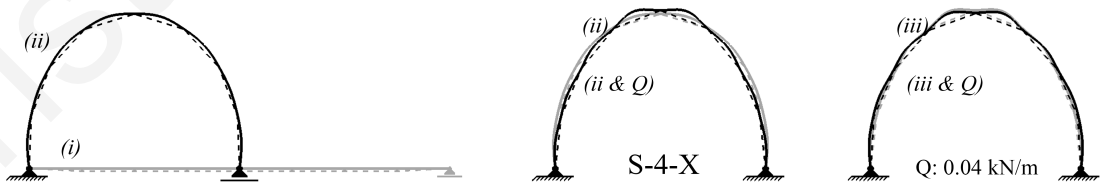

Figure 6.11 Deformation diagrams for S-8cs with non-uniform cable activation

Table 6.6 Numerical results for S-8cs under non-uniform cable activation (cGRP)

System	Δl_c [mm]	N_x [kN]	V_z [kN]	M_y [kNm]	σ_x [MPa]	H [m]	L/H
(ii)	10/10/20/30	0.49	0.14	0.05	12.01	2.94	1.36
(iii)	0/0/0/40	1.23	0.48	0.11	26.76	3.01	1.33
(iii) & Q	-	1.21	0.50	0.11	27.40	2.96	1.35

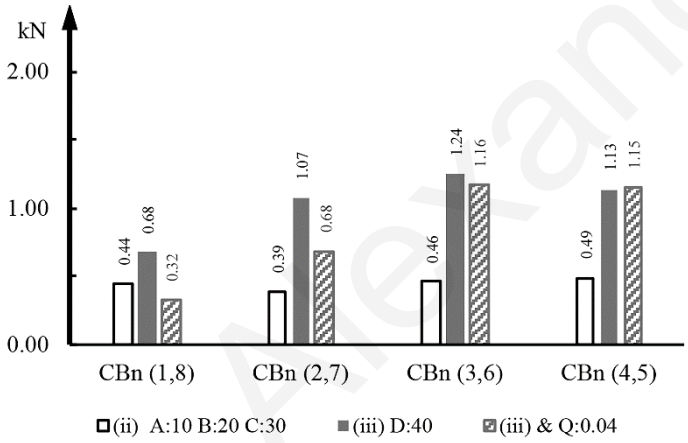

Figure 6.12 Cables' maximum axial force in S-8cs with non-uniform cable activation

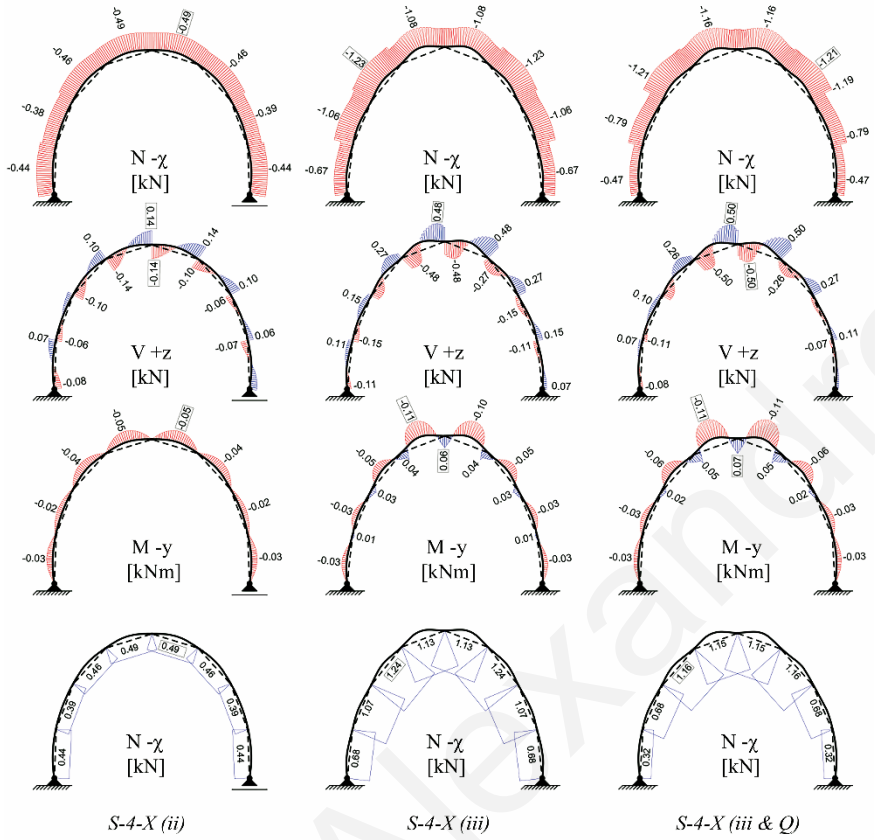

Figure 6.13 Inner forces and cables' axial force development at erection *(ii)*, post-tensioned *(iii)* configuration and consecutive vertical loading stage *(iii&Q)* for S-8cs with non-uniform cable activation

6.5 Conclusions

The present Chapter investigated a planar hybrid cable bending-active system series acting as extension of Unit 1 configuration. The system consists of an elastic stripe of continuous length, interconnected with cable elements at equal length intervals of 1 m. A total of seven system configurations, with two to eight cable segments, have been analyzed. The proposed systems are assembled in planar arrangement *(i)*, erected *(ii)* through uniform cable length reduction and post-tensioned *(iii)* through further cable length reduction. The post-formed load-deformation behaviour of the systems has been examined at the end of the erection *(ii&Q)* and post-tensioning stage *(iii&Q)*. The analysis conducted proves that the hybridization of the elastic member with cables contributes positively towards alternative erection and simultaneous post-formed stiffening of the systems. At the

erection stage *(ii)*, the cable pretension improves the systems' load-deformation behaviour. A higher amount of tension force, introduced in the elements at the post-tensioning stage *(iii)*, improves further the load-deformation behaviour of the systems, due to the ability of cables to withstand higher amounts of compression loads imposed, prior to their relaxation. However, morphological aspects such as the horizontal alignment of the cables close to mid-span, and the small angle of the cables as to the horizontal plane, close to the supports, counteract the cables' strengthening action. In this frame, an explicit activation approach has been adopted for the eight-cable system in the post-tensioning stage *(iii)* through respective activation of individual - or set - of cable groups, in order to avoid inefficient geometrical configurations. Apart from the constraint of not exceeding the elastic member's yield strength, the activation approach is sensitive with regard to inverse deformations of adjacent elastic member segments as to the respective cable acting ones. S-1-D, S-2-CD and S-3-BCD prove that selective cable group reduction may further improve the load-deformation behaviour of the systems. Furthermore, under vertical loading of the specific systems, compared to their respective response at the erection stage *(ii&Q)*, these are vertically deformed at a percentage of 48, 53 and 39 %, with a cable pretension utilization of 14 % in only the first case, and by extent, an elastic member's stress utilization of up to 66, 81 and 100 % respectively. Finally, a system's erection *(ii)* and post-tensioning, through non-uniform cable reduction, have been applied by considering the respective geometrical conditions of the members. This activation scenario of the system has confirmed a considerable improvement of its load-deformation behaviour.

CHAPTER 7 NUMERICAL ANALYSIS OF MULTI-SEGMENT STRUCTURAL CONFIGURATIONS – S2

7.1 Multi-Segment Structural Configuration

This Chapter stands as an extension of the previous one, for a longer span, multi-segment structural system analysis. The structural combosition of a multi-segment cable bending-active structure is generated from a linear arrangement of multible single-segment configurations of a coupled case, with two elastic stipes fastened together at midspan (Chapter 4, Unit 5, Fig. 4.1). The multi-segment structure is composed of continuous length elastic stripes and take into consideration the principle geometrical configuration characteristics of Unit 5. In the current System analysis, only the eight-segment configuration case is examined.

7.2 Hybrid System Analysis

The System is examined in its form-found shape acquisition *(ii)* and respective load-deformation behaviour under uniform vertical loading *(ii & Q)*. The results obtained are presented in Fig 7.1 and Table 7.1. The system's erection is enabled through secondary cable elements length reduction, linking the elastic stripes fastening points, and sliding of the three ground supports (endpoints of the undeformed elastic stripes) in longitudinal direction (x-axis). Throughout the fastening process, due to the length differentiation of the secondary and primary elastic member, the force interaction between the two members causes a self-induced gradual bending and forces the overall system to obtain a global semi-circular shape. During the erection stage and subsequently the elastic stripes upward deformation and inward displacement, the system's supports conditions are modified to fixed at an intermideate stage, to preserve the target span length of 4 m ($L_0/2$ of the lower elastic member). The fastening stage and consequently the erection process

constinues until the secondary cables length reduction reaches 99 %. The cables are then replaced with strut elements to provide a shear resistance conditions between the members. The vertical loading applied at the end of the erection stage *(ii & Q)* amounts to 0.04 kN/m. This loading value has been selected and applied on the system on purpose, so that the desired analysis results may be compared to the respective ones of System 1 (Chapter 6). The form-found configuration of the system is examined in its load-deformation behaviour with and without primary cables. Compared to System 1, no post-tensioning is applicable in this case, due to an already high stress utilisation of the secondary elastic member.

7.2.1 Erection stage (form-found shape)

The erection stage is divided into three intermediate substages. At intial undeformed conditions *(i)* the elastic members are only fastened together at midspan. The primary elastic stripe's ground supports are set to fixed on one side and to sliding in the other respectively. The secondary elastic stripe's ground supports are set to sliding conditions. In substage 1, the secondary cables that link the two elastic stripes ground supports are activated. The amount of secondary cables length reduction reaches 100 % until the two end supports of both members are aligned. Both support groups are then unified and set to act together. In the subsequent substage 2, the secondary cables, which link the inner elastic members division points (i.e. every 1 m of the primary member and every 1.4 m of the secondary elastic member) are activated and gradually reduced in legth until the unified sliding support reaches the target displacement of 4 m ($L_0/2$ of the primary elastic member). The unified sliding support is then turned to fixed and the secondary cables continue to shrink until their length reduces to zero. The final shape acquisition of the system at the end of each substage is presented Fig. 7.2.

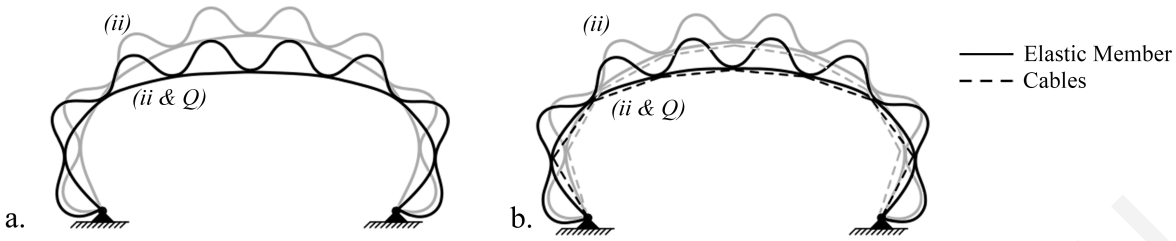

Figure 7.1 System 2 coupled configuration without (a) and with (b) cables at erected *(ii)* and subsequent vertical loading stage *(ii & Q)*

Table 7.1 Numerical results for System 2 at all intermediate stages of the erection stage (*ii)*, vertical loading with and without* cables *(ii & Q)*

System	N_x [kN]	V_z [kN]	M_y [kNm]	σ_x [MPa]	N_x [kN]	V_z [kN]	M_y [kNm]	σ_x [MPa]	H [m]	L/H
	Primary el. member				Secondary el. member					
(ii) - 1	0.03	0.02	0.03	7.39	0.03	0.03	0.04	9.90	2.02	3.34
(ii) - 2	0.16	0.08	0.05	13.1	0.14	0.84	0.06	13.9	2.56	1.56
(ii) - 3	1.12	0.30	0.06	24.2	1.03	0.90	0.23	57.1	2.44	1.64
*(ii) & Q**	1.27	0.34	0.14	33.2	10.4	0.93	0.23	59.1	1.93	2.07
(ii) & Q	0.83	0.45	0.13	31.4	1.05	0.92	0.23	58.6	2.07	1.93

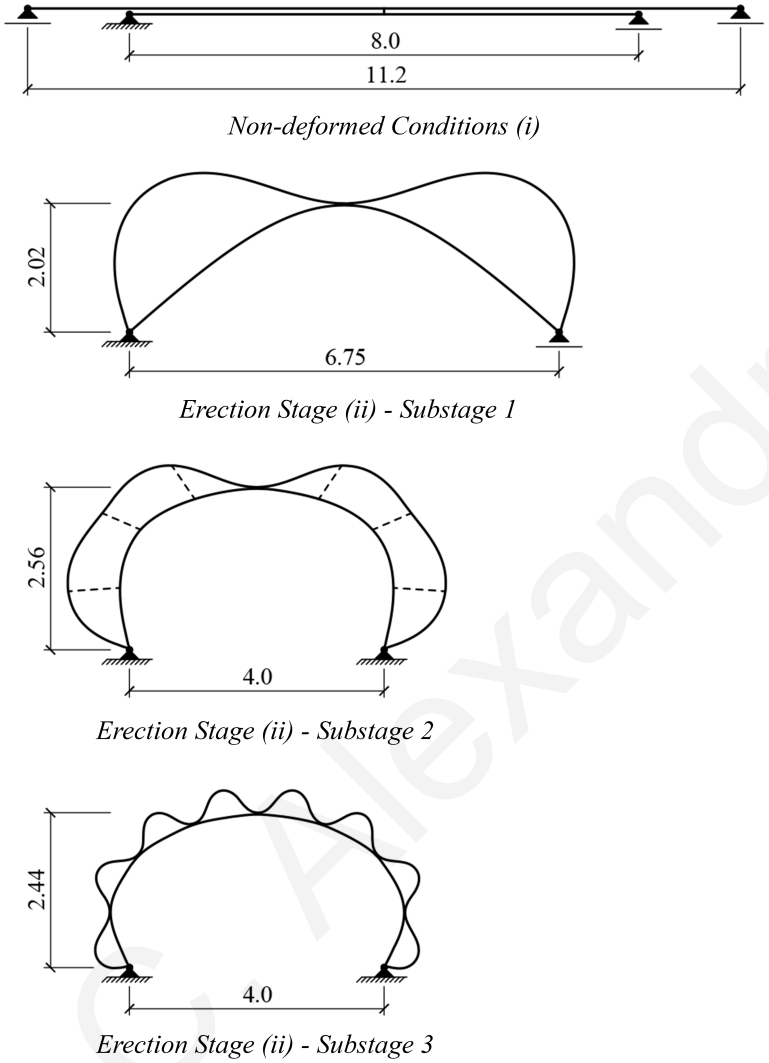

Figure 7.2 System 2 erection intermediate stages

The erection process and therefore the fastening of the elastic members may be accomplished under successive fastening actions or supports conditions control. The secondary cable elements used as contracting elements for the fastening of the elastic members is the only mean possible to enable such actions in FEA software. In actual construction this method can be handled by machinery, or any other form of externally induced force or pressure. The proposed erection approach adopted, takes into consideration both actual contraction constraints and possible FEA tools, i.e. supports condition shifting and contracting elements to act as externally induced forces. Aim is to

enable a simple erection process, while maintaining the fastening substeps as low as possible.

The system is form-found resulting into a span to height ratio of 1.64, and reaching a total height of 2.44 m at midspan. Through the fastening process, the secondary elastic member forces the primary elastic member to bend in an almost uniform manner. Therefore, the former develops exclusively compression axial forces, registering a maximum value of 1.03 kN, whereas, the latter is only stressed in tension, registering a respective maximum axial force of 1.12 kN. The secondary elastic member develops a maximum bending moment of 0.23 kNm, 74 % higher compared to the primary elastic member. The stress utilisation in the secondary elastic member exceeds the material's ultimate elastic limit at a percentage of 20 %, reaching a maximum stress value of 57.1 MPa. The respective value in the primary elastic member reaches 69 %, exhibiting a maximum stress value of 33.2 MPa. All values of inner force for the intermediate stages are included in Table 7.1. All inner forces diagrams at the end of the erection stage *(ii)* are presented in Fig. 7.3.

Load-deformation behaviour

The system exceeds the stress utilisation of its secondary elastic member and no further post-tensioning is possible. At this stage, the system is examined in its load-deformation behaviour with and without cable elements, Fig. 7.1. The cables are therefore used as post-bracing additions to the coupled bending-active structure. The amount of uniform vertical loading is set to 0.04 kN for comparison purposes of the load-deformation behaviour with the System 1.

In System 2 without cables, the secondary elastic member's compression force records a slight increase from 1.03 to 1.04 kN, while the primary elastic member's tension force also increases at a percentage of 13 %, down to 1.27 kN (Fig. 7.3). The primary elastic member undergoes further bending deformation, increasing its maximum bending moment to 133 %, 0.14 kNm, and shear force to 13 %, up to 0.34 kN. The secondary elastic

member's shear force and bending moment undergo negligible increase. The primary elastic member's stress increases at a percentage of 37 %, 33.2 MPa. The system exhibits a high vertical deformation at midspan of 0.51 m, resulting into a span to height ratio of 2.07.

In System 2 with cables, the system's stability is improved slightly. The cables close to midspan, i.e. cable group C & D, develop 0.74 and 1.56 kN axial force respectively (Fig. 7.4), eliminating any primary elastic member's tension force increase. The primary member's tension force is decreased at a percentage of 26 %, 0.83 kN, whereas the secondary elastic member's compression force is slightly increased from 1.03 to 1.05 kN. The primary elastic member's maximum shear force increases by 50 %, 0.45 kN, and the bending moment to 117 %, 0.13 kNm. The secondary elastic member's shear force and bending moment undergo a negligible increase. The system deforms vertically at midspan at a magnitude of 0.37 m, resulting into a span to height ratio of 1.93.

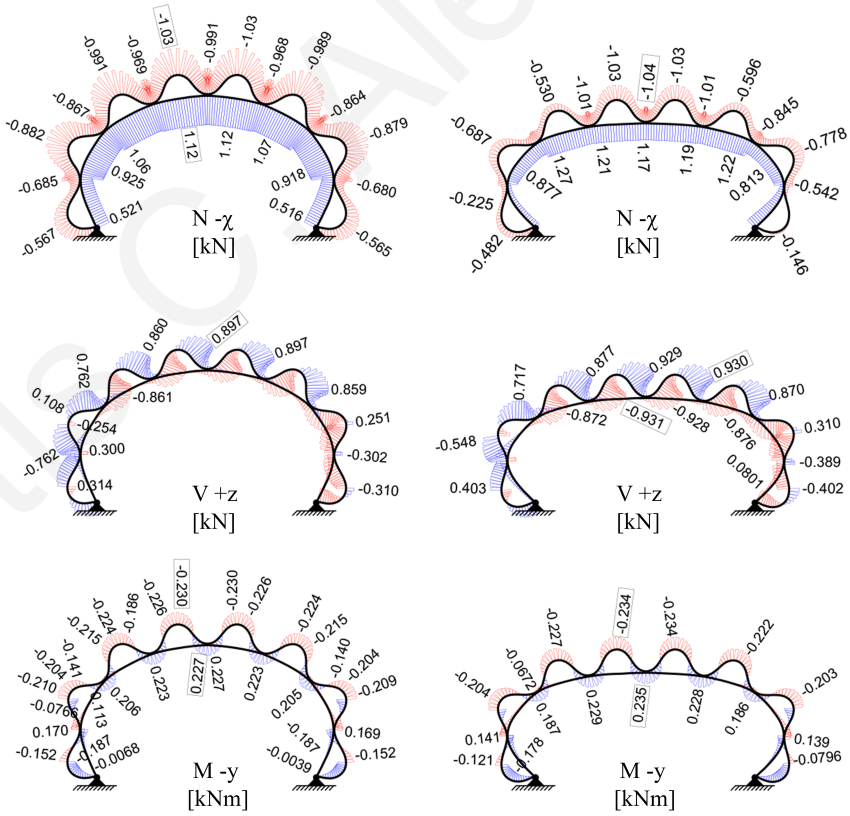

a. (ii) *b. (ii & Q)*

Figure 7.3 System 2 without cables. Inner forces diagrams at erected *(ii)* and subsequent verical loading stage *(ii & Q)*

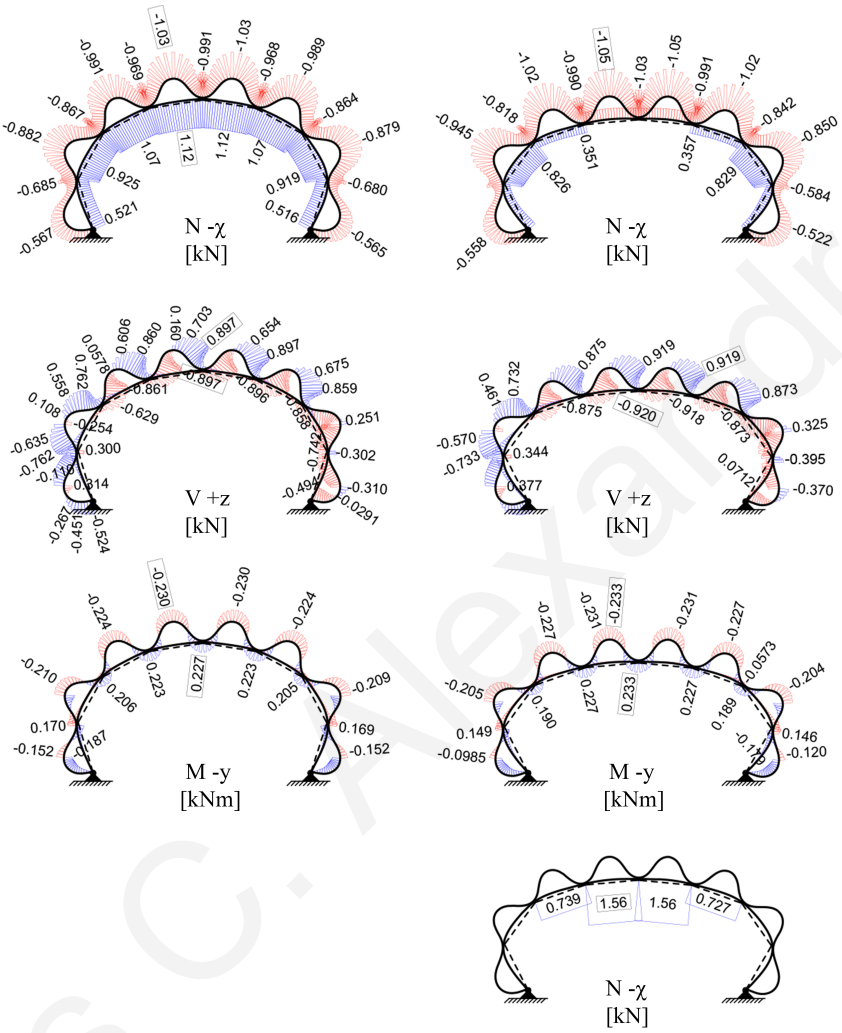

*a. (ii) **

*b. (ii & Q) **

Figure 7.4 System 2 with cables. Inner forces diagrams at erected *(ii)* and subsequent verical loading stage *(ii & Q)*

7.3 Comparison with System 1

Although System 2 with cable elements establises an improved load-deformation behaviour compared to the respective coupled configuration without cables, System 1 (Chapter 6, Fig. 6.21 S-8cs *(ii)*) at the equivalent erected state, results into even higher stability. System 1 erected state followed by uniform vertical loading of 0.04 kN/m *(ii & Q)*,

absorbed the imposed load in the form of compression in the elastic member, through increase of its maximum axial force by 42 %, and through the cables' tension force decrease of 100 % in cables groups close to the supports and through a smaller respective increase in cables close to midspan, of approcimately 60 %. On the other hand, System 2 with cables, absorbed the imposed load through a slight increase of the compression force in the secondary elastic member, at a percentage of 2 %, and a decrease of the primary elastic member's tension force at a percentage of 35 %. Despite the reserves of the primary elastic member in tension, System 2 results into a higher magnitude of vertical deformation at midspan, of 37 cm, compared to System 1 with a respective value of only 13 cm.

CHAPTER 8 **CONCLUSIONS**

8.1 Research Contribution

The present thesis focuses on the form-finding and load-deformation behaviour of single- and multi-segment hybrid cable bending-active structure configurations. The application of bending-active principles provides an alternative solution for the design of lightweight temporary structures, through the unique assembly, construction and members' stress attitudes generated. A key feature of bending-active structures is their ability to provide natural shapes without undertaking cold-formed processes or high-volume transportation of the structural members. The need to examine and associate the form-found shape of such systems with their respective load-deformation behaviour has led the present study to the investigation and evaluation of cable bending-active systems of exclusive configurational characteristics, consisting of primary elastic members and secondary cable elements.

Following a state-of-the-art review on bending-active structures, the integration of secondary cable elements with elastic members, as proposed in the current thesis, provides enhanced structural characteristics in terms of simplified erection, global stiffening and post form-found load-deformation capacity and control. The results obtained give an insight in the role of the cable elements to enable an alternative vertical erection of the systems through their own length reduction and the simultaneous absorption of a high amount of tension forces, enabling the systems to resist a high amount of uniformly distributed vertical load. By extent, the shape reconfiguration capability and respective load-deformation behaviour of possible structure reconfigurations, have been investigated through individual cable groups activation scenarios and stepwise incremental vertical loading.

The hybrid cable bending-active systems investigated are composed of an initial single-segment configuration of fundamental pairing attitudes (Unit 1). A further configuration exploration focuses on the participation of two elastic members, followed by simply paired and paired-interconnected fastening techniques (Unit 2 to 6). All configurations are designed to enable a simple assembly and erection process, activated through gradual cable's length reduction. Longer span hybrid systems of multi-segment configurations with identical fastening characteristics as to the single-segment units (System 1 and 2) are developed, in order to enable a broader assessment of the cables' contribution in the systems erection, stiffening and post form-found load-deformation capacity and control.

The numerical investigations conducted in the present thesis are primarily based on the accuracy of the FEA adopted, initially yielding the form-finding of the hybrid cable bending-active structures. The analyses take into consideration the nonlinear geometrical characteristics of the systems that govern the bending-active members deformability. The contribution of the cables to serve both as alternative erection mediator and post-stiffening addition is discussed in Chapter 3. The analysis workflow and simulation tools utilised for the establishment of the analysis framework, by using FEA software SOFiSTiK and the alternative input tool TEDDY, are presented in Chapter 4. The analysis methodology applied addresses the elastic members fastening through gradual auxiliary cables' length shortening. The fastening techniques, explored for the single-segment configurations, including the elastic members' thickness variations, are presented in Chapter 5. Finally, in Chapters 6 and 7, Unit 1 and 5 are explored in multi-segment configurations of longer spans.

8.2 Research Results

Main characteristics in the construction of pure or hybrid bending-active structures comprise the stress utilisation of the elastic members, that should not exceed the material's yield strength. In the case of a linear elastic material and single-axis bending deformation, the material's stress constraint can be monitored through the curvature value of the bending deformation or bending moments development, which by extent is

proportional to the member's thickness. Design-wise, critical aspects that influence the deformation control of two-member constituent bending-active structures are the kinematic constraints of the ground supports and the members' fastening distance. In hybrid cable bending-active structures, the latter aspect refers to the connectivity distance between the elastic member and the cable elements.

In terms of the single-segment structural configurations' form-finding, the following remarks can be drawn, with regard to the fastening technique applied:

Simply-paired configurations (single member)

- An adequate system stiffness with a cables maximum axial force is primarily achieved by the elastic member's thickness.
- The cable's maximum tension force corresponds to the elastic member's compression force.

Simply-paired configurations (dual members)

- The system stiffness is negatively affected by the length of the secondary elastic member, irrespectively of the cables tension force.

Paired-interconnected configurations

- The units result into higher stiffness due to the members' interfastening conditions. However, the material's yield strength may be reached. The elastic member's thickness and the secondary elastic member's length differentiation should remain low in case of multiple interfastening points between the members.
- Hybridisation with cable elements may be insignificant or even non-applicable, due to the already high amount of bending deformation achieved through the elastic member's initial internal fastening.

In the case of the post-form found load-deformation behaviour, the remarks are as follows:

Simply-paired configurations (single and dual members)

- The elastic member's compression force corresponds to the cable's axial force.
- The lower is the deformed curvature of the elastic member, the higher is the axial force increase in both elements.
- The lower is the bending curvature of the elastic member (low static height), the lower is the system vulnerability to vertical deformations at midspan (caused by lateral buckling of the elastic member).

Paired-interconnected configurations

- Both elastic members undergo axial force reductions (higher in the primary elastic member), while the cables axial force remains almost constant.
- The internal fastening of the members leads to reduced system deformations at midspan (constrains the elastic members lateral buckling). However, the role of the cables is less apparent in terms of enhancing the system stability.

The two fastening techniques applied in Unit 1 (cable's length reduction) and Unit 5 (paired-interconnected dual members) have been investigated in longer span hybrid configurations, in System 1 and 2 respectively.

In System 1 the following remarks can be made:

In uniform cables length reduction

- The cable elements verify their role as alternative erection mediator achieved through their own length reduction.
- The cable elements pretension significantly improves the load-bearing capacity and load-deformation behaviour of the system by restraining the elastic member's lateral buckling and the development of compression forces instead of bending

moments. By extent, the cable elements absorve the imposed loads in form of compression in cable groups closed to the ground supports and tension in cables groups closed to midspan.

In non-uniform cables length reduction

- The cable groups individual length reduction provides unique morphological variability to the overall system resulting in differentiated span to height ratios.
- The post-tensioning stage enables the cables to further increase their axial force, and consequently, to absorb a higher amount of external loads.
- The cables axial force development is not associated with their length reduction. Higher cables axial force is traced in adjacent system segmentations of higher length reduction.
- The cables high tension force is not solely important for improving the system's load-deformation behaviour and capacity. A low system's span to height ratio (i.e. smaller angle between the cables close to the supports and the horizontal axis) acts positively with regard to the loads distribution control.

In System 2 the following remarks can be made:

- The cable elements can only be applied as form-found stiffeners, and they only contribute towards the system's load-deformation control.
- The primary elastic member works in a similar manner as to the cable elements through a tension force decrease, while the secondary elastic member slightly increases its compression.
- The cable elements could possibly be used for post-tensioning purposes, if the secondary elastic member's length differentiation compared to the primary one is

lower (i.e. lower percentage of elastic member's stress utilisation at the end of the erection – fastening stage).

8.3 Future Work

Compared to conventional design schemes followed by the employment of rigid structural members and realised on the basis of a top-down approach, the soft mechanical approach renders the possibility of generating organic shapes though repetitive nonlinear geometrical form-finding processes. Despite its engineering novelty in dealing with natural shapes, the soft approach ends up becoming complex and time consuming in cases where complex shapes are desired. This is directly affected by several parameters, such as the members' planar shape and construction details with regard to the fastening technique applied for the elastic members. The investigations conducted in the current thesis enable a simplified design approach towards generating a synthesis of curvilinear structural forms of planar or spatial elastic members configurations.

In principle, the use of regular planar stripes and the introduction of cable elements enable a respective morphological exploration process of hybrid bending-active structures. The internally connected cable elements provide segmental deformation to the elastic members enabling in this respect higher amounts of stability and deformation control at global scale. The results obtained in the analysis are based on the specific sections and material properties used for the systems. Further investigations of hybrid cable bending-active structures may address the load-deformation behaviour and deformation control of the systems under asymmetrical vertical and horizontal loading. In addition, further experimental investigations of the systems will serve as proof-of concept for the proposed erection and activation approach. The generation of automated optimization processes with regard to the configurations and load-deformation objectives may also demonstrate the possible design space and applicability of the systems towards the achievement of adaptive features.

REFERENCES

AA Twist installation (2015). Available at: http://www.archdaily.com/775842/emtechs-twist-displayed-at-the-timber-expo-in-birmingham.

Adaptable (2016). Available at: https://en.oxforddictionaries.com/definition/adaptable (Accessed: 10 October 2015).

Adaptive (2016). Available at: https://en.oxforddictionaries.com/definition/adaptive (Accessed: 10 October 2015).

Adriaenssens, S., Block, P., Veenendaal, D. and Williams, C. (2014) *Shell Structures for Architecture: Form Finding and Optimization*. Edited by C. W. Sigrid Adriaenssens, Philippe Block, Diederik Veenendaal. Routledge. doi: 10.4324/9781315849270.

Adriaenssens, S. M. L. and Barnes, M. R. (2001) 'Tensegrity spline beam and grid shell structures', *Engineering Structures*, 23(1), pp. 29–36. doi: 10.1016/S0141-0296(00)00019-5.

Ahlquist, S., Kampowski, T., Torghabehi, O. O., Menges, A. and Speck, T. (2014) 'Development of a digital framework for the computation of complex material and morphological behavior of biological and technological systems', *Computer-Aided Design*, 60, pp. 84–104. doi: 10.1016/j.cad.2014.01.013.

Alexandrou, K. (2017) 'Bending-active systems: On exploring morphological configurations through coupling with tension-only members', *archi DOCT*, 5(1), pp. 89–103.

Alexandrou, K. and Phocas, M. C. (2017) 'Hybrid bending-active structures with multiple cables', in Bögle, A. and Grohmann, M. (eds) *The International Association for Shell Structures, IASS*.

Anastasiadou, I., Alexandrou, K. and Phocas, M. C. (2018) 'Deformation Control of Hybrid Bending-active Structures by Multible Cables', in Müller, C. and Adriaenssens, S. (eds) *The International association for Shell Structures, IASS 2018, Creativity in Structural Design*. (In preparation).

Bending active membrane roofing Marrakech (2012). Available at: http://www.structure.com/en/what/research-and-development/reference/bending-active-membrane-roofing-marrakech-itke-university-of-stuttgart-2011/ (Accessed: 22 November 2016).

Chini, S. A. and Wolde-Tinsae, A. M. (1988) 'Effect of Prestressing on Elastica Arches', *Journal of Engineering Mechanics*, 114(10), pp. 1791–1800. doi: 10.1061/(ASCE)0733-9399(1988)114:10(1791).

D'Amico, B., Kermani, A. and Zhang, H. (2014) 'Form finding and structural analysis of actively bent timber grid shells', *Engineering Structures*. Elsevier Ltd, 81, pp. 195–207. doi: 10.1016/j.engstruct.2014.09.043.

Deleuran, A. H., Tamke, M. and Thomsen, M. R. (2011) 'Designing with Deformation - Sketching material and aggregate behaviour of actively deforming structures', *Symposium on Simulation for Architecture and Urban Design*, pp. 5–12. Available at: http://simaud.com/proceedings/.

Dieringer, F., Philipp, B., Wüchner, R. and Bletzinger, K. (2013) 'Numerical Methods for the Design and Analysis of Hybrid Structures', *International Journal of Space Structures*, 28(3–4), pp. 149–160.

Elkhayat, Y. O. (2014) 'Interactive movement in kinetic architecture', *Journal of Engineering Sciences*, 42(3), pp. 816–845.

EmTech Pavilion (2012). Available at: http://www.archdaily.com/221650/pavilion-emtech-aa-eth (Accessed: 24 January 2014).

Escrig, F. (2013) 'Emilio pérez piñero: Inventor of deployability', in *2nd International*

Conference on Structures and Architecture, ICSA 2013, pp. 42–57.

Ferre, A. (2007) *Patent Constructions: New Architecture made in Catalonia*. Actar.

Fertis, D. G. (2006) *Nonlinear Structural Engineering. With Unique Theories and Methods to Solve Effectively Complex Nonlinear Problems*, *Nonlinear Structural Engineering. With unique theories and methods to solve effectively complex nonlinear problems*. Springer-Verlag Berlin Heidelberg. doi: 10.1007/978-3-540-32976-3.

Fox, M. (ed.) (2016) *Interactive Architecture: Adaptive World (Architecture Briefs)*. New York: Princeton Architectural Press.

Fox, M. A. and Yeh, B. P. (2000) 'Intelligent Kinetic Systems in Architecture', in Paddy Nixon, Gerard Lacey, D. S. (ed.) *Managing Interactions in Smart Environments*. London: Springer, pp. 91–103.

Fröling, M. and Persson, K. (2013) 'Computational Methods for Laminated Glass', *Journal of Engineering Mechanics*, 139, pp. 780–790. doi: 10.1061/(ASCE)EM.1943-7889.0000527.

Harris, R., Romer, J., Kelly, O. and Johnson, S. (2003) 'Design and construction of the Downland Gridshell', *Building research and information*, 31(6), pp. 427–454. doi: 10.1080/0961321032000088007.

Harris, R. and Roynon, J. (2008) 'The Savill Garden Gridshell Design and Construction', *Structural Engineer*, 86(17), pp. 27–34.

Hensel, M., Menges, A. and Weinstock, M. (2013) *Emergent Technologies and Design: Towards a bilogical aradigm for architecture* ". Oxford, UK: Routledge.

Hensel, M. U. (2013) *Performance-oriented Architecture Towards a Biological Paradigm for Architectural Design and the Built Environment*, *John Wiley & Sons*. Chichester, UK.

Hypermembrane Project (2013). Available at: http://www.formakers.eu/project-1083-hybrida- sylvia-felipe-jordi-truco-hypermembrane-modular-complexit (Accessed: 21

November 2016).

Khoo, C. K., Salim, F. and Burry, J. (2012) 'Designing Architectural Morphing Skins with Elastic Modular Systems', *International Journal of Architectural Computing*, 9(4), pp. 397–420. doi: 10.1260/1478-0771.9.4.397.

Kilian, A. and Ochsendorf, J. (2005) 'Particle Spring Systems for Structural Form Finding', *Journal of the International Association for Shell and Spatial Structures*, 46(2), pp. 77–84. Available at: http://cumincad.scix.net/data/works/att/744e.content.03334.pdf.

Kontovourkis, O., Phocas, M. C., Alexandrou, K. and Frangogiannopoulos, S. (2016) 'Configuration and Deformation Control of a Hybrid Bending-Active Structure', *Computational Methods and Experimental Measurements, WIT press*, 5(4), pp. 475–483.

Kontovourkis, O., Phocas, M. and Tryfonos, G. (2013) 'Prototyping of an adaptive structure based on physical conditions', *International Journal of Architectural Computing*, 11(2), pp. 205–226. doi: 10.1260/1478-0771.11.2.205.

Kooi, B. W. (1981) 'On the mechanics of the bow and arrow', *Journal of Engineering Mathematics*, 15(2), pp. 119–145. doi: 10.1007/BF00052515.

Kotelnikova-Weiler, N., Douthe, C., Hernandez, E. L., Baverel, O., Gengnagel, C. and Caron, J.-F. (2013) 'Materials for actively-Bent structures', *International Journal of Space Structures*, 28(3–4), pp. 229–240. doi: 10.1260/0266-3511.28.3-4.229.

Lafuente-Hernandez, E., Baverel, O. and Gengnagel, C. (2013) 'On the design and construction of elastic gridshells with irregular meshes', *International Journal of Space Structures*, 28(3–4), pp. 161–174.

Levien, R. L. (2009) *From Spiral to Spline : Optimal Techniques in Interactive Curve Design Copyright by Raphael Linus Levien*, *Bernoulli*. University of California, Berkeley.

Lewis, W. J. (2003) *Tension Structures: Form and behaviour*. London, UK: Thomas Telford.

Liddell, I. (2015) 'Frei Otto and the development of gridshells', *Case Studies in Structural Engineering*. Elsevier Ltd, 4, pp. 39–49. doi: 10.1016/j.csse.2015.08.001.

Lienhard, J. (2014) 'Bending-Active Structures : form-finding strategies using elastic deformation in static and kinematic systems and the structural potentials therein.' Ph.D. Thesis: University of Stuttgart: Institute of Building Structures and Structural Design.

Lienhard, J., Ahlquist, S., Menges, A. and Knippers, J. (2013) 'Finite element modelling in integral design strategies of form- and bending-active hybrid structures', in *Proceedings of the VI International Conference on Textile Composites and Inflatable Structures: Structural Membrane*. Munich, pp. 39–50.

Lienhard, J., Alpermann, H., Gengnagel, C. and Knippers, J. (2013) 'Active Bending, A Review on Structures where Bending is used as a Self-Formation Process', *International Journal of Space Structures*, 28(3), pp. 187–196. doi: 10.1260/0266-3511.28.3-4.187.

Lienhard, J. and Knippers, J. (2013) 'Considerations on the Scaling of Bending-Active Structures', *International Journal of Space Structures*, 28(3), pp. 137–148. doi: 10.1260/0266-3511.28.3-4.137.

Lienhard, J., La Magna, R. and Knippers, J. (2014) 'Form-finding Bending-active structures with temporary ultra-elastic construction elements', in *Mobile and rabidly assembled structures IV*. Ostend: WIT Press, pp. 107–115.

Liuti, A. (2016) 'Erection of post-formed gridshells by means of inflatable membrane technology membrane technology', in Stephan, R. H. C. and A. (ed.) *International Conference of the Architectural Science Association 2015*. Melbourne: Taylor & Francis, pp. 678–687.

Mele, T. Van, Laet, L. De, Veenendaal, D., Mollaert, M., Block, P. and Mele, V. (2013) 'Shaping Tension Structures with Actively Bent Linear Elements', *International Journal of Space Structures*, 28(3–4), pp. 127–135.

Menges, A. (2012) *Material computation: higher integration in morphogenetic design, Architectural Design. Vol. 82, No. 2*. Edited by A. Menges. London: Wiley Academy.

Menges, A. and Ahlquist, S. (2011) *Computational Design Thinking*. Chichester, Uk: John Wiley & Sons.

Moon, F. C. (2003) 'Franz Reuleaux: Contributions to 19th C. Kinematics and Theory of Machines', *The American Society of Mechanical Engineers - ASME*, 56(2), pp. 261–285. doi: 10.1115/1.1523427.

Nicholas, P. and Tamke, M. (2013) 'Computational Strategies for the Architectural Design of Bending Active Structures', *International Journal of Space Structures*, 28(3–4), pp. 215–228. doi: 10.1260/0266-3511.28.3-4.215.

Olsson, J. (2012) 'Form finding and size optimization - Implementation of beam elements and size optimization in real time'. Chalmers University of Technology, p. 97.

Phocas, M. C. (2015) 'Interdisciplinary Technology-Driven Design Processes in Architecture', *archi DOCT*, 3(1), pp. 10–19.

Phocas, M. C. (2017) 'Design and Analysis of Form-active Systems. Spanning from Tensile to Hybrid Bending-active Structures', *archi DOCT*, 5(1), pp. 11–25.

Phocas, M. C., Alexandrou, K. and Zakou, C. (2018) 'Design and Analysis of an Adaptive Bending-active Plate Gridshell', *Journal of the International Association for Shell and Spatial Structures, J.IASS*, (Submitted).

Phocas, M. C., Charmpis, D. C., Alexandrou, K. and Athini, S. (2018) 'Design and Analysis of an Adaptive Hybrid Structure', *Engineering Structures*, (In preparation).

Phocas, M. C., Christoforou, E. G. and Matheou, M. (2015) 'Design, motion planning and control of a reconfigurable hybrid structure', *Engineering Structures*, 101, pp. 376–385. doi: 10.1016/j.engstruct.2015.07.036.

Phocas, M. C., Kontovourkis, O. and Alexandrou, K. (2013) 'Design of a Controlled Cable Bending-Active Structure', in *International Conference on Adaptation and Movement in Architecture, ICAMA 2013*. Toronto, Canada, pp. 224–236.

Phocas, M. C., Kontovourkis, O. and Nicolaou, N. (2014) 'Design Concept of a Kinetic Form-active Hybrid Envelope Structure', *International Journal of Design and Nature and Ecodynamics*, 9(1), pp. 13–30. doi: 10.2495/DNE-V9-N1-13-30.

Quagliaroli, M., Malerba, P. G., Albertin, A. and Pollini, N. (2015) 'The Role of Prestress and its Optimization in Cable Domes Design', *Computers and Structures,*. Elsevier Ltd, 161, pp. 17–30. doi: 10.1016/j.compstruc.2015.08.017.

Quinn, G. and Gengnagel, C. (2014) 'A Review of Elastic Grid Shells, their Erection Methods and the Potential Use of Pneumatic Formwork', in *Mobile and Rapidly Assembled Structures IV*. Ostend: WIT Press, pp. 129–144. doi: 10.2495/MAR140111.

Reuleaux, F. and Ferguson, E. S. (2012) *Kinematics of Machinery: Outlines of a Theory of Machines*. Courier Corporation.

Saitoh, M. (1998) 'Role of string: aesthetics and technology of tension structures', in *Long-Span and High-Rise Structures, IABSE Symposium*. Kope, Japan: IABSE, pp. 699–710.

Saitoh, M. and Okada, A. (1999) 'The role of string in hybrid string structure', *Engineering Structures*, 21(8), pp. 756–769. doi: 10.1016/S0141-0296(98)00029-7.

Schleicher, S., Rastetter, A., La Magna, R., Schönbrunner, A., Haberbosch, N. and Knippers, J. (2015) *Form-Finding and Design Potentials of Bending-Active Plate Structures*, *Modelling Behaviour: Design Modelling Symposium 2015*. Edited by F. S. Mette Ramsgaard Thomsen, Martin Tamke, Christoph Gengnagel, Billie Faircloth. Springer. doi: 10.1007/978-3-319-24208-8.

Schnädelbach, H. (2010) 'Adaptive Architecture: A Conceptual Framework', in *Proceedings of MediaCity 2010*. Weimar, pp. 532–555.

Schumacher, M. (2010) *MOVE: Architecture in Motion - Dynamic components and elements*. Basel: Birkhäuser Architecture.

Shelter Systems (2016). Available at: http://www.shelter-systems.com/tensegrity.html (Accessed: 12 September 2016).

SOFiSTiK AG (2014a) 'ASE: General Static Analysis of Finite Element Structures'. Oberschleissheim, Germany: SOFiSTiK AG.

SOFiSTiK AG (2014b) 'SOFiLOAD: Loadgenerator for Finite Elements and Frameworks'. Oberschleissheim, Germany: SOFiSTiK AG.

Sterk, T. d'Estree (2003) 'Using Actuated Tensegrity Structures to Produce a Responsive Architecture', in *ACADIA22: Connecting Crossroads of Digital Discourse*, pp. 84–93.

Takahashi, K., Körner, A., Koslowski, V. and Knippers, J. (2016) 'Scale effect in bending-active plates and a novel concept for elastic kinetic roof systems', in Kawaguchi, K., Ohsaki, M., and Takeuchi, T. (eds) *Proceedings of the IASS Annual Symposium 2016, Special Structures in the 21st Century,*. Tokyo, Japan, pp. 1–10.

Temporary shading structure (2012). Available at: Temporary shading structure (Accessed: 21 November 2016).

Terzopoulost, D., Platt, J., Barr, A. and Fleischert, K. (1987) 'Elastically Deformable Models', *ACM Siggraph Computer Graphics*, 21(4), pp. 205–214.

Textile Hybrid M1 (2013). Available at: http://icd.uni-stuttgart.de (Accessed: 26 November 2016).

Toussaint, M. (2007) *A design tool for timber gridshells*. Delft University of Technology. Available at: http://scholar.google.com/scholar?hl=en&btnG=Search&q=intitle:A+Design+Tool+for+Timber+Gridshells#0.

Veenendaal, D. and Block, P. (2012) 'An overview and comparison of structural form finding methods for general networks', *International Journal of Solids and Structures*, 49(26), pp. 3741–3753. doi: 10.1016/j.ijsolstr.2012.08.008.

Veltkamp, M. (2007) 'Free Form Structural Design'. Delft: Technical University of Delft. Available at: http://repository.tudelft.nl/assets/uuid:a6c9d911-a548-4092-9d89-12ca37ceb8c3/arc_veltkamp_20070917-2.pdf.

Woodbury, R. (2010) *Elements of Parametric Design*. 1st edn. United Kingdom: Taylor Francis Ltd.

Yurd-dome (2013). Available at: http://www.shelter-systems.com/solor-dome (Accessed: 22 November 2016).

APPENDIX

Table A1. Single-segment structural configuration 1

T: 5 W:240	Displacement		Primary elastic Member			Secondary elastic Member			Cable
	$U_{(z)}$ [mm]	$U_{(x)}$ [mm]	$N_{(x)}$ [KN]	$V_{(z)}$ [KN]	$M_{(y)}$ [KNm]	$N_{(x)}$ [KN]	$V_{(z)}$ [KN]	$M_{(y)}$ [KNm]	N [KN]
Fastened	0	0	0	0	0				
Step 1	190	100	0.1	0.04	0.01				0.0634
Step 2	261	200	0.1	0.05	0.02				0.0675
Step 3	309	300	0.1	0.07	0.02				0.072
Step 4	343	400	0.1	0.07	0.03				0.0769
Step 5	367	500	0.1	0.08	0.03				0.0825
Q	Not Applicable								
T: 10 W:240									
Fastened	0	0	0	0	0				
Step 1	190	100	0.5	0.30	0.10				0.5071
Step 2	261	200	0.5	0.43	0.14				0.5402
Step 3	309	300	0.6	0.52	0.18				0.5752
Step 4	343	400	0.6	0.60	0.21				0.6146
Step 5	367	500	0.7	0.66	0.25				0.6599
Q	362	500	1.3	0.85	0.23				0.8757

T: 15 W:240	Displacement		Primary elastic Member			Secondary elastic Member			Cable
	$U_{(z)}$ [mm]	$U_{(x)}$ [mm]	$N_{(x)}$ [KN]	$V_{(z)}$ [KN]	$M_{(y)}$ [KNm]	$N_{(x)}$ [KN]	$V_{(z)}$ [KN]	$M_{(y)}$ [KNm]	N [KN]
Fastened	0	0	0	0	0				
Step 1	190	100	1.7	1.02	0.33				1.7115
Step 2	261	200	1.8	1.45	0.48				1.8230
Step 3	309	300	1.9	1.76	0.61				1.9412
Step 4	343	400	2.1	2.01	0.72				2.0741
Step 5	367	500	2.2	2.22	0.83				2.2270
Q	365	500	2.5	2.38	0.81				2.4513
T: 20 W: 240									
Fastened	0	0	0	0	0				
Step 1	190	100	4.1	2.42	0.79				4.0559
Step 2	261	200	4.3	3.42	1.15				4.3202
Step 3	309	300	4.6	4.17	1.44				4.6005
Step 4	343	400	4.9	4.77	1.71				4.9154
Step 5	367	500	5.3	5.26	1.96				5.2776
Q	367	500	5.5	5.41	1.95				5.5040

T: 25 W:240	Displacement		Primary elastic Member			Secondary elastic Member			Cable
	$U_{(z)}$ [mm]	$U_{(x)}$ [mm]	$N_{(x)}$ [KN]	$V_{(z)}$ [KN]	$M_{(y)}$ [KNm]	$N_{(x)}$ [KN]	$V_{(z)}$ [KN]	$M_{(y)}$ [KNm]	N [KN]
Fastened	0	0	0	0	0				
Step 1	190	100	7.9	4.72	1.53				7.9191
Step 2	261	200	8.4	6.68	2.24				8.4354
Step 3	309	300	9.0	8.13	2.81				8.9825
Step 4	343	400	9.6	9.30	3.34				9.5972
Step 5	367	500	10.3	10.28	3.84				10.3042
Q	367	500	10.5	10.42	3.82				10.5317
T: 10 W: 80									
Fastened	0	0	0	0	0				
Step 1	190	100	0.2	0.10	0.03				0.1691
Step 2	261	200	0.2	0.14	0.05				0.1801
Step 3	309	300	0.2	0.17	0.06				0.1918
Step 4	343	400	0.2	0.20	0.07				0.2049
Step 5	367	500	0.2	0.22	0.08				0.2201
Q	Not Applicable								

T: 10 W:160	Displacement		Primary elastic Member			Secondary elastic Member			Cable
	$U_{(z)}$ [mm]	$U_{(x)}$ [mm]	$N_{(x)}$ [KN]	$V_{(z)}$ [KN]	$M_{(y)}$ [KNm]	$N_{(x)}$ [KN]	$V_{(z)}$ [KN]	$M_{(y)}$ [KNm]	N [KN]
Fastened	0	0	0	0	0				
Step 1	190	100	0.3	0.13	0.04				0.3236
Step 2	261	200	0.3	0.24	0.08				0.3469
Step 3	309	300	0.4	0.31	0.11				0.3693
Step 4	343	400	0.4	0.37	0.13				0.3936
Step 5	367	500	0.4	0.41	0.15				0.4213
Q	Not Applicable								
T: 10 W: 240									
Fastened	0	0	0	0	0				
Step 1	190	100	0.5	0.30	0.10				0.5071
Step 2	261	200	0.5	0.43	0.14				0.5402
Step 3	309	300	0.6	0.52	0.18				0.5752
Step 4	343	400	0.6	0.60	0.21				0.6146
Step 5	367	500	0.7	0.66	0.25				0.6599
Q	362	500	1.3	0.85	0.23				0.8757

T: 10 W:320	Displacement		Primary elastic Member			Secondary elastic Member			Cable
	$U_{(z)}$ [mm]	$U_{(x)}$ [mm]	$N_{(x)}$ [KN]	$V_{(z)}$ [KN]	$M_{(y)}$ [KNm]	$N_{(x)}$ [KN]	$V_{(z)}$ [KN]	$M_{(y)}$ [KNm]	N [KN]
Fastened	0	0	0	0	0				
Step 1	190	100	0.7	0.40	0.13				0.6762
Step 2	261	200	0.7	0.57	0.19				0.7202
Step 3	309	300	0.8	0.69	0.24				0.7670
Step 4	343	400	0.8	0.79	0.29				0.8195
Step 5	367	500	0.9	0.88	0.33				0.8799
Q	364	500	1.3	1.05	0.31				1.0989

Table A2. Single-segment structural configuration 2

T: 5 W:240	Displacement		Primary elastic Member			Secondary elastic Member			Cable
	$U_{(z)}$ [mm]	$U_{(x)}$ [mm]	$N_{(x)}$ [KN]	$V_{(z)}$ [KN]	$M_{(y)}$ [KNm]	$N_{(x)}$ [KN]	$V_{(z)}$ [KN]	$M_{(y)}$ [KNm]	N [KN]
Fastened	0	0	0	0	0	0	0	0	0
Step 1	190	100	0.1	0.04	0.01	0.1	0.04	0.01	0.1268
Step 2	261	200	0.1	0.05	0.02	0.1	0.05	0.02	0.1350
Step 3	309	300	0.1	0.07	0.02	0.1	0.07	0.02	0.1440
Step 4	343	400	0.1	0.07	0.03	0.1	0.07	0.03	0.1538
Step 5	367	500	0.1	0.08	0.03	0.1	0.08	0.03	0.1650
Q	Not Applicable								
T: 10 W: 240									
Fastened	0	0	0	0	0	0	0	0	0
Step 1	190	100	0.5	0.30	0.10	0.5	0.30	0.10	1.0142
Step 2	261	200	0.5	0.43	0.14	0.5	0.43	0.14	1.0804
Step 3	309	300	0.6	0.52	0.18	0.6	0.52	0.18	1.1504
Step 4	343	400	0.6	0.60	0.21	0.6	0.60	0.21	1.2292
Step 5	367	500	0.7	0.66	0.25	0.7	0.66	0.25	1.3198
Q	362	500	1.3	0.85	0.23	1.3	0.85	0.23	1.7514

T: 15 W:240	Displacement		Primary elastic Member			Secondary elastic Member			Cable
	$U_{(z)}$ [mm]	$U_{(x)}$ [mm]	$N_{(x)}$ [KN]	$V_{(z)}$ [KN]	$M_{(y)}$ [KNm]	$N_{(x)}$ [KN]	$V_{(z)}$ [KN]	$M_{(y)}$ [KNm]	N [KN]
Fastened	0	0	0	0	0	0	0	0	0
Step 1	190	100	1.7	1.02	0.33	1.7	1.02	0.33	3.4230
Step 2	261	200	1.8	1.45	0.48	1.8	1.45	0.48	3.6460
Step 3	309	300	1.9	1.76	0.61	1.9	1.76	0.61	3.8824
Step 4	343	400	2.1	2.01	0.72	2.1	2.01	0.72	4.1482
Step 5	367	500	2.2	2.22	0.83	2.2	2.22	0.83	4.4540
Q	365	500	2.5	2.38	0.81	2.5	2.38	0.81	4.9026
T: 20 W: 240									
Fastened	0	0	0	0	0	0	0	0	0
Step 1	190	100	4.1	2.42	0.79	4.1	2.42	0.79	8.1118
Step 2	261	200	4.3	3.42	1.15	4.3	3.42	1.15	8.6404
Step 3	309	300	4.6	4.17	1.44	4.6	4.17	1.44	9.2010
Step 4	343	400	4.9	4.77	1.71	4.9	4.77	1.71	9.8308
Step 5	367	500	5.3	5.26	1.96	5.3	5.26	1.96	10.5552
Q	367	500	5.5	5.41	1.95	5.5	5.41	1.95	11.0080

T: 25 W:240	Displacement		Primary elastic Member			Secondary elastic Member			Cable
	$U_{(z)}$ [mm]	$U_{(x)}$ [mm]	$N_{(x)}$ [KN]	$V_{(z)}$ [KN]	$M_{(y)}$ [KNm]	$N_{(x)}$ [KN]	$V_{(z)}$ [KN]	$M_{(y)}$ [KNm]	N [KN]
Fastened	0	0	0	0	0	0	0	0	0
Step 1	190	100	7.9	4.72	1.53	7.9	4.72	1.53	15.8382
Step 2	261	200	8.4	6.68	2.24	8.4	6.68	2.24	16.8708
Step 3	309	300	9.0	8.13	2.81	9.0	8.13	2.81	17.9650
Step 4	343	400	9.6	9.30	3.34	9.6	9.30	3.34	19.1944
Step 5	367	500	10.3	10.28	3.84	10.3	10.28	3.84	20.6084
Q	367	500	10.5	10.42	3.82	10.5	10.42	3.82	21.0634
T: 10 W: 80									
Fastened	0	0	0	0	0	0	0	0	0
Step 1	190	100	0.2	0.10	0.03	0.2	0.10	0.03	0.3382
Step 2	261	200	0.2	0.14	0.05	0.2	0.14	0.05	0.3602
Step 3	309	300	0.2	0.17	0.06	0.2	0.17	0.06	0.3836
Step 4	343	400	0.2	0.20	0.07	0.2	0.20	0.07	0.4098
Step 5	367	500	0.2	0.22	0.08	0.2	0.22	0.08	0.4402
Q	Not Applicable								

T: 10 W:160	Displacement		Primary elastic Member			Secondary elastic Member			Cable
	$U_{(z)}$ [mm]	$U_{(x)}$ [mm]	$N_{(x)}$ [KN]	$V_{(z)}$ [KN]	$M_{(y)}$ [KNm]	$N_{(x)}$ [KN]	$V_{(z)}$ [KN]	$M_{(y)}$ [KNm]	N [KN]
Fastened	0	0	0	0	0	0	0	0	0
Step 1	190	100	0.3	0.13	0.04	0.3	0.13	0.04	0.6472
Step 2	261	200	0.3	0.24	0.08	0.3	0.24	0.08	0.6938
Step 3	309	300	0.4	0.31	0.11	0.4	0.31	0.11	0.7386
Step 4	343	400	0.4	0.37	0.13	0.4	0.37	0.13	0.7872
Step 5	367	500	0.4	0.41	0.15	0.4	0.41	0.15	0.8426
Q	Not Applicable								
T: 10 W: 240									
Fastened	0	0	0	0	0	0	0	0	0
Step 1	190	100	0.5	0.30	0.10	0.5	0.30	0.10	1.0142
Step 2	261	200	0.5	0.43	0.14	0.5	0.43	0.14	1.0804
Step 3	309	300	0.6	0.52	0.18	0.6	0.52	0.18	1.1504
Step 4	343	400	0.6	0.60	0.21	0.6	0.60	0.21	1.2292
Step 5	367	500	0.7	0.66	0.25	0.7	0.66	0.25	1.3198
Q	362	500	1.3	0.85	0.23	1.3	0.85	0.23	1.7514

T: 10 W:320	Displacement		Primary elastic Member			Secondary elastic Member			Cable
	$U_{(z)}$ [mm]	$U_{(x)}$ [mm]	$N_{(x)}$ [KN]	$V_{(z)}$ [KN]	$M_{(y)}$ [KNm]	$N_{(x)}$ [KN]	$V_{(z)}$ [KN]	$M_{(y)}$ [KNm]	N [KN]
Fastened	0	0	0	0	0	0	0	0	0
Step 1	190	100	0.7	0.4	0.13	0.7	0.4	0.13	1.3524
Step 2	261	200	0.7	0.57	0.19	0.7	0.57	0.19	1.4404
Step 3	309	300	0.8	0.69	0.24	0.8	0.69	0.24	1.5340
Step 4	343	400	0.8	0.79	0.29	0.8	0.79	0.29	1.6390
Step 5	367	500	0.9	0.88	0.33	0.9	0.88	0.33	1.7598
Q	364	500	1.3	1.05	0.31	1.3	1.05	0.31	2.1978

Table A3 Single-segment structural configuration 3

T: 5 W: 240	Displacement		Primary elastic Member			Secondary elastic Member			Cable
	$U_{(z)}$ [mm]	$U_{(x)}$ [mm]	$N_{(x)}$ [KN]	$V_{(z)}$ [KN]	$M_{(y)}$ [KNm]	$N_{(x)}$ [KN]	$V_{(z)}$ [KN]	$M_{(y)}$ [KNm]	N [KN]
Fastened	425	0	0	0	0	0	0.03	0.02	0
Step 1	463	100	0.1	0.03	0.01	0.0	0.03	0.02	0.0983
Step 2	493	200	0.1	0.04	0.01	0.0	0.04	0.02	0.1017
Step 3	516	300	0.1	0.05	0.02	0.0	0.04	0.02	0.1075
Step 4	534	400	0.1	0.07	0.03	0.0	0.04	0.02	0.1141
Step 5	547	500	0.1	0.08	0.03	0.0	0.05	0.03	0.1213
Q	Not Applicable								
T: 10 W: 240									
Fastened	425	0	0	0	0	0.3	0.26	0.13	0
Step 1	463	100	0.5	0.30	0.10	0.3	0.29	0.14	0.8121
Step 2	493	200	0.5	0.43	0.14	0.3	0.31	0.16	0.8602
Step 3	516	300	0.6	0.52	0.18	0.3	0.34	0.18	0.9121
Step 4	534	400	0.6	0.60	0.21	0.4	0.36	0.19	0.9701
Step 5	547	500	0.7	0.66	0.25	0.4	0.38	0.21	1.0361
Q	Not Applicable								

T: 15 W: 240	Displacement		Primary elastic Member			Secondary elastic Member			Cable
	$U_{(z)}$ [mm]	$U_{(x)}$ [mm]	$N_{(x)}$ [KN]	$V_{(z)}$ [KN]	$M_{(y)}$ [KNm]	$N_{(x)}$ [KN]	$V_{(z)}$ [KN]	$M_{(y)}$ [KNm]	N [KN]
Fastened	425	0	0	0	0	1.0	0.88	0.42	0
Step 1	463	100	1.7	1.02	0.33	1.0	0.97	0.48	2.7397
Step 2	493	200	1.8	1.44	0.48	1.1	1.06	0.54	2.9021
Step 3	516	300	1.8	2.01	0.61	1.1	1.12	0.59	3.0766
Step 4	534	400	2.1	1.76	0.72	1.2	1.13	0.65	3.2727
Step 5	547	500	2.2	2.22	0.83	1.3	1.27	0.70	3.4969
Q	537	500	2.2	2.22	0.83	1.4	1.66	0.65	3.5481
T: 20 W: 240									
Fastened	425	0	0	0	0	2.3	2.07	1.0	0
Step 1	463	100	4.1	2.41	0.78	2.4	2.31	1.14	6.4898
Step 2	493	200	4.3	3.42	1.14	2.6	2.5	1.27	6.8742
Step 3	516	300	4.6	4.16	1.44	2.7	2.68	1.40	7.2877
Step 4	534	400	4.9	4.76	1.71	2.8	2.84	1.53	7.7517
Step 5	547	500	5.3	5.26	1.96	3.0	3.01	1.66	8.2825
Q	543	500	5.3	5.26	1.96	3.1	3.34	1.61	8.3476

T: 25 W: 240	Displacement		Primary elastic Member			Secondary elastic Member			Cable
	$U_{(z)}$ [mm]	$U_{(x)}$ [mm]	$N_{(x)}$ [KN]	$V_{(z)}$ [KN]	$M_{(y)}$ [KNm]	$N_{(x)}$ [KN]	$V_{(z)}$ [KN]	$M_{(y)}$ [KNm]	N [KN]
Fastened	425	0	0	0	0	4.5	4.05	1.95	0
Step 1	463	100	7.9	4.69	1.52	4.8	4.50	2.22	12.6639
Step 2	493	200	8.4	6.66	2.23	5.0	4.89	2.48	13.4139
Step 3	516	300	9.0	8.11	2.81	5.3	5.24	2.74	14.2203
Step 4	534	400	9.6	9.28	3.33	5.5	5.54	2.99	15.1251
Step 5	547	500	10.3	10.26	3.83	5.9	5.87	3.24	16.1596
Q	545	500	10.3	10.26	3.83	5.9	6.15	3.19	16.2303
T: 10 W: 80									
Fastened	425	0	0	0	0	0.1	0.09	0.04	0
Step 1	463	100	0.2	0.10	0.03	0.1	0.10	0.05	0.2707
Step 2	493	200	0.2	0.14	0.05	0.1	0.10	0.05	0.2868
Step 3	516	300	0.2	0.17	0.06	0.1	0.11	0.06	0.3041
Step 4	534	400	0.2	0.20	0.07	0.1	0.12	0.06	0.3234
Step 5	547	500	0.2	0.22	0.08	0.1	0.13	0.07	0.3456
Q	Not Applicable								

T: 10 W: 160	Displacement		Primary elastic Member			Secondary elastic Member			Cable
	$U_{(z)}$ [mm]	$U_{(x)}$ [mm]	$N_{(x)}$ [KN]	$V_{(z)}$ [KN]	$M_{(y)}$ [KNm]	$N_{(x)}$ [KN]	$V_{(z)}$ [KN]	$M_{(y)}$ [KNm]	N [KN]
Fastened	425	0	0	0	0	0.2	0.17	0.08	0
Step 1	463	100	0.3	0.20	0.07	0.2	0.19	0.10	0.5414
Step 2	493	200	0.4	0.29	0.10	0.2	0.21	0.11	0.5735
Step 3	516	300	0.4	0.35	0.12	0.2	0.22	0.12	0.6091
Step 4	534	400	0.4	0.40	0.14	0.2	0.24	0.13	0.6468
Step 5	547	500	0.4	0.44	0.16	0.3	0.25	0.14	0.6911
Q	Not Applicable								
T: 10 W: 240									
Fastened	425	0	0	0	0	0.3	0.26	0.13	0
Step 1	463	100	0.3	0.29	0.14	0.5	0.30	0.13	0.8121
Step 2	493	200	0.3	0.31	0.16	0.5	0.43	0.14	0.8602
Step 3	516	300	0.3	0.34	0.18	0.6	0.52	0.18	0.9121
Step 4	534	400	0.4	0.36	0.19	0.6	0.60	0.21	0.9701
Step 5	547	500	0.4	0.38	0.21	0.7	0.66	0.25	1.0361
Q	Not Applicable								

T: 10 W: 320	Displacement		Primary elastic Member			Secondary elastic Member			Cable
	$U_{(z)}$ [mm]	$U_{(x)}$ [mm]	$N_{(x)}$ [KN]	$V_{(z)}$ [KN]	$M_{(y)}$ [KNm]	$N_{(x)}$ [KN]	$V_{(z)}$ [KN]	$M_{(y)}$ [KNm]	N [KN]
Fastened	425	0	0	0	0	0.4	0.35	0.17	0
Step 1	463	100	0.7	0.40	0.13	0.4	0.38	0.19	1.0828
Step 2	493	200	0.7	0.57	0.18	0.4	0.42	0.21	1.1469
Step 3	516	300	0.8	0.69	0.24	0.4	0.45	0.23	1.2159
Step 4	534	400	0.8	0.79	0.28	0.5	0.47	0.26	1.2934
Step 5	547	500	0.9	0.88	0.33	0.5	0.50	0.28	1.3821
Q	Not Applicable								

Table A4 Single-segment structural configuration 4

T: 5 W: 240	Displacement		Primary elastic Member			Secondary elastic Member			Cable
	$U_{(z)}$ [mm]	$U_{(x)}$ [mm]	$N_{(x)}$ [KN]	$V_{(z)}$ [KN]	$M_{(y)}$ [KNm]	$N_{(x)}$ [KN]	$V_{(z)}$ [KN]	$M_{(y)}$ [KNm]	N [KN]
Fastened	425	0	0	0	0	0	0.03	0.02	0
Step 1	463	100	0.1	0.03	0.01	0.0	0.03	0.02	0.0983
Step 2	493	200	0.1	0.04	0.01	0.0	0.04	0.02	0.1017
Step 3	516	300	0.1	0.05	0.02	0.0	0.04	0.02	0.1075
Step 4	534	400	0.1	0.07	0.03	0.0	0.04	0.02	0.1141
Step 5	547	500	0.1	0.08	0.03	0.0	0.05	0.03	0.1213
Q	Not Applicable								
T: 10 W: 240									
Fastened	425	0	0	0	0	0.3	0.26	0.13	0
Step 1	463	100	0.5	0.30	0.10	0.3	0.29	0.14	0.8121
Step 2	493	200	0.5	0.43	0.14	0.3	0.31	0.16	0.8602
Step 3	516	300	0.6	0.52	0.18	0.3	0.34	0.18	0.9121
Step 4	534	400	0.6	0.60	0.21	0.4	0.36	0.19	0.9701
Step 5	547	500	0.7	0.66	0.25	0.4	0.38	0.21	1.0361
Q	Not Applicable								

T: 15 W: 240	Displacement		Primary elastic Member			Secondary elastic Member			Cable
	$U_{(z)}$ [mm]	$U_{(x)}$ [mm]	$N_{(x)}$ [KN]	$V_{(z)}$ [KN]	$M_{(y)}$ [KNm]	$N_{(x)}$ [KN]	$V_{(z)}$ [KN]	$M_{(y)}$ [KNm]	N [KN]
Fastened	425	0	0	0	0	1.0	0.88	0.42	0
Step 1	463	100	1.7	1.02	0.33	1.0	0.97	0.48	2.7397
Step 2	493	200	1.8	1.44	0.48	1.1	1.06	0.54	2.9021
Step 3	516	300	1.8	2.01	0.61	1.1	1.12	0.59	3.0766
Step 4	534	400	2.1	1.76	0.72	1.2	1.13	0.65	3.2727
Step 5	547	500	2.2	2.22	0.83	1.3	1.27	0.70	3.4969
Q	537	500	2.2	2.22	0.83	1.4	1.66	0.65	3.5481
T: 20 W: 240									
Fastened	425	0	0	0	0	2.3	2.07	1.0	0
Step 1	463	100	4.1	2.41	0.78	2.4	2.31	1.14	6.4898
Step 2	493	200	4.3	3.42	1.14	2.6	2.5	1.27	6.8742
Step 3	516	300	4.6	4.16	1.44	2.7	2.68	1.40	7.2877
Step 4	534	400	4.9	4.76	1.71	2.8	2.84	1.53	7.7517
Step 5	547	500	5.3	5.26	1.96	3.0	3.01	1.66	8.2825
Q	543	500	5.3	5.26	1.96	3.1	3.34	1.61	8.3476

T: 25 W: 240	Displacement		Primary elastic Member			Secondary elastic Member			Cable
	$U_{(z)}$ [mm]	$U_{(x)}$ [mm]	$N_{(x)}$ [KN]	$V_{(z)}$ [KN]	$M_{(y)}$ [KNm]	$N_{(x)}$ [KN]	$V_{(z)}$ [KN]	$M_{(y)}$ [KNm]	N [KN]
Fastened	425	0	0	0	0	4.5	4.05	1.95	0
Step 1	463	100	7.9	4.69	1.52	4.8	4.50	2.22	12.6639
Step 2	493	200	8.4	6.66	2.23	5.0	4.89	2.48	13.4139
Step 3	516	300	9.0	8.11	2.81	5.3	5.24	2.74	14.2203
Step 4	534	400	9.6	9.28	3.33	5.5	5.54	2.99	15.1251
Step 5	547	500	10.3	10.26	3.83	5.9	5.87	3.24	16.1596
Q	545	500	10.3	10.26	3.83	5.9	6.15	3.19	16.2303
T: 10 W: 80									
Fastened	425	0	0	0	0	0.1	0.09	0.04	0
Step 1	463	100	0.2	0.10	0.03	0.1	0.10	0.05	0.2707
Step 2	493	200	0.2	0.14	0.05	0.1	0.10	0.05	0.2868
Step 3	516	300	0.2	0.17	0.06	0.1	0.11	0.06	0.3041
Step 4	534	400	0.2	0.20	0.07	0.1	0.12	0.06	0.3234
Step 5	547	500	0.2	0.22	0.08	0.1	0.13	0.07	0.3456
Q	Not Applicable								

T: 10 W: 160	Displacement		Primary elastic Member			Secondary elastic Member			Cable
	$U_{(z)}$ [mm]	$U_{(x)}$ [mm]	$N_{(x)}$ [KN]	$V_{(z)}$ [KN]	$M_{(y)}$ [KNm]	$N_{(x)}$ [KN]	$V_{(z)}$ [KN]	$M_{(y)}$ [KNm]	N [KN]
Fastened	425	0	0	0	0	0.2	0.17	0.08	0
Step 1	463	100	0.3	0.20	0.07	0.2	0.19	0.10	0.5414
Step 2	493	200	0.4	0.29	0.10	0.2	0.21	0.11	0.5735
Step 3	516	300	0.4	0.35	0.12	0.2	0.22	0.12	0.6091
Step 4	534	400	0.4	0.40	0.14	0.2	0.24	0.13	0.6468
Step 5	547	500	0.4	0.44	0.16	0.3	0.25	0.14	0.6911
Q	Not Applicable								
T: 10 W: 240									
Fastened	425	0	0	0	0	0.3	0.26	0.13	0
Step 1	463	100	0.3	0.29	0.14	0.5	0.30	0.13	0.8121
Step 2	493	200	0.3	0.31	0.16	0.5	0.43	0.14	0.8602
Step 3	516	300	0.3	0.34	0.18	0.6	0.52	0.18	0.9121
Step 4	534	400	0.4	0.36	0.19	0.6	0.60	0.21	0.9701
Step 5	547	500	0.4	0.38	0.21	0.7	0.66	0.25	1.0361
Q	Not Applicable								

T: 10 W: 320	Displacement		Primary elastic Member			Secondary elastic Member			Cable
	$U_{(z)}$ [mm]	$U_{(x)}$ [mm]	$N_{(x)}$ [KN]	$V_{(z)}$ [KN]	$M_{(y)}$ [KNm]	$N_{(x)}$ [KN]	$V_{(z)}$ [KN]	$M_{(y)}$ [KNm]	N [KN]
Fastened	425	0	0	0	0	0.4	0.35	0.17	0
Step 1	463	100	0.7	0.40	0.13	0.4	0.38	0.19	1.0828
Step 2	493	200	0.7	0.57	0.18	0.4	0.42	0.21	1.1469
Step 3	516	300	0.8	0.69	0.24	0.4	0.45	0.23	1.2159
Step 4	534	400	0.8	0.79	0.28	0.5	0.47	0.26	1.2934
Step 5	547	500	0.9	0.88	0.33	0.5	0.50	0.28	1.3821
Q	Not Applicable								

Table A5 Single-segment structural configuration 5

T: 5 W: 240	Displacement		Primary elastic Member			Secondary elastic Member			Cable
	$U_{(z)}$ [mm]	$U_{(x)}$ [mm]	$N_{(x)}$ [KN]	$V_{(z)}$ [KN]	$M_{(y)}$ [KNm]	$N_{(x)}$ [KN]	$V_{(z)}$ [KN]	$M_{(y)}$ [KNm]	N [KN]
Fastened	216	114	0.2	0.14	0.03	0.2	0.22	0.04	
Step 2	265	200	0.2	0.16	0.03	0.2	0.20	0.04	0.0443
Step 3	312	300	0.2	0.16	0.03	0.2	0.19	0.04	0.0727
Step 4	346	400	0.2	0.17	0.04	0.2	0.18	0.04	0.0934
Step 5	370	500	0.2	0.17	0.05	0.2	0.17	0.04	0.1115
Q	Not Applicable								
T: 10 W: 240									
Fastened	216	125	1.9	1.13	0.22	1.9	1.75	0.32	
Step 2	265	200	1.6	1.24	0.26	1.8	1.64	0.32	0.2957
Step 3	312	300	1.4	1.30	0.30	1.7	1.54	0.31	0.5291
Step 4	346	400	1.3	1.33	0.34	1.6	1.45	0.30	0.6978
Step 5	370	500	1.3	1.35	0.38	1.5	1.38	0.30	0.8435
Q	363	500	0.5	0.76	0.32	1.8	1.98	0.31	0.8223

T: 15 W: 240	Displacement		Primary elastic Member			Secondary elastic Member			Cable
	$U_{(z)}$ [mm]	$U_{(x)}$ [mm]	$N_{(x)}$ [KN]	$V_{(z)}$ [KN]	$M_{(y)}$ [KNm]	$N_{(x)}$ [KN]	$V_{(z)}$ [KN]	$M_{(y)}$ [KNm]	N [KN]
Fastened	216	124	6.5	3.74	0.70	6.5	5.81	1.08	
Step 2	265	200	5.4	4.03	0.84	6.0	5.45	1.06	0.9761
Step 3	312	300	4.7	4.25	0.99	5.6	5.11	1.03	1.7446
Step 4	346	400	4.4	4.38	1.12	5.2	4.83	1.01	2.2983
Step 5	370	500	4.3	4.46	1.24	4.9	4.59	1.01	2.7747
Q	368	500	3.5	3.79	1.18	5.1	5.14	1.01	2.7801
T: 20 W: 240									
Fastened	216	123	15.1	8.46	1.58	15.1	13.53	2.54	
Step 2	265	200	12.7	9.16	1.91	14.1	12.71	2.48	2.2779
Step 3	312	300	11.0	9.73	2.26	13.1	11.9	2.41	4.0659
Step 4	346	400	10.2	10.08	2.57	12.3	11.25	2.38	5.3495
Step 5	370	500	9.9	10.32	2.85	11.4	10.70	2.37	6.4501
Q	368	500	9.2	9.68	2.79	11.6	11.24	2.37	6.5006

T: 25 W: 240	Displacement		Primary elastic Member			Secondary elastic Member			Cable
	$U_{(z)}$ [mm]	$U_{(x)}$ [mm]	$N_{(x)}$ [KN]	$V_{(z)}$ [KN]	$M_{(y)}$ [KNm]	$N_{(x)}$ [KN]	$V_{(z)}$ [KN]	$M_{(y)}$ [KNm]	N [KN]
Fastened	216	120	29.2	15.89	2.98	29.2	26.05	4.90	
Step 2	265	200	24.4	17.31	3.61	27.1	24.49	4.79	4.4061
Step 3	312	300	21.2	18.48	4.31	25.4	22.95	4.67	7.8535
Step 4	346	400	19.7	19.24	4.89	23.7	21.71	4.61	10.3195
Step 5	370	500	19.1	19.78	5.42	22.1	20.65	4.59	12.4270
Q	370	500	18.3	19.16	5.38	22.3	21.19	4.59	12.4538
T: 10 W: 80									
Fastened	216	125	0.7	0.39	0.07	0.7	0.59	0.11	
Step 2	265	200	0.5	0.42	0.09	0.6	0.55	0.11	0.0986
Step 3	312	300	0.5	0.44	0.10	0.6	0.52	0.10	0.1764
Step 4	346	400	0.4	0.45	0.12	0.5	0.49	0.10	0.2328
Step 5	370	500	0.4	0.45	0.13	0.5	0.46	0.10	0.2815
Q	Not Applicable								

T: 10 W: 160	Displacement		Primary elastic Member			Secondary elastic Member			Cable
	$U_{(z)}$ [mm]	$U_{(x)}$ [mm]	$N_{(x)}$ [KN]	$V_{(z)}$ [KN]	$M_{(y)}$ [KNm]	$N_{(x)}$ [KN]	$V_{(z)}$ [KN]	$M_{(y)}$ [KNm]	N [KN]
Fastened	216	125	1.3	0.78	0.15	1.3	1.17	0.22	
Step 2	265	200	1.1	0.83	0.17	1.2	1.10	0.21	0.1972
Step 3	312	300	1.0	0.87	0.20	1.1	1.03	0.21	0.3528
Step 4	346	400	0.9	0.89	0.23	1.1	0.97	0.20	0.4655
Step 5	370	500	0.9	0.91	0.25	1.0	0.92	0.20	0.5627
Q	357	500	0.4	0.46	0.19	1.4	1.56	0.22	0.5251
T: 10 W: 240									
Fastened	216	125	1.9	1.13	0.22	1.9	1.75	0.32	
Step 2	265	200	1.6	1.24	0.26	1.8	1.64	0.32	0.2957
Step 3	312	300	1.4	1.30	0.30	1.7	1.54	0.31	0.5291
Step 4	346	400	1.3	1.33	0.34	1.6	1.45	0.30	0.6978
Step 5	370	500	1.3	1.35	0.38	1.5	1.38	0.30	0.8435
Q	363	500	0.5	0.76	0.32	1.8	1.98	0.31	0.8223

T: 10 W: 320	Displacement		Primary elastic Member			Secondary elastic Member			Cable
	$U_{(z)}$ [mm]	$U_{(x)}$ [mm]	$N_{(x)}$ [KN]	$V_{(z)}$ [KN]	$M_{(y)}$ [KNm]	$N_{(x)}$ [KN]	$V_{(z)}$ [KN]	$M_{(y)}$ [KNm]	N [KN]
Fastened	216	125	2.6	1.54	0.29	2.6	2.33	0.43	
Step 2	265	200	2.2	1.65	0.34	2.4	2.18	0.42	0.3941
Step 3	312	300	1.9	1.73	0.40	2.2	2.04	0.41	0.7051
Step 4	346	400	1.8	1.77	0.46	2.1	1.93	0.40	0.9299
Step 5	370	500	1.7	1.79	0.50	2.0	1.83	0.40	1.1238
Q	365	500	0.9	1.15	0.44	2.2	2.42	0.41	1.1107

Table A6 Single-segment structural configuration 6

T: 5 W: 240	Displacement		Primary elastic Member			Secondary elastic Member			Cable
	$U_{(z)}$ [mm]	$U_{(x)}$ [mm]	$N_{(x)}$ [KN]	$V_{(z)}$ [KN]	$M_{(y)}$ [KNm]	$N_{(x)}$ [KN]	$V_{(z)}$ [KN]	$M_{(y)}$ [KNm]	N [KN]
Fastened	403	332	0.8	0.28	0.03	0.7	0.66	0.06	
Step 4	420	400	0.7	0.28	0.04	0.7	0.63	0.06	0.0195
Step 5	438	500	0.6	0.29	0.04	0.6	0.58	0.06	0.4351
Q	Not Applicable								
T: 10 W: 240									
Fastened	425	427	5.8	2.33	0.30	5.8	4.9	0.49	
Step 5	438	500	5.3	2.34	0.32	5.4	4.63	0.48	0.1523
Q	432	500	5.7	2.47	0.32	5.7	4.63	0.48	0.0026
T: 15 W: 240									
Fastened	424	422	19.5	7.83	1.00	18.2	16.51	1.66	
Step 5	431	500	17.9	7.85	1.07	18.4	15.61	1.62	0.5128
Q	435	500	18.2	7.91	1.06	18.7	15.61	1.62	0.5262

T: 20 W: 240	Displacement		Primary elastic Member			Secondary elastic Member			Cable
	$U_{(z)}$ [mm]	$U_{(x)}$ [mm]	$N_{(x)}$ [KN]	$V_{(z)}$ [KN]	$M_{(y)}$ [KNm]	$N_{(x)}$ [KN]	$V_{(z)}$ [KN]	$M_{(y)}$ [KNm]	N [KN]
Fastened	412	384	44.9	17.24	2.24	41.3	37.58	3.86	
Step 4	416	400	44	17.28	2.28	40.7	37.11	3.84	0.2862
Step 5	434	500	38.4	18.02	2.49	37.3	34.28	3.74	1.9000
Q	434	500	38.7	17.59	2.48	37.6	34.27	3.73	1.9080
T: 25 W: 240									
Fastened	400	352	84.7	31.21	4.15	77.6	70.54	7.28	
Step 4	412	400	79.1	31.41	4.36	74.3	67.79	7.17	1.7001
Step 5	431	500	68.6	34.10	4.83	67.8	62.39	6.99	4.7433
Q	430	500	68.8	33.68	4.81	68.1	62.36	6.98	4.7492
T: 10 W: 80									
Fastened	427	427	1.9	0.78	0.10	1.8	1.65	0.17	
Step 5	438	500	1.8	0.78	0.11	1.7	1.54	0.16	0.0503
Q	Not Applicable								

T: 10 W: 160	Displacement		Primary elastic Member			Secondary elastic Member			Cable
	$U_{(z)}$ [mm]	$U_{(x)}$ [mm]	$N_{(x)}$ [KN]	$V_{(z)}$ [KN]	$M_{(y)}$ [KNm]	$N_{(x)}$ [KN]	$V_{(z)}$ [KN]	$M_{(y)}$ [KNm]	N [KN]
Fastened	425	427	3.8	1.55	0.20	3.6	3.26	0.33	
Step 5	438	500	3.5	1.56	0.21	3.4	3.08	0.32	0.1016
Q	Not Applicable								
T: 10 W: 240									
Fastened	425	427	5.8	2.33	0.30	5.8	4.9	0.49	
Step 5	438	500	5.3	2.34	0.32	5.4	4.63	0.48	0.1523
Q	Not Applicable								
T: 10 W: 320									
Fastened	425	427	7.7	3.11	0.40	7.2	6.54	0.66	
Step 5	438	500	7	3.12	0.42	6.7	6.18	0.64	0.2031
Q	434	500	7.5	3.27	0.43	7.0	6.16	0.64	0.0062

Table B1. Multi-segment structural configuration. Two to eight segments

System	Δl_c [mm]	σ_x (MPa)	H [m]	L/H	$C_{1,8}$	$C_{2,7}$	$C_{3,6}$	$C_{4,5}$
S-2cs								
(ii)	211.6	36.43	0.63	1.59	0.56			
(ii) & Q: 1.3	-	37.60	0.63	1.59	0.00			
(iii)	64	45.98	0.54	1.83	0.79			
(iii) & Q: 1.3	-	47.88	0.55	1.83	0.01			
S-3cs								
(ii)	116.6	25.48	1.04	1.44	0.53	0.52		
(ii) & Q: 0.6	-	26.19	1.03	1.46	0.00	0.61		
(iii)	105	46.80	0.99	1.52	0.91	1.30		
(iii) & Q: 0.6	-	47.95	0.99	1.52	0.29	1.19		
S-4cs								
(ii)	67.6	19.09	1.35	1.48	0.48	0.46		
(ii) & Q: 0.25	-	21.98	1.17	1.71	0.00	0.55		
(iii)	105	45.49	1.09	1.83	0.88	1.42		
(iii) & Q: 0.25	-	47.96	0.91	2.20	0.42	1.43		
S-5cs								
(ii)	46.5	15.49	1.72	1.45	0.48	0.45	0.45	
(ii) & Q: 0.12	-	16.65	1.60	1.56	0.00	0.29	0.71	
(iii)	100	46.10	1.53	1.63	0.85	1.45	1.62	
(iii) & Q: 0.12	-	47.89	1.35	1.85	0.48	1.40	1.70	
S-6cs								
(ii)	33.9	12.88	2.05	1.46	0.45	0.41	0.41	
(ii) & Q: 0.08	-	13.96	1.89	1.59	0.00	0.07	0.63	

System	Δl_{cr} [mm]	σ_x (MPa)	H [m]	L/H	$C_{1,8}$	$C_{2,7}$	$C_{3,6}$	$C_{4,5}$
(iii)	95	45.53	1.59	1.89	0.81	1.42	1.69	
(iii) & Q: 0.08	-	48.00	1.26	2.38	0.43	1.28	1.79	
S-7cs								
(ii)	26.6	11.17	2.42	1.45	0.44	0.39	0.39	0.39
(ii) & Q: 0.05	-	11.74	2.29	1.53	0.00	0.00	0.45	0.69
(iii)	93	46.08	2.00	1.75	0.77	1.37	1.70	1.79
(iii) & Q: 0.05	-	47.96	1.64	2.13	0.43	1.16	1.80	1.89
S-8cs								
(ii)	21.6	9.88	2.76	1.45	0.43	0.37	0.38	0.38
(ii) & Q: 0.04	-	11.90	2.43	1.65	0.00	0.00	0.49	0.92
(iii)	90	46.06	2.02	1.98	0.74	1.32	1.69	1.83
(iii) & Q: 0.04	-	48.01	1.48	2.70	0.37	1.01	1.78	1.95

Table B2. Multi-segment structural configuration. Eight-segment model with and without* cables

			Elastic Member			Displacement	
System 1 SC1:	Δl_c [mm]	$N_{(x)}$ [KN]	$V_{(z)}$ [KN]	$M_{(y)}$ [KNm]	σ_x [MPa]	H [m]	L/H
(ii)*	-	0.18	0.01	0.03	7.93	3.01	1.33
(ii) & Q:0.03*	-	0.28	0.10	0.07	18.57	1.48	2.70
(ii)	21.6	0.43	0.11	0.04	9.88	2.76	1.45
(ii) & Q:0.03	-	0.61	0.34	0.04	9.80	2.63	1.52
			Cable Groups				
	$C_{1,8}$	$C_{2,7}$	$C_{3,6}$	$C_{4,5}$			
(ii)	0.44	0.37	0.38	0.38			
(ii) & Q:0.03	0.08	0	0.31	0.60			

Table B3. Multi-segment structural configuration (8-cs)

			Elastic Member			Displacement	
System 1 SC1:	Δl_c [mm]	$N_{(x)}$ [KN]	$V_{(z)}$ [KN]	$M_{(y)}$ [KNm]	σ_x [MPa]	H [m]	L/H
(ii)	21.6	0.43	0.11	0.04	9.88	2.757	1.45
(ii) & Q:0.04	-	0.93	0.19	0.05	11.90	2.429	1.65
(ii)	21.6	0.43	0.11	0.04	9.88	2.757	1.45
(iii)	90	1.72	1.01	0.18	46.06	2.019	1.98
(iii) & Q:0.04	-	1.84	1.08	0.19	48.01	1.477	2.71

	Cable Groups			
	$C_{1,8}$	$C_{2,7}$	$C_{3,6}$	$C_{4,5}$
(ii)	0.434	0.372	0.375	0.376
(ii) & Q:0.04	0	0	0.486	0.919
(ii)	0.434	0.372	0.375	0.376
(iii)	0.735	1.319	1.694	1.833
(iii) & Q:0.04	0.366	1.011	1.783	1.946

Table B4. Multi-segment structural configuration (8-cs). Scenario 1 – Single group activation

			Elastic Member			Displacement	
System 1 SC1:	Δl_c [mm]	$N_{(x)}$ [KN]	$V_{(z)}$ [KN]	$M_{(y)}$ [KNm]	σ_x [MPa]	H [m]	L/H
(ii)	21.6	0.43	0.11	0.04	9.88	2.757	1.45
(iii)	A: 290	0.94	0.54	0.18	45.97	1.997	2.00
(iii) & Q:0.04	-	1.47	0.94	0.17	43.48	1.205	3.32

	Cable Groups			
	$C_{1,8}$	$C_{2,7}$	$C_{3,6}$	$C_{4,5}$
(ii)	0.434	0.372	0.375	0.376
(iii)	0.586	0.692	0.872	0.963
(iii) & Q:0.04	0.301	0	0.997	1.501

Table B4. Multi-segment structural configuration (8-cs). Scenario 1 – Single group activation

			Elastic Member			Displacement	
System 1 SC1:	Δl_c [mm]	$N_{(x)}$ [KN]	$V_{(z)}$ [KN]	$M_{(y)}$ [KNm]	σ_x [MPa]	H [m]	L/H
(ii)	21.6	0.43	0.11	0.04	9.88	2.757	1.45
(iii)	B:190	1.61	0.89	0.16	40.69	1.847	2.17
(iii) & Q:0.02	-	1.74	1.08	0.15	38.90	1.494	2.68

	Cable Groups			
	$C_{1,8}$	$C_{2,7}$	$C_{3,6}$	$C_{4,5}$
(ii)	0.434	0.372	0.375	0.376
(iii)	0.769	0.872	1.596	1.674
(iii) & Q:0.02	0.450	0.721	1.727	1.803

Table B4. Multi-segment structural configuration (8-cs). Scenario 1 – Single group activation

			Elastic Member			Displacement	
System 1 SC1:	Δl_c [mm]	$N_{(x)}$ [KN]	$V_{(z)}$ [KN]	$M_{(y)}$ [KNm]	σ_x [MPa]	H [m]	L/H
(ii)	21.6	0.43	0.11	0.04	9.88	2.757	1.45
(iii)	C:170	1.91	1.05	0.17	42.56	2.366	1.69
(iii) & Q:0.01	-	1.95	1.09	0.17	42.45	2.286	1.75

	Cable Groups			
	$C_{1,8}$	$C_{2,7}$	$C_{3,6}$	$C_{4,5}$
(ii)	0.43	0.37	0.375	0.38
(iii)	0.76	1.43	1.08	1.96
(iii) & Q:0.01	0.69	1.37	1.06	2.01

Table B4. Multi-segment structural configuration (8-cs). Scenario 1 – Single group activation

			Elastic Member			Displacement	
System 1 SC1:	Δl_c [mm]	$N_{(x)}$ [KN]	$V_{(z)}$ [KN]	$M_{(y)}$ [KNm]	σ_x [MPa]	H [m]	L/H
(ii)	21.6	0.43	0.11	0.04	9.88	2.757	1.45
(iii)	D:80	1.51	0.54	0.12	30.89	2.943	1.36
(iii) & Q:0.04	-	1.43	0.78	0.13	31.80	2.773	1.44

	Cable Groups			
	$C_{1,8}$	$C_{2,7}$	$C_{3,6}$	$C_{4,5}$
(ii)	0.43	0.37	0.38	0.38
(iii)	0.68	1.09	1.42	1.11
(iii) & Q:0.04	0.25	0.57	1.41	1.13

Table B5. Multi-segment structural configuration (8-cs). Scenario 2 – Two group activation

			Elastic Member			Displacement	
System 1 SC1:	Δl_c [mm]	$N_{(x)}$ [KN]	$V_{(z)}$ [KN]	$M_{(y)}$ [KNm]	σ_x [MPa]	H [m]	L/H
(ii)	21.6	0.43	0.11	0.04	9.88	2.757	1.45
(iii)	A:160 B:160	1.34	0.54	0.10	26.43	2.005	2.00
(iii) & Q:0.01	-	1.71	0.93	0.15	38.32	1.419	2.82

	Cable Groups			
	$C_{1,8}$	$C_{2,7}$	$C_{3,6}$	$C_{4,5}$
(ii)	0.43	0.37	0.38	0.38
(iii)	0.58	0.79	1.298	1.38
(iii) & Q:0.01	0.58	0.91	1.73	1.80

Table B5. Multi-segment structural configuration (8-cs). Scenario 2 – Two group activation

			Elastic Member			Displacement	
System 1 SC1:	Δl_c [mm]	$N_{(x)}$ [KN]	$V_{(z)}$ [KN]	$M_{(y)}$ [KNm]	σ_x [MPa]	H [m]	L/H
(ii)	21.6	0.43	0.11	0.04	9.88	2.757	1.45
(iii)	A:230 C:80	1.67	0.88	0.17	42.70	1.99	2.01
(iii) & Q:0.01	-	1.77	0.77	0.16	41.06	1.81	2.21

	Cable Groups			
	$C_{1,8}$	$C_{2,7}$	$C_{3,6}$	$C_{4,5}$
(ii)	0.43	0.37	0.38	0.38
(iii)	0.67	1.35	1.12	1.71
(iii) & Q:0.01	0.54	1.10	1.11	1.83

Table B5. Multi-segment structural configuration (8-cs). Scenario 2 – Two group activation

			Elastic Member			Displacement	
System 1 SC1:	Δl_c [mm]	$N_{(x)}$ [KN]	$V_{(z)}$ [KN]	$M_{(y)}$ [KNm]	σ_x [MPa]	H [m]	L/H
(ii)	21.6	0.43	0.11	0.04	9.88	2.757	1.45
(iii)	A:70 D:70	1.44	0.56	0.12	30.62	2.672	1.50
(iii) & Q:0.03	-	1.57	0.90	0.12	30.56	2.470	1.62

	Cable Groups			
	$C_{1,8}$	$C_{2,7}$	$C_{3,6}$	$C_{4,5}$
(ii)	0.43	0.37	0.38	0.38
(iii)	0.61	1.09	1.48	1.18
(iii) & Q:0.03	0.33	0.56	1.53	1.17

Table B5. Multi-segment structural configuration (8-cs). Scenario 2 – Two group activation

			Elastic Member			Displacement	
System 1 SC1:	Δl_c [mm]	$N_{(x)}$ [KN]	$V_{(z)}$ [KN]	$M_{(y)}$ [KNm]	σ_x [MPa]	H [m]	L/H
(ii)	21.6	0.43	0.11	0.04	9.88	2.757	1.45
(iii)	B:110 C:80	1.56	0.53	0.10	25.79	2.31	1.73
(iii) & Q:0.04	-	2.00	0.83	0.14	34.35	2.017	1.98

	Cable Groups			
	$C_{1,8}$	$C_{2,7}$	$C_{3,6}$	$C_{4,5}$
(ii)	0.43	0.37	0.38	0.38
(iii)	0.68	0.88	1.10	1.60
(iii) & Q:0.04	0.84	1.01	1.29	2.06

Table B5. Multi-segment structural configuration (8-cs). Scenario 2 – Two group activation

			Elastic Member			Displacement	
System 1 SC1:	Δl_c [mm]	$N_{(x)}$ [KN]	$V_{(z)}$ [KN]	$M_{(y)}$ [KNm]	σ_x [MPa]	H [m]	L/H
(ii)	21.6	0.43	0.11	0.04	9.88	2.757	1.45
(iii)	B:20 D:60	1.39	0.51	0.11	28.47	2.777	1.44
(iii) & Q:0.04	-	1.43	0.92	0.11	29.18	2.537	1.58

	Cable Groups			
	$C_{1,8}$	$C_{2,7}$	$C_{3,6}$	$C_{4,5}$
(ii)	0.43	0.37	0.38	0.38
(iii)	0.67	0.93	1.42	1.16
(iii) & Q:0.04	0.15	0.43	1.42	1.19

Table B5. Multi-segment structural configuration (8-cs). Scenario 2 – Two group activation

			Elastic Member			Displacement	
System 1 SC1:	Δl_c [mm]	$N_{(x)}$ [KN]	$V_{(z)}$ [KN]	$M_{(y)}$ [KNm]	σ_x [MPa]	H [m]	L/H
(ii)	21.6	0.43	0.11	0.04	9.88	2.757	1.45
(iii)	C:90 D:50	1.46	0.72	0.15	37.29	2.813	1.42
(iii) & Q:0.04	-	1.40	0.77	0.15	38.76	2.660	1.50

	Cable Groups			
	$C_{1,8}$	$C_{2,7}$	$C_{3,6}$	$C_{4,5}$
(ii)	0.43	0.37	0.38	0.38
(iii)	0.78	1.48	1.34	1.37
(iii) & Q:0.04	0.40	1.05	1.30	1.42

Table B6. Multi-segment structural configuration (8-cs). Scenario 3 – Three group activation

			Elastic Member			Displacement	
System 1 SC1:	Δl_c [mm]	$N_{(x)}$ [KN]	$V_{(z)}$ [KN]	$M_{(y)}$ [KNm]	σ_x [MPa]	H [m]	L/H
(ii)	21.6	0.43	0.11	0.04	9.88	2.757	1.45
(iii)	A:30 B:40 C:60	1.64	0.60	0.11	27.99	2.236	1.79
(iii) & Q:0.02	-	1.82	0.76	0.11	28.03	1.982	2.02

	Cable Groups			
	$C_{1,8}$	$C_{2,7}$	$C_{3,6}$	$C_{4,5}$
(ii)	0.43	0.37	0.38	0.38
(iii)	0.65	0.96	1.13	1.68
(iii) & Q:0.02	0.44	0.75	1.11	1.86

Table B6. Multi-segment structural configuration (8-cs). Scenario 3 – Three group activation

			Elastic Member			Displacement	
System 1 SC1:	Δl_c [mm]	$N_{(x)}$ [KN]	$V_{(z)}$ [KN]	$M_{(y)}$ [KNm]	σ_x [MPa]	H [m]	L/H
(ii)	21.6	0.43	0.11	0.04	9.88	2.757	1.45
(iii)	A:20 B:20 D:60	1.45	0.53	0.11	28.87	2.704	1.48
(iii) & Q:0.03	-	1.51	0.88	0.12	29.35	2.485	1.61

	Cable Groups			
	$C_{1,8}$	$C_{2,7}$	$C_{3,6}$	$C_{4,5}$
(ii)	0.43	0.37	0.38	0.38
(iii)	0.63	0.66	1.47	1.18
(iii) & Q:0.03	0.30	0.56	1.50	1.21

Table B6. Multi-segment structural configuration (8-cs). Scenario 3 – Three group activation

			Elastic Member			Displacement	
System 1 SC1:	Δl_c [mm]	$N_{(x)}$ [KN]	$V_{(z)}$ [KN]	$M_{(y)}$ [KNm]	σ_x [MPa]	H [m]	L/H
(ii)	21.6	0.43	0.11	0.04	9.88	2.757	1.45
(iii)	A:30 C:30 D:100	1.43	0.73	0.15	38.29	2.767	1.45
(iii) & Q:0.04	-	1.47	0.77	0.16	39.51	2.549	1.57

	Cable Groups			
	$C_{1,8}$	$C_{2,7}$	$C_{3,6}$	$C_{4,5}$
(ii)	0.43	0.37	0.38	0.38
(iii)	0.69	1.44	1.46	1.34
(iii) & Q:0.04	0.32	0.88	1.46	1.38

Table B6. Multi-segment structural configuration (8-cs). Scenario 3 – Three group activation

			Elastic Member			Displacement	
System 1 SC1:	Δl_c [mm]	$N_{(x)}$ [KN]	$V_{(z)}$ [KN]	$M_{(y)}$ [KNm]	σ_x [MPa]	H [m]	L/H
(ii)	21.6	0.43	0.11	0.04	9.88	2.757	1.45
(iii)	B:40 C:80 D:120	1.55	0.98	0.19	47.41	2.522	1.59
(iii) & Q:0.04	-	1.61	1.01	0.19	48.05	2.323	1.72

	Cable Groups			
	$C_{1,8}$	$C_{2,7}$	$C_{3,6}$	$C_{4,5}$
(ii)	0.43	0.37	0.38	0.38
(iii)	0.93	1.30	1.62	1.62
(iii) & Q:0.04	0.48	1.03	1.57	1.66

Table B7. Multi-segment structural configuration (8-cs). Scenario 4 – Custom group activation

			Elastic Member			Displacement	
System 1 SC1:	Δl_c [mm]	$N_{(x)}$ [KN]	$V_{(z)}$ [KN]	$M_{(y)}$ [KNm]	σ_x [MPa]	H [m]	L/H
(ii)	A:10 B:20 C:30	0.49	0.14	0.05	12.01	2.942	1.36
(iii)	D:40	1.74	0.82	0.11	26.76	3.009	1.33
(iii) & Q:0.04	-	1.92	0.92	0.11	27.40	2.96	1.35

	Cable Groups			
	$C_{1,8}$	$C_{2,7}$	$C_{3,6}$	$C_{4,5}$
(ii)	0.44	0.39	0.46	0.49
(iii)	0.68	1.07	1.24	1.13
(iii) & Q:0.04	0.32	0.68	1.16	1.15

Table C1. Multi-segment structural configuration (8-cs). System 2 with and without* cables

System	$N_{(x)}$ [KN]	$V_{(z)}$ [KN]	$M_{(y)}$ [KNm]	σ_x [MPa]	$U_{(z)}$ [m]	$V_{(z)}$ [KN]	$M_{(y)}$ [KNm]	σ_x [MPa]	H [m]	L/H [m/m]
		Primary el. member				Secondary el. member				
(ii) - 1	0.03	0.02	0.03	7.39	0.03	0.03	0.04	9.90	2.02	3.34
(ii) - 2	0.16	0.08	0.05	13.1	0.14	0.84	0.06	13.9	2.56	1.56
(ii) - 3	1.12	0.30	0.06	24.2	1.03	0.90	0.23	57.1	2.44	1.64
*(ii) & Q**	1.27	0.34	0.14	33.2	10.4	0.93	0.23	59.1	1.93	2.07
(ii) & Q	0.83	0.45	0.13	31.4	1.05	0.92	0.23	58.6	2.07	1.93